

University of Mosul
College of Electronic Engineering



Study of sidelobes reduction methods in circular antenna array

Mohammed Zuhair Mohammed Fawzi

M.Sc. Dissertation in

Communication Engineering

Supervised by

Dr. Abdullah Hasan. Aboud

2018 A.C

Mosul-Iraq

1439 A.H

University of Mosul
College of Engineering



Study of sidelobes reduction methods in circular antenna array

A Dissertation Submitted

by

Mohammed Zuhair Mohammed Fawzi

To

The Council of College of Electronic Engineering

University of Mosul

*In Partial Fulfillment of the Requirements
For the Degree of Master of Science*

In

Communication Engineering

Supervised by

Dr. Abdullah Hasan. Aboud

2018 A.C

Mosul-Iraq

1439 A.H

Supervisor's Certification

We certify that the dissertation entitled (**Study of sidelobes reduction methods in circular antenna array**) was prepared by **Mohammed Zuhair Mohammed Fawzi** under our supervision at the Department of Communication Engineering, University of Mosul, as a partial requirement for the Master of Science Degree in Communication Engineering.

Signature:

Dr. Abdullah Hassan Aboud

Date: / / 2018

Report of Linguistic Reviewer

I certify that the linguistic review of this dissertation was carried out by me and it is accepted linguistically and in expression.

Signature:

Name:

Date:: / / 2018

Report of the Head of Postgraduate Studies Committee

According to the recommendations presented by the supervisor of this dissertation and the linguistic reviewer, I nominate this dissertation to be forwarded to discussion.

Signature:

Name:

Date: / / 2018

Report of the Head of Department

I certify that this dissertation was carried out in the Department of Communication Engineering. I nominate it to be forwarded to discussion.

Signature:

Name:

Date: / / 2018

Committee Certification

We the examining committee, certify that we have read this dissertation entitled (**Study of sidelobes reduction methods in circular antenna array**) and have examined the postgraduate student(**Mohammed Zuhair Mohammed Fawzi**)in its contents and that in our opinion it meets the standards of a dissertation for the degree of Master of Science in Communication Engineering.

Signature:
Name:
Head of committee
Date: / /2018

Signature:
Name:
Member
Date: / /2018

Signature:
Name:
Member
Date: / /2018

Signature:
Name:
Member and Supervisor
Date: / /2018

Signature:
Name:
Member
Date: / /2018

Signature:
Name:
Member
Date: / /2018

The college council, in its..... meeting on / /2018, has decided to award the degree of Master of Science in Communication Engineering to the candidate.

Signature:
Name:
Dean of the College
Date: / /2018

Signature:
Name:
Council registrar
Date: / /2018

Table of Contents

Sub. No.	Subject	Page No.
	Abstract	I
	Acknowledgements	III
	List of Figures	IV
	List of tables	X
	List of symbols	XI
	List of Abbreviations	XIII
CHAPTER 1- Introduction		1
1.1	General consideration	1
1.2	Historical reviews	2
1.3	Aim of the work	6
1.4	Scope of the Dissertation	6
CHAPTER 2 -Study and Analysis of Arrays		7
2.1	Introduction	7
2.2	Linear antenna array	8
2.3	Directivity of antenna array	11
2.4	Circular antenna array	12
2.5	Vertical pattern for circular antenna array	18
2.5.1	Nulls of the vertical pattern	19
2.5.2	Maxima of minor lobes of the vertical pattern	19
2.5.3	The HPBW of the major lobe of the vertical pattern	19
2.6	Horizontal pattern for circular antenna array	20
2.6.1	Nulls of the horizontal pattern	21
2.6.2	Maxima of minor lobes of the horizontal pattern	21
2.6.3	The HPBW of the major lobe of the horizontal pattern	21
2.7	Results of a uniform circular array	24

CHAPTER 3- Sidelobes Level Reduction of Circular Antenna Array using Genetic Algorithm		27
3.1	Introduction	27
3.2	Genetic algorithm	27
3.2.1	Sidelobes level reduction using genetic algorithm	28
3.2.2	Results and discussion	29
3.3	Sidelobes level reduction with modification in the selected elements of the circular antenna array	34
3.3.1	Analysis and results of modified excitations of circular array	34
3.3.2	Sidelobes level reduction using modified spacing between two collinear elements at specified angular positions	51
CHAPTER 4- Sidelobes level Reduction Using Concentric Circular Antenna Array		58
4.1	Introduction	58
4.2	Equation of concentric circular antenna array	59
4.3	Sidelobes level reduction by using concentric circular array	60
4.3.1	Sidelobes level reduction for 12-element concentric circular array	61
4.3.2	Sidelobes level reduction for 14-element concentric circular array	61
4.3.3	Sidelobes level reduction for 18-element concentric circular array	62
4.3.4	Sidelobes level reduction for 24-element concentric circular array	66
a-(10-14) concentric circular array		66
b-(8-16) concentric circular array		68
c-(6-18) concentric circular array		70
4.4	Discussions for the results of concentric circular antenna array	73

CHAPTER 5 -Conclusions and Suggestions for Future Work		84
5.1	Circular antenna arrays	85
5.2	Suggestions for Future Work	89
References		90

Abstract

Communication and radar systems require radiation pattern of high directivity and low sidelobes level. It is necessary to look for an antenna to achieve such purpose. An antenna array can help us to reach this duty. Antenna array posses good directivity and low sidelobes level as compared with the antenna of a single element. The sidelobes level of the array still high and need to be reduced to overcome the interference from unwanted signals. In this work we used circular antenna array. Many methods were used to obtain the suitable excitation for the elements of the array for low sidelobes level.

A genetic algorithm is a technique presented in this work for reducing the sidelobes structure in the radiation pattern of a circular antenna array. The fitness function used in the algorithm is the area under the sidelobes. In order to obtain good results in the reduction of the sidelobes level, we should obtain the lowest value for the fitness function, taking into consideration the small increase in the beamwidth of the main beam.

Results of computer simulations showed good reductions in the sidelobes level.

Modification in the weights and radial distance of certain specified elements of a circular antenna array is also presented for reducing the sidelobes. This method involves adjusting the current weights or the radial distance or both of them. The idea of modification in the current weights was developed for two, four, six and eight elements.

Computer simulations showed better results in reduction of the sidelobes level as compared with that obtained by genetic algorithm method.

Concentric circular antenna array is also presented. The elements used in the single ring of a circular array were distributed over two concentric rings. Three examples of concentric antenna array were used. The first one we measured the performance of the array by varying the radii of the concentric array in steps guided by the ratio of the elements in the outer ring to that in the inner ring. The second one we measured is the performance of the array by varying the radius of the outer ring while keeping the radius of the inner one unchanged at value less than the radius of the original circular array. The third one we measured is the performance of the array by varying the radius of the inner ring in the concentric antenna array keeping the outer ring constant at value equal to radius of the original circular array.

Computer simulations showed better results in the performance of the concentric circular antenna array as compared with that of single ring circular antenna array.

Acknowledgements

I would like to express my deep sense of gratitude and thanks to my supervisor, **Dr. Abdullah H. Abood** for his valuable supervision and helpful suggestions throughout the progression of this work.

In addition I would like to extend my thanks and appreciation to professor **Dr. Khalil Hassan sayidmarie** for his valuable observations during the course of study and research period

I would also like to thank the head of communication engineering department, and all staff members who provided the help. Thanks are to all my friends for their assistance in the completion of this work.

Finally, I would like to thank all the members of my family especially my father and mother for their support, encouragement and patience throughout the duration of this work.

List of Figures		
Fig. No.	Figure Description	Page No.
2.1	Linear antenna array of N elements positioned along z-axis	9
2.2	a&b -Plot of the array factor for 12-element uniformly linear excited array	10
2.3	Plot of beamwidth for linear antenna array versus $d(\lambda)$ for different values of N	11
2.4	Directivity for uniform linear array versus d for different number of the elements	12
2.5	Geometry of circular antenna array of N elements positioned in x-y plane	13
2.6	Section of the circular antenna shows two consecutive elements of the array on the arc of a circle	14
2.7	plot of vertical pattern of circular antenna array for $N = 12, d = 0.75\lambda$	20
2.8	plot of horizontal pattern of circular antenna array for $N = 12, d = 0.75\lambda$	22
2.9	Plot of beamwidth for circular antenna array versus $d(\lambda)$ for different values of N	22
2.10	Directivity for uniform circular array versus radius $a(\lambda)$ for different number of the elements	23
2.11	Angular positions of 1 st , 2 nd null and sidelobes for 18 elements uniform circular array versus elements spacing $d(\lambda)$	24
3.1	Geometry of a circular antenna array positioned in x-y plane	29
3.2	a&b -Radiation pattern for 12-element circular antenna array using genetic algorithm shows a reduction in the sidelobes level $\phi_0 = 0, \theta_0 = 0$	31

3.3	a&b -Radiation pattern for 18-element circular antenna array using genetic algorithm shows a reduction in the sidelobes level $\phi_0 = 0, \theta_0 = 0$	32
3.4	a&b -Radiation pattern for 20 elements circular antenna array using genetic algorithm shows a reduction in the sidelobes level $\phi_0 = 0, \theta_0 = 0$	33
3.5	Improvement factor versus angular positions for each pair of elements locations in the resting plane for 12 elements uniform circular array	35
3.6	Geometry of modified excitation circular antenna array in x-y plane	36
3.7	a&b - Radiation pattern of 12-element circular array with unity excitation of all elements except two elements with 0.1 positioned at angles $30^\circ, 210^\circ$	40
3.8	a&b -Radiation pattern of 12-element circular array with unity excitation of all elements except 4 elements with excitation 0.3 positioned at angles in (deg.) 30,210,150,330	41
3.9	a&b - Radiation pattern of 18-element circular array with unity excitation of all elements except 4 elements with excitation 0.1 positioned at angles in (deg.) 20,160,200,340	42
3.10	a&b - Radiation pattern of 18-element circular array with unity excitation of all elements except 6 elements with modified excitation 0.2 at angular positions in (deg.) 20,140,160,200,320,340	43
3.11	a&b - Radiation pattern of 24-element circular array with unity excitation of all elements except 6 elements with excitation 0.1 positioned at angles in (deg.) 15,30,180,195,210,360	44
3.12	a&b - Radiation pattern of 24-element circular array with unity excitation of all elements except 8 elements with modified excitation 0.1 at angular positions in (deg.) 15,30,45,180,195,210,225,360	45
3.13	Plot of beamwidth for uniform circular array, final array and modified array versus N at $d=0.5\lambda$	46

3.14	Plot of Directivity for modified excitation circular antenna array with $N=12$ & $d=0.75\lambda$ versus amplitude excitation for selected elements, $Nr=2$ at $(\phi_1 = 30^\circ, \phi_7 = 210^\circ)$ and $Nr=4$ at $(\phi_1 = 30^\circ, \phi_5 = 150^\circ, \phi_7 = 210^\circ, \phi_{11} = 330^\circ)$	47
3.15	Plot of first and second Sidelobes level for modified excitation circular antenna array with $N=12$ & $d=0.75\lambda$ versus amplitude excitation for selected elements, $Nr=2$ at $(\phi_1 = 30^\circ, \phi_7 = 210^\circ)$ and $Nr=4$ at $(\phi_1 = 30^\circ, \phi_5 = 150^\circ, \phi_7 = 210^\circ, \phi_{11} = 330^\circ)$	47
3.16	Plot of beamwidth for modified excitation circular antenna array with $N=12$ & $d=0.75\lambda$ versus amplitude excitation for selected elements, $Nr=2$ at $(\phi_1 = 30^\circ, \phi_7 = 210^\circ)$ and $Nr=4$ at $(\phi_1 = 30^\circ, \phi_5 = 150^\circ, \phi_7 = 210^\circ, \phi_{11} = 330^\circ)$	48
3.17	Plot of AUC ratio for modified excitation circular Antenna array with $N=12$ & $d=0.75\lambda$ versus amplitude excitation for selected elements, $Nr=2$ at $(\phi_1 = 30^\circ, \phi_7 = 210^\circ)$ and $Nr=4$ at $(\phi_1 = 30^\circ, \phi_5 = 150^\circ, \phi_7 = 210^\circ, \phi_{11} = 330^\circ)$	48
3.18	Plot of first and second Sidelobes level for modified excitation circular antenna array with $N=24$ & $d=0.65\lambda$ versus amplitude excitation for selected elements, $Nr=2$ at $(\phi_1 = 15^\circ, \phi_{13} = 195^\circ)$, $Nr=4$ at $(\phi_1 = 15^\circ, \phi_2 = 30^\circ, \phi_{13} = 195^\circ, \phi_{14} = 210^\circ)$ $Nr=6$ at $(\phi_1 = 15^\circ, \phi_2 = 30^\circ, \phi_{12} = 180^\circ, \phi_{13} = 195^\circ, \phi_{14} = 210^\circ, \phi_{24} = 360^\circ)$ $Nr=8$ at $(\phi_1 = 15^\circ, \phi_2 = 30^\circ, \phi_3 = 45^\circ, \phi_{13} = 195^\circ, \phi_{14} = 210^\circ, \phi_{15} = 225^\circ, \phi_{16} = 240^\circ, \phi_{24} = 360^\circ)$	49
3.19	Plot of beamwidth for modified excitation circular antenna array with $N=24$ & $d=0.65\lambda$ versus amplitude excitation for selected elements, $Nr=2$ at $(\phi_1 = 15^\circ, \phi_{13} = 195^\circ)$, $Nr=4$ at $(\phi_1 = 15^\circ, \phi_2 = 30^\circ, \phi_{13} = 195^\circ, \phi_{14} = 210^\circ)$, $Nr=6$ at $(\phi_1 = 15^\circ, \phi_2 = 30^\circ, \phi_{12} = 180^\circ, \phi_{13} = 195^\circ, \phi_{14} = 210^\circ, \phi_{24} = 360^\circ)$ $Nr=8$ at $(\phi_1 = 15^\circ, \phi_2 = 30^\circ, \phi_3 = 45^\circ, \phi_{13} = 195^\circ, \phi_{14} = 210^\circ, \phi_{15} = 225^\circ, \phi_{16} = 240^\circ, \phi_{24} = 360^\circ)$	50

3.20	Plot of area under the curve ratio for modified excitation circular antenna array with $N=24$ & $d=0.65\lambda$ versus amplitude excitation for selected elements, Nr=2 at $(\phi_1 = 15^\circ, \phi_{13} = 195^\circ)$, Nr=4 at $(\phi_1 = 15^\circ, \phi_2 = 30^\circ, \phi_{13} = 195^\circ, \phi_{14} = 210^\circ)$ Nr=6 $(\phi_1 = 15^\circ, \phi_2 = 30^\circ, \phi_{12} = 180^\circ, \phi_{13} = 195^\circ, \phi_{14} = 210^\circ, \phi_{24} = 360^\circ)$ Nr=8 at $(\phi_1 = 15^\circ, \phi_2 = 30^\circ, \phi_3 = 45^\circ, \phi_{13} = 195^\circ, \phi_{14} = 210^\circ, \phi_{15} = 225^\circ, \phi_{16} = 240^\circ, \phi_{24} = 360^\circ)$	50
3.21	Geometry of reconfigure circular antenna array in x-y plane	51
3.22	a&b -Radiation pattern of 12-element uniform circular antenna array with radiation pattern of 12-element modified spacing between the two collinear selected elements	53
3.23	a&b -Radiation pattern of 12-element uniform circular antenna array with radiation pattern of 12-element for modified spacing between the two collinear elements and modified excitation for the same selected elements	54
3.24	Plot of first and second sidelobes level for $N=12$ modified circular array versus spacing between the two collinear elements at $(\phi_1 = 30^\circ, \phi_7 = 210^\circ)$	56
3.25	Plot of area ratio for $N=12$ modified circular array versus spacing between the two collinear elements at $(\phi_1 = 30^\circ, \phi_7 = 210^\circ)$	56
3.26	Plot of the improvement factor versus modified spacing between the two collinear elements at $(\phi_1 = 30^\circ, \phi_7 = 210^\circ)$	57
4.1	Geometry of concentric circular antenna array position in x-y plane	58
4.2	a&b -Radiation pattern for concentric circular array with inner ring of 4 elements and outer ring of 8 elements	63

4.3	a&b -Radiation pattern for concentric circular array with inner ring of 4 elements and outer ring of 10 elements	64
4.4	a&b - Radiation pattern for concentric circular array using 18 elements in two rings, inner ring of 6 elements and outer ring of 12 elements	65
4.5	a&b - Radiation pattern for concentric circular array using two rings with inner ring contains 10 elements and outer ring contains 14 elements	67
4.6	a&b -Radiation pattern for concentric circular array using(8 -16) element antenna for uniform array c --Radiation pattern for concentric circular array for (8-16) using modified amplitude excitation for element antenna	69,70
4.7	a&b -Radiation pattern for concentric circular array using (6-18) element antenna for uniform array, c -Radiation pattern for concentric circular array for (6-18) using modified amplitude excitation for specified elements	71,72
4.8	Plot of beamwidth for concentric circular antenna array versus spacing between the elements at $d1=d2$	75
4.9	Plot of ratio of area under the curve for different state of concentric circular antenna array versus spacing between the elements for ' $d1=d2$ '	75
4.10	Plot of directivity for different state of concentric circular antenna array versus spacing between the elements for ' $d1=d2$ '	76
4.11	Plot of sidelobes level versus spacing between the rings for a - uniform concentric circular array $N1=10, N2=14$ b - uniform concentric circular array $N1 =8, N2=16$ c - uniform concentric circular array $N1 =6, N2=18$	76,77

4.12	a- Plot of beamwidth for concentric circular antenna array versus spacing between the rings b- Plot of the beamwidth difference for concentric circular antenna array versus spacing between the rings	78
4.13	Plot of ratio of area under the curve for different state of concentric circular antenna array versus spacing between the rings	79
4.14	Plot of directivity for different state of concentric Circular antenna array versus spacing between the rings	79
4.15	Plot of sidelobes level versus spacing between therings for a- uniform concentric circular array $N_1=10, N_2=14$ b- uniform concentric circular array $N_1 =8, N_2=16$ c- uniform concentric circular array $N_1 =6, N_2=18$	81,82
4.16	Plot of beamwidth for concentric circular antenna array versus spacing between the rings.	82
4.17	Plot of ratio of area under the curve for different state of concentric circular antenna array versus spacing between the rings	83
4.18	Plot of directivity for different state of concentric circular antenna array versus spacing between the rings	83

List of Tables

Tab. No.	Table Description	Page No.
2-1	Maximum peak sidelobes level in dB and beamwidth for uniform linear broadside arrays at $d=0.5\lambda$.	10
2-2	Maximum peak sidelobes level in dB and beamwidth for uniform circular broadside arrays at $d=0.5\lambda$	25
2-3	Maximum sidelobes angular positions in degrees for uniform circular broadside arrays at $d=0.5\lambda$	25
2-4	Comparisons between the uniform linear array and uniform circular array of spacing between the elements $d=0.5\lambda$ in broadside array	26
3-1	Normalized amplitude excitation obtained from genetic algorithm for different number of elements in circular antenna array	30
3-2	Normalized amplitude excitations obtained from Modified excitation for selected the elements in circular antenna array	38

List of Symbols	
Symbol	Symbol Description
a	Radius of the circular ring in meter
a_m	Radius of ring m of the concentric circular ring in meter
a_n	Excitation coefficients (amplitude and phase) of n th element
d	Straight line inter-elements spacing in meter
d_{arc}	Arc line inter-elements spacing in meter
d_m	Inter-element spacing of concentric circular m th ring
d_1	Inter-elements spacing of inner ring in meter
d_2	Inter-elements spacing of outer ring in meter.
D	Directivity of antenna array.
D_i	Directivity of uniform antenna array
D_o	Directivity of obtained antenna array
E	Electric field
k	Wave number
N	Number of elements of an array
N_r	Number of elements selected of modified array
N_m	Number of elements in concentric circular ring
N_1	Number of elements in inner ring
N_2	Number of elements in outer ring
β	Progressive phase shift between the array elements
m	The running index
M	Number of concentric circular rings.
θ	Observation angle in degrees

θ_n	The n th null of the array pattern
θ_h	3dB angle location of the array factor
θ_s	Angular position of the minor lobes
ϕ	Angle in degrees in the azimuth plane perpendicular to the slot axis
ϕ_n	Angular position of n th element on x - y plane
ϕ_m	Angular position for the selected elements in the modified circular array
ϕ_{mn}	Angular position of concentric circular with respect to $\phi = 0^\circ$
$\Delta\phi_n$	Angular position difference between consecutive elements
I_n	Amplitude excitation of the n th element
I_r	Amplitude excitation of the selected the elements in modified array
I_{nm}	Amplitude excitation of concentric circular for n element of the m ring
α_n	phase excitation(relative to the array center) of the n th element
R_n	Distance from the n th element to the observation point
λ	Wavelength
ψ	Phase difference in the far field

List of Abbreviations	
CAA	Circular antenna array
UCAA	Uniform circular antenna array
CCAA	Concentric circular antenna array
UCCAA	Uniform concentric circular antenna array
BW	Beamwidth
BWi	Beamwidth of uniform antenna array
BW _o	Beamwidth of obtained antenna array
<i>HPBW</i>	Half power beamwidth
FSSL	First sidelobe level
FNBW	First null beamwidth
AUC	Area under the curve
$J_0(\rho k)$	Zero order Bessel function principal term
$AF_v(\theta, \phi)$	Array factor in vertical pattern
$AF_h(\theta, \phi)$	Array factor in horizontal pattern
$AF_{Nr}(\theta, \phi)$	Array factor of selected elements for modified array
$AF_{mod}(\theta, \phi)$	Array factor of modified excitation array
$AF_r(\theta, \phi)$	Array factor of modified spacing between two collinear elements

CHAPTER ONE

Introduction

1.1- General Consideration:

An antenna is a transducer that converts electric currents into electromagnetic waves which are radiated into the free space making the antenna as an essential component in any wireless communication system. In many applications it is necessary to design antennas with good directivity to meet the demands of less interfering signals and of long communication distance. A large number of antenna designs have been done to achieve a reduced sidelobes with good directivity. These demands can be achieved by using array of antennas. Array of antennas have been widely used specially in radar, sonar, and wireless communications. Array of antennas can provide the capability of steerable beams in smart antennas. Such antennas are composed of a number of sources arranged in one of the forms (linear, circular, rectangular...). [1]. In circular array of a uniform distribution, it is possible to have a high gain, but the sidelobes level is relatively high, the first sidelobe is at -8dB.

The high level of the sidelobes is responsible for interferences with the main signal in many applications of antennas. Design techniques that gives low sidelobes level are desirable. Changing the parameters of the array such as amplitude excitation, phase excitation of elements and space between the elements will help in reducing the sidelobes level of the array pattern. There are many techniques that can be used

to change the performance of the array. Genetic algorithm, particle swarm optimization, invasive weed optimization and differential evolution etc. In this work genetic algorithm technique, non-uniform excitations for certain specified elements and concentric circular array of two rings were used to obtain a reduced sidelobes level in the radiation pattern of the circular array.

1.2 -Historical Review:

Since the radiation pattern of the antenna array suffers from high sidelobes level, pattern synthesis is the necessary process of choosing the antenna parameters to obtain the desired radiation pattern.

In literature, there are many works concerned with the synthesis of antenna array. In 1967 Cockrell and Crosswell utilized general method for designing circular array antennas to obtain quasi-omnidirectional patterns [2]. In 1978 Hodjat et al. used non-uniformly spaced uniformly excited linear and planar arrays of antennas for sidelobes reduction. He used the iterative method to solve a set of linear equations for establishing the spaces between the elements [3].

In 1980 Tseng used a technique of producing an array pattern that posses a reduced sidelobes and a deep null in certain direction. He discussed the effect of sidelobes on the noise and interferences [4]. In 1990 Hassan used the principle of non-uniformly spaced array to obtain the desired radiation pattern. He obtained a radiation pattern approximately similar to that of Chebyshev array [5].

In 1994 Anderson et al. used genetic algorithmic in element position perturbation for obtaining nulling in the pattern [6].

In 1996 he used genetic algorithm for antenna pattern synthesis and sidelobe reduction. This technique, takes to consideration the effects of mutual coupling between the array elements [7]. In 1997 Yan and Yilong utilized genetic algorithm for sidelobe reduction in linear array-pattern. This approach avoids coding, and directly deals with real or complex excitation vectors[8]. In 1999 Kumar and Branner designed unequally spaced arrays utilizing a simple inversion algorithm to obtain the element spacing from prescribed far-zone electric field and current distribution[9].In 2003 Dennis and Yahya Rahmat used particle swarm optimization algorithm for reconfigurable phase differentiated array design [10].In 2006 Dessouky, M. et al. used efficient sidelobe reduction technique for small-size concentric circular arrays [11].

In 2008 Sayidmarie et al. used Position perturbation of the array elements for reducing the sidelobe structure in the radiation pattern of phased arrays. The obtained results of computer simulations showed good improvements in the sidelobe structure as compared to the equal size linear array [12]. In the same year Najjar Y. et al. designed a non-uniform excitation of circular antenna array with optimum reduction of sidelobes level using particle swarm optimization (PSO) method. This method used to determine an optimum set of weights and antenna element separations that provide a radiation pattern with maximum sidelobe reduction [13].

In 2009 Zuniga, V. et al. made a modification of the circular array geometry by placing antenna element in the center of the array. By adjusting the phase of the central element, this modification in the

geometry of the circular array showed good performance in the directivity and beamwidth of the array pattern[14].

In 2010 Mandal et al. designed a three concentric circular array with maximum reduction in sidelobes level. He used particle swarm optimization method for three successive concentric rings[15].In the same year Siddharth et al. used a differential invasive weed optimization algorithm to reduce the sidelobes level and the major lobe beamwidth as much as possible [16].In 2011 Das et al. synthesized broadside uniform circular antenna array along with the resting plane. It has been shown analytically that, good performance of the on-resting plane array pattern was obtained with proper choice of the number of elements and radius of the array [17]. In 2011 Singh and Kamal used biogeography-based optimization to find out an optimal set of weights and antenna element separations to provide a radiation pattern with maximum sidelobes level reduction[18].In 2012 Ghosh et al. used evolutionary algorithm to achieve minimum sidelobes level for a specific first null beam-width and also a minimum size of the circumference by an optimization-based design method for non-uniform excitation circular antenna arrays [19].

In 2013 Reddy et al. used artificial neural networks to design a circular antenna array for a given gain and beamwidth by finding the parameters of the radiation pattern of a uniform circular antenna array. The designed model has given a quick speed of convergence and improved accuracy [20].In 2014 Albagory used Kaiser Window to design uniform concentric circular arrays for sidelobes reduction. This technique is based on tapering the current amplitudes of the rings in the array,

whereas all elements in an individual ring are weighted in amplitude by the same value. Based on establishing some mapping curves, this novel tapering window is optimized in its parameters to have the lowest possible sidelobes level [21]. In the same year Mohab A. et al. designed circular arrays and hexagonal arrays with low sidelobes level and high directivity by increasing the number of array elements, which leads to a high undesired mutual coupling. Also he designed multi-ring concentric and concentric configurations using a hybrid enhanced particle swarm optimization and differential evolution optimization technique. The presented optimum concentric circular array and concentric hexagonal array have perfect invariant sidelobes level and high directivity with low mutual coupling by keeping the inter-element spacing not less than half a wavelength which is not possible to be achieved in circular array and hexagonal array arrangements [22].

In 2015 Rezioui used differential search algorithm for synthesizing a one-and a three-ring circular and concentric circular antenna array with thirty elements. This synthesis is done by finding the optimum inter-element spacing of rings, phases and positions that give optimum sidelobes level. [23].

In 2016 Raju et al. used differential evolution algorithm for sidelobes level reduction for concentric ring arrays by amplitude only synthesis method along with thinning the array at the same time. A differential evaluation algorithm is employed for obtaining optimum array configurations. [24].

In 2017 Mohammed & Sayidmarie, used a controlled edge elements for synthesizing asymmetric sidelobe pattern with steered nulling in

non-uniformly excited linear array. Therefore the difference in the sidelobes level on both sides of the main beam is achieved by varying the phase excitations of the two-edge elements[25].

1.3 -Aim of the Work:

In this work genetic algorithm technique is presented for sidelobe reduction in circular antenna array. Genetic algorithm is used to obtain an optimized weights for the elements used to design a reduced sidelobes level in circular array. A modification method for an existing circular antenna array is introduced here and it is shown that larger reduction in the sidelobes level is obtained. Concentric circular antenna array of two rings is also presented in this work for reducing the sidelobes level, and it is shown that good result is obtained as compared to a circular array of the same number of elements.

1.4-Scope of the Dissertation:

This dissertation consists of five chapters. Chapter two covers the antenna array analysis.

In Chapter three, the results of using genetic algorithm, modified excitations and modified radial distance of the selected elements in circular antenna array for sidelobes reduction are covered.

Chapter four covers the results of using concentric circular array of two rings for sidelobes reduction in circular array.

Chapter five gives the conclusions obtained from this work and lists of some suggestions for future work.

CHAPTER TWO

Study and Analysis of Antenna Arrays

2.1 Introduction:

A large variety of antenna have been developed starting from simple structures such as monopoles and dipoles to complex structures such as phased arrays. The radiation pattern of a single element antenna is very wide and it provides low value of directivity. High value of directivity can be achieved by increasing the size of the antenna. Another way of increasing the directivity is to enlarge an antenna by considering a set of individual elements in a geometrical configuration this arrangement is known as antenna array [1]. It is convenient that the elements of the array are identical to enable a simpler analysis and design. Antenna array has an important role in detecting and processing signals arriving from different directions. Antenna arrays are preferred over single element antenna in the values of its directivity and bandwidth. Antenna arrays overcome the low directivity and high beamwidth associated with the single element. Design of any structure of antenna array is basically accomplished in finding the allocation of the array elements and its weights in the configuration used. The total field of the array is determined by the vector addition of the fields radiated by the individual elements. The pattern of the antenna array, to be more directives in the desired direction, the individual fields of the array added constructively and interfere destructively in the remaining space. In an antenna array of

identical elements, the controls that can be used to obtain the desired pattern of the antenna are:

1. General array shape (linear, circular, planar, etc.).
2. Elements spacing.
3. Elements excitation amplitude.
4. Elements excitation phase.
5. Patterns of array elements.

2.2 Linear antenna array:

In linear antenna arrays all the elements are positioned in one-dimensional form as shown in Fig. (2.1).

In the uniform array, all the elements have identical magnitudes with β progressive phase lead current excitation relative to the preceding one. The array factor can be obtained by considering the elements to be isotropic sources. In terms of the inter-element spacing which is assumed to be uniform across the array, the array factor for the N-element array is given by:

$$AF(\theta) = \sum_{n=1}^N I_n e^{j(n-1)(kd \cos(\theta) + \beta)} \dots\dots\dots (2.1)$$

$k = 2\pi/\lambda$ is the wave number, λ is the wavelength, d is the displacement between the elements, ' θ ' is the angular position of the field point and β is the progressive phase excitation difference between the elements [1].

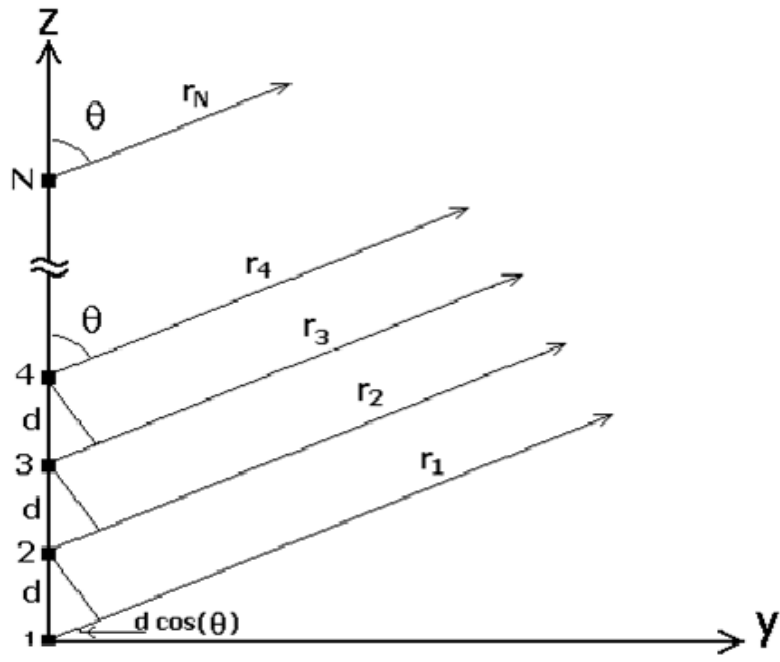
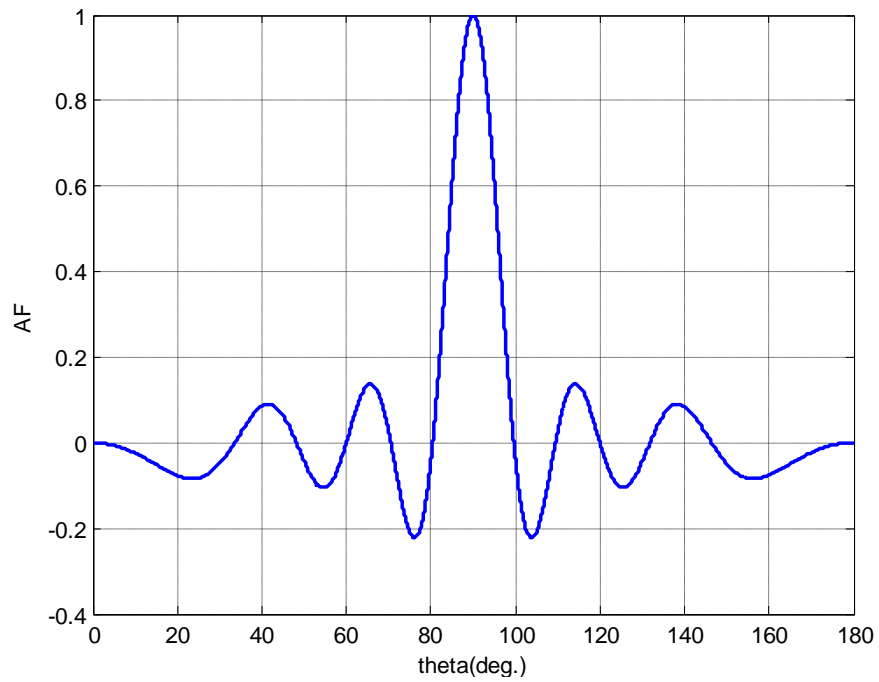
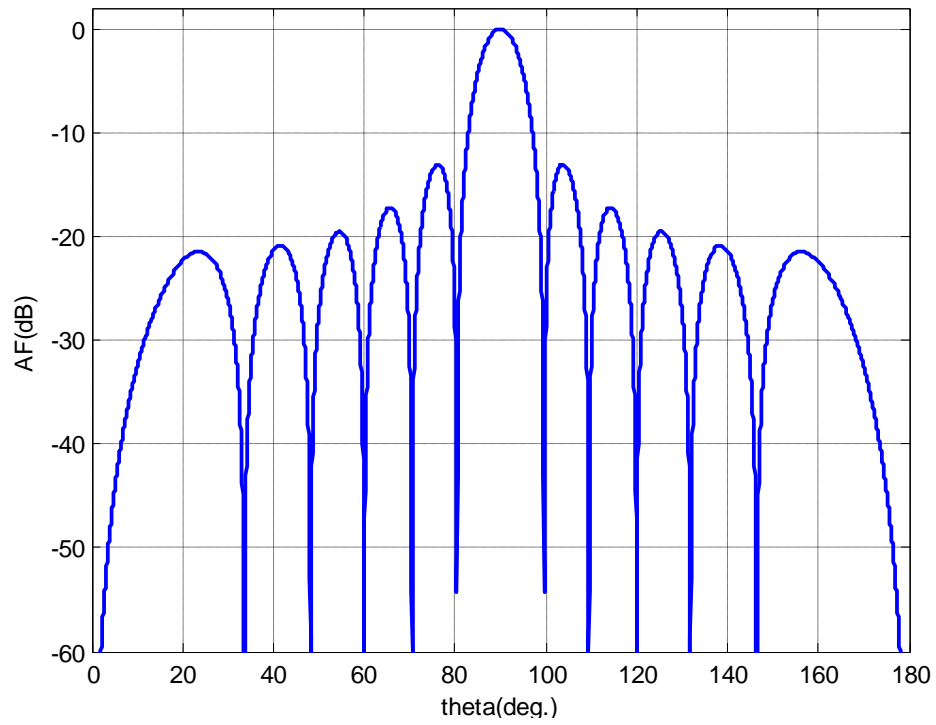


Fig. (2.1) Linear antenna array of N elements positioned along z - axis.



-a-



-b-

Fig. (2.2) a&b- Plot of the array factor for 12-element uniformly excited linear array pattern.

Table 2.1 Maximum peak sidelobes level in dB and beamwidth for uniform linear broadside arrays at $d=0.5\lambda$.

N	Bwi	1st	2nd	3rd	4th	5th
8	12.9°	-12.8	-16.43	-17.8	0	0
12	8.5°	-13.06	-17.2	-19.5	-20.9	0
18	5.6°	-13.21	-17.5	-20.2	-22	-23
24	4.2°	-13.22	-17.6	-20.5	-22.4	-23.9

Table (2.1) gives results regarding the information about beamwidth and level of sidelobes for spacing between the elements $d = 0.5\lambda$ and different number of elements 'N'.

Figure (2.3) shows the beamwidth plot of a uniform broadside linear array of isotropic elements versus spacing between the elements $d(\lambda)$ for different values of 'N'. It is clear from the plot that the beamwidth decreases with the increasing elements number 'N', and it is inversely proportional with spacing between the elements 'd'.

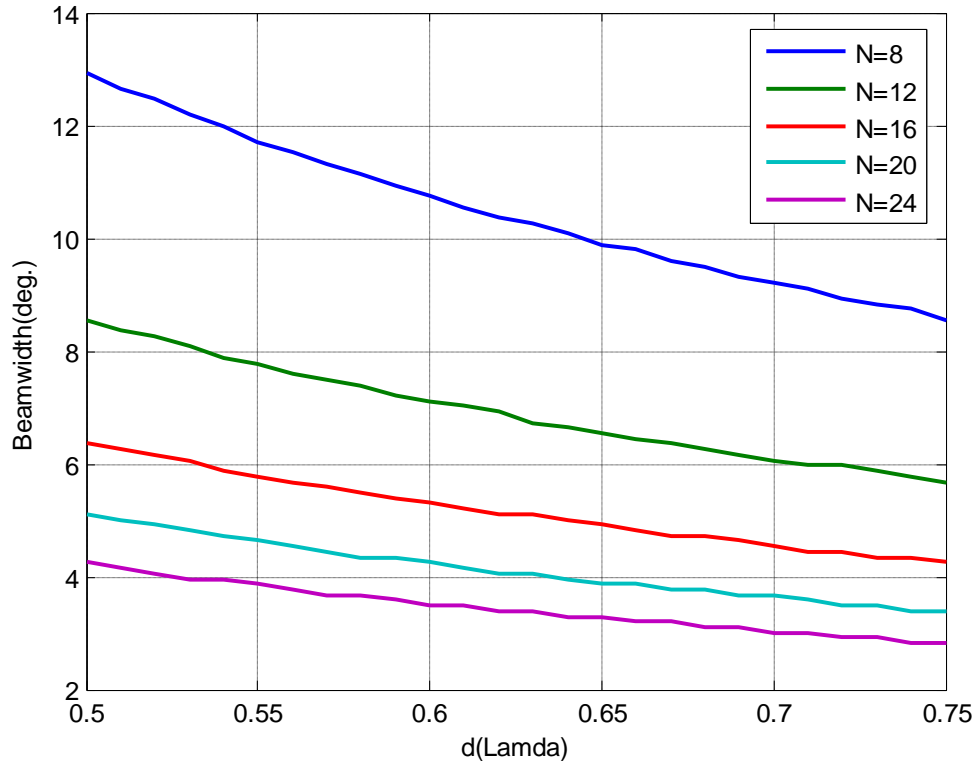


Fig. (2.3) Plot of beamwidth for linear antenna array versus $d(\lambda)$ for different values of N.

2.3- Directivity of the Array Antenna:

Directivity gives a measure for the ability of the antenna to direct its power towards a given direction; the directivity is a figure-of-merit describing how well the radiator directs energy in a certain direction. The directivity of an antenna is defined as the ratio of the radiation intensity in a given direction from the antenna to the radiation intensity averaged over all directions.

Figure (2.4) shows the directivity plot of a uniform broadside linear array of isotropic elements versus spacing between the elements $d(\lambda)$ for different values of 'N'. It is clear from Fig. (2.4) that the directivity equals 'N' at integer multiples of half-wavelength. From the directivity curves for each value of 'N' we note that the directivity curve takes steep decline for integer multiple of wavelength between the elements due to the emergence of grating lobes into the visible region.

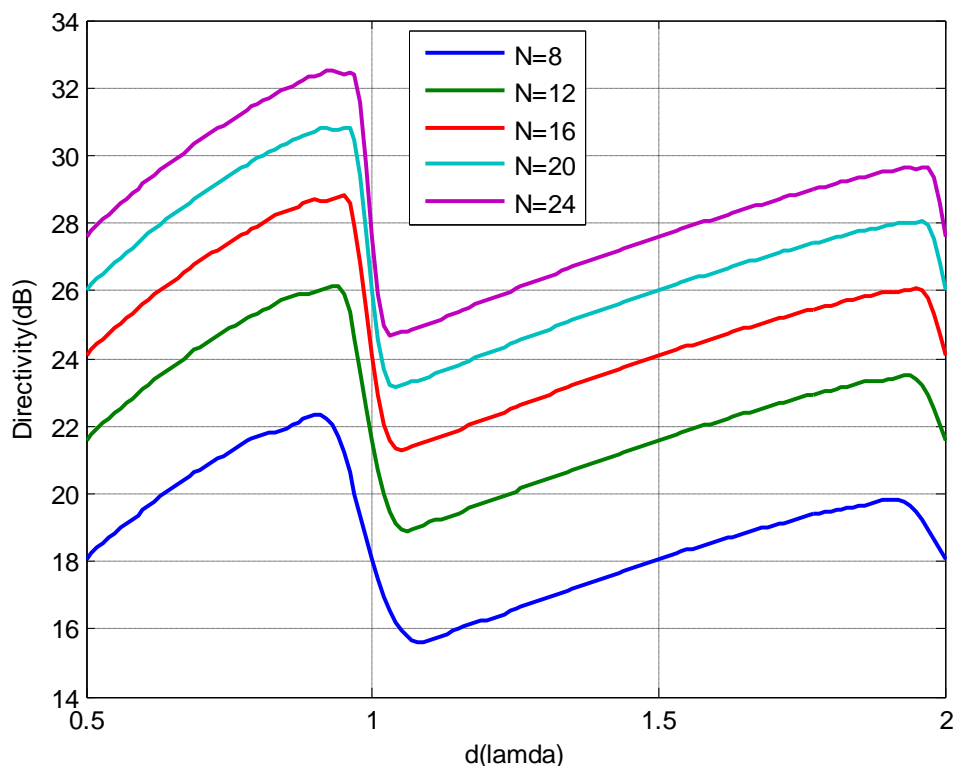


Fig. (2.4) Directivity for uniform linear array versus d for different number of the elements.

2.4 Circular antenna Array:

One of many antenna array geometries is the circular antenna arrays. The elements of the array lie in two dimensions. Its applications include space navigation, underground propagation, radar, sonar, radio direction finding, mobile and commercial satellite

communications systems [26-29]. The advantage of circular antenna array is its ability to steering the main beam electronically through all azimuth angles without any change in the beamwidth and sidelobes level [26]. The radiation pattern of a circular array depends on the radius of the circular antenna array, number of elements in the array, excitation and phase of each element that constitute the array. In the uniform antenna array, all the elements have identical magnitudes and each succeeding element has a progressive phase leading current excitation relative to the preceding one. Fig. (2.5) shows a circular array consisting of N -element that are allocated on a circle of radius a in the x - y plane.

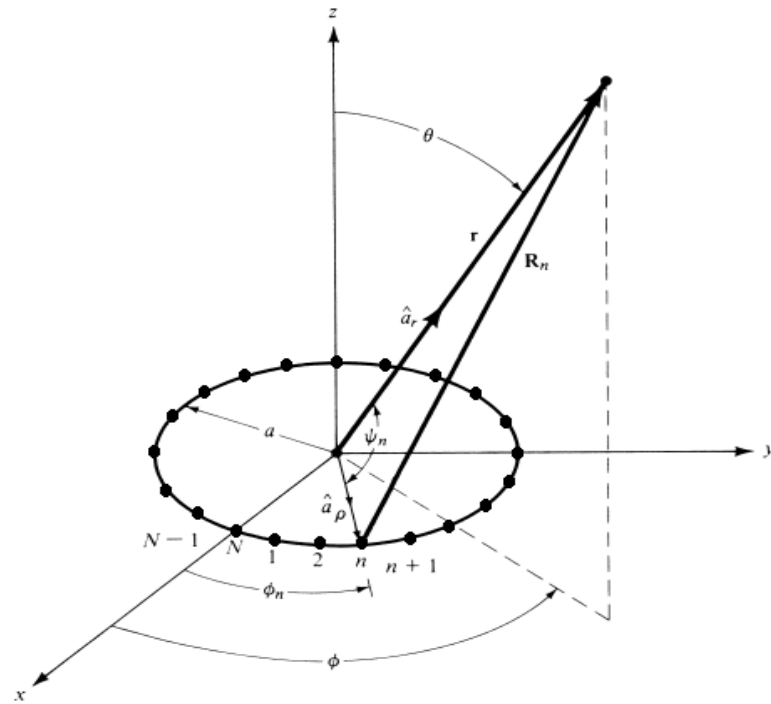


Fig. (2.5) Geometry of circular antenna array of N elements positioned in x - y plane.

Array Factor of circular antenna array:

Consider N isotropic radiators distributed in circular ring of radius a placed in x-y plane. The origin of the coordinate system is located at the center of the array. The array factor can be obtained by considering the elements to be isotropic sources. If the actual elements are not isotropic sources, the total field can be formed by multiplying the array factor of the isotropic sources by the field of the single element. This is known as the pattern multiplication rule, and it applies only for arrays of identical elements.

The array factor of N-element array shown in Fig. (2.5) can be given by:

$$E_n = \sum_{n=1}^N a_n \frac{e^{-jkR_n}}{R_n} \dots\dots\dots (2.2)$$

$$R_n = r - a \sin(\theta) \cos(\phi - \phi_n) \dots\dots\dots (2.3)$$

Where R_n is the distance from the nth element to the observation point (θ) , (ϕ) elevation and azimuth angle respectively.

Let the linear distance between two consecutive elements is d as shown in Fig. (2.6).

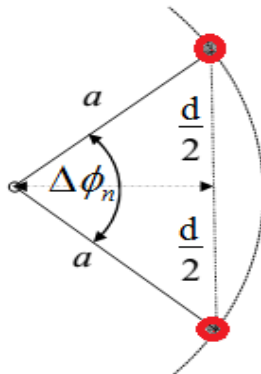


Fig.(2.6) Section of the circular antenna shows two consecutive elements of the array on the arc of a circle

Angular position difference between consecutive elements is [18].

$$\Delta\phi_n = \phi_n - \phi_{n-1} = \frac{2\pi}{N}$$

From the Fig. (2.6) and the geometry of a circle, the following relation can be written,

$$\sin \frac{\Delta\phi_n}{2} = \frac{d}{2a}$$

$$a = \frac{d}{2 \sin \frac{\pi}{N}}$$

Where a is the radius of the circular antenna array.

a_n is the excitation coefficient of the n th element, I_n amplitude excitation of the n th element, α_n phase excitation (relative to the array center) of the n th element.

$$a_n = I_n e^{j\alpha_n} \dots\dots\dots (2.4)$$

The angular position of the n th element ϕ_n on the resting plane is given by:

$$\phi_n = \frac{2\pi n}{N}, \quad n = (1,2,3,\dots, N) \dots\dots\dots (2.5)$$

For amplitude variations $R_n = r$, then the equation (2.2) can be written as:

$$E_n(r, \theta, \phi) = \frac{e^{-jkr}}{r} \sum_{n=1}^N a_n e^{+jka \sin(\theta) \cos(\phi - \phi_n)} \dots\dots\dots (2.6)$$

$$E_n(r, \theta, \phi) = \frac{e^{-jkr}}{r} [AF(\theta, \phi)] \dots\dots\dots (2.7)$$

Then the array factor can be written as:

$$AF(\theta, \phi) = \sum_{n=1}^N I_n e^{j(ka \sin \theta \cos(\phi - \phi_n) + \alpha_n)} \dots\dots\dots (2.8)$$

Equation (2.8) represents the array factor of a circular array of N equally spaced elements. To direct the peak of the main beam in the (θ_0, ϕ_0) direction, the phase excitation of the nth element can be chosen to be

$$\alpha_n = -ka \sin \theta_0 \cos(\phi_0 - \phi_n), \quad n = 1, 2, \dots, N \quad \dots\dots\dots (2.9)$$

Thus, the array factor can be written as.

$$AF(\theta, \phi) = \sum_{n=1}^N I_n e^{jka[\sin \theta \cos(\phi - \phi_n) - \sin \theta_0 \cos(\phi_0 - \phi_n)]} \dots\dots\dots (2.10)$$

$$AF(\theta, \phi) = \sum_{n=1}^N I_n e^{jka[\cos \psi - \cos \psi_0]} \dots\dots\dots (2.11)$$

To reduce equation (2.11) to a simpler form we define ρ as

$$\rho = a \left[(\sin \theta \cos \phi - \sin \theta_0 \cos \phi_0)^2 + (\sin \theta \sin \phi - \sin \theta_0 \sin \phi_0)^2 \right]^{1/2} \dots\dots\dots (2.12)$$

The exponential in equation (2.11) takes the form of

$$ka(\cos \psi - \cos \psi_0)$$

$$= \frac{k\rho[\sin \theta \cos(\phi - \phi_n) - \sin \theta_0 \cos(\phi_0 - \phi_n)]}{[(\sin \theta \cos \phi - \sin \theta_0 \cos \phi_0)^2 - (\sin \theta \sin \phi - \sin \theta_0 \cos \phi_0)^2]^{1/2}} \dots\dots\dots (2.13)$$

Which when expanded reduced to

$$ka(\cos \psi - \cos \psi_0) = k\rho \left\{ \frac{\cos \phi_n (\sin \theta \cos \phi - \sin \theta_0 \cos \phi_0) + \sin \phi_n (\sin \theta \sin \phi - \sin \theta_0 \sin \phi_0)}{[(\sin \theta \cos \phi - \sin \theta_0 \cos \phi_0)^2 - (\sin \theta \sin \phi - \sin \theta_0 \cos \phi_0)^2]^{1/2}} \right\} \dots\dots\dots (2.14)$$

Defining

$$\cos \gamma = \frac{\sin \theta \cos \phi - \sin \theta_0 \cos \phi_0}{(\rho/a)} \dots\dots\dots (2.15)$$

$$\sin \gamma = [1 - \cos^2 \gamma]^{1/2}$$

$$\sin \gamma = \frac{\sin \theta \sin \phi - \sin \theta_0 \sin \phi_0}{[(\sin \theta \cos \phi - \sin \theta_0 \cos \phi_0)^2 - (\sin \theta \sin \phi - \sin \theta_0 \cos \phi_0)^2]^{1/2}} \dots\dots\dots (2.16)$$

Thus equation (2.14) and equation (2.11) can be rewritten, respectively as

$$ka(\cos \psi - \cos \psi_0) = k\rho(\cos \phi_n \cos \gamma + \sin \phi_n \sin \gamma) \\ ka(\cos \psi - \cos \psi_0) = k\rho \cos(\phi_n - \gamma) \dots\dots\dots (2.17)$$

$$AF(\theta, \phi) = \sum_{n=1}^N I_n e^{jka(\cos \psi - \cos \psi_0)} = \sum_{n=1}^N I_n e^{jk\rho \cos(\gamma - \phi_n)} \dots\dots\dots (2.18)$$

For a uniform amplitude excitation of each element ($I_n = I$) and equally space between the elements the equation (2.18) can be written as:

$$AF(\theta, \phi) = NI \sum_{m=-\infty}^{\infty} \exp \left[jmN \left(\frac{\pi}{2} - \gamma \right) \right] J_{mN}(k\rho) \dots\dots\dots (2.19)$$

Where m is the running index.

The term with the zero-order Bessel function $J_0(\rho k)$ is called the principal term, and the rest are residuals. For a circular array with a large number of elements, the term $J_0(\rho k)$ alone can be used to approximate the two-dimensional principal-plane patterns. The remaining terms in (2.19) contribute negligibly because Bessel functions of larger orders are very small [1, 30].

2.5 -Vertical pattern for circular antenna array:

From equation above for vertical pattern in broadside array where $(\theta_0 = 0, \phi_0 = 0)$, we have.

$$\alpha_n = 0$$

$$\rho_{vertical} = a \sin \theta$$

$$\cos \gamma = \cos \phi$$

$$\therefore \gamma = \phi$$

Array factor in equation (2.19) can be represented as:

$$AF_v(\theta, \phi) = NI \sum_{m=-\infty}^{\infty} \exp \left[jmN \left(\frac{\pi}{2} - \phi \right) \right] J_{mN}(ka \sin \theta) \dots\dots\dots (2.20)$$

2.5.1-Nulls of the vertical Pattern:

To find the nulls of the vertical pattern, the term of the array factor in Eq. (2.20) is set to zero, ($J_{mN}(k a \sin \theta) = 0$) which gives the nulls at.

$$k a \sin \theta = x, \quad x = (2.4, 5.5, 8.6, 11.6, 14.9, \dots)$$

$$\theta_n = \sin^{-1} \left(\frac{x \lambda}{N d_{arc}} \right) = \sin^{-1} \left(\frac{x \lambda}{2 \pi a} \right)$$

The number of nulls that can exist will be a function of the element spacing d_{arc} and the number of elements N.

2.5.2- Maxima of Minor Lobes of the vertical Pattern:

The maximum of the minor lobes occurs approximately when the term $J_{mN}(k a \sin \theta) = \pm 1$ of Eq. (2.20), that is:

$$k a \sin \theta = s, \quad s = (3.8, 7, 10, 13, \dots)$$

$$\theta_s = \sin^{-1} \left(\frac{s \lambda}{N d_{arc}} \right)$$

2.5.3- HPBW of the Major Lobe of the vertical Pattern:

The Half Power Beamwidth (HPBW) of the main lobe can be calculated by setting the value of the array factor to its 3dB point i.e. $AF = 0.707$, which leads to:

$$k a \sin \theta = 1.14$$

$$\theta_h = \sin^{-1} \left(\frac{1.14 \lambda}{N d_{arc}} \right).$$

For a symmetrical pattern around the angle of maximum radiation, the HPBW can be calculated as:

$$HPBW = 2 \theta_h$$

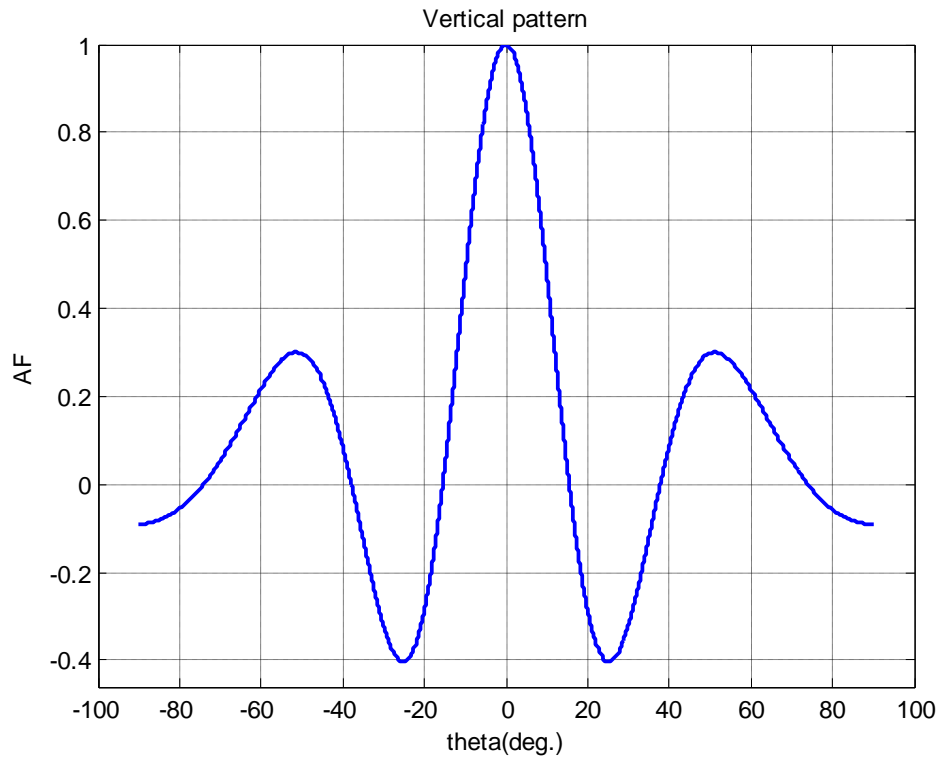


Fig. (2.7) plot of vertical pattern of circular antenna array for $N = 12, d = 0.75\lambda$

2.6-Horizontal pattern for circular antenna array:

For the horizontal (azimuth) pattern $\left(\theta_0 = \frac{\pi}{2}, \phi_0 = 0\right)$ we have

$$\alpha_n = -ka \cos \phi_n$$

$$\rho_{horizontal} = 2a \sin \frac{\phi}{2}$$

$$\cos \gamma_{horizontal} = -\sin \frac{\phi}{2}$$

$$\therefore \gamma_{horizontal} = \frac{\pi + \phi}{2}$$

$$AF_h(\theta, \phi) = NI \sum_{m=-\infty}^{\infty} \exp\left(\frac{-jmN\phi}{2}\right) J_{mN} \left(2ka \sin \frac{\phi}{2}\right) \dots\dots\dots (2.21)$$

2.6.1-Nulls of the horizontal Pattern:

To find the nulls of the horizontal pattern, the term of the array factor $J_{mN}\left(2ka\sin\frac{\phi}{2}\right)$ in Eq. (2.21) is set to zero.

$(J_{mN}\left(2ka\sin\frac{\phi}{2}\right)=0)$ which gives nulls at.

$$2ka\sin\frac{\phi}{2} = x, \quad x = (2.4, 5.5, 8.6, 11.7, 14.6, 18.1, 21.2, 24.3, 27.5, \dots)$$

$$\phi_n = 2\sin^{-1}\left(\frac{x\lambda}{2Nd_{arc}}\right)$$

The number of nulls that can exist will be a function of the element spacing d , and the number of elements N .

2.6.2- Maxima of Minor Lobes of the horizontal Pattern:

The maximum of the minor lobes occurs approximately when the term $J_{mN}\left(2ka\sin\frac{\phi}{2}\right) = \pm 1$ of Eq. (2.21) attains maxima, that is:

$$2ka\sin\frac{\phi}{2} = s, \quad s = (3.8, 7, 10, 13, \dots)$$

$$\phi_s = 2\sin^{-1}\left(\frac{s\lambda}{2Nd_{arc}}\right)$$

2.6.3- The HPBW of the Major Lobe of the horizontal Pattern:

The Half Power Beamwidth (HPBW) of the main lobe can be calculated by setting the value of the array factor to its 3dB point i.e. $AF = 0.707$, which leads to:

$$2ka\sin\frac{\phi}{2} = 1.14$$

$$\phi_h = 2\sin^{-1}\left(\frac{0.57\lambda}{Nd_{arc}}\right).$$

For a symmetrical pattern around the angle of maximum radiation, the HPBW can be calculated as:

$$\text{HPBW} = 2 \phi_h$$

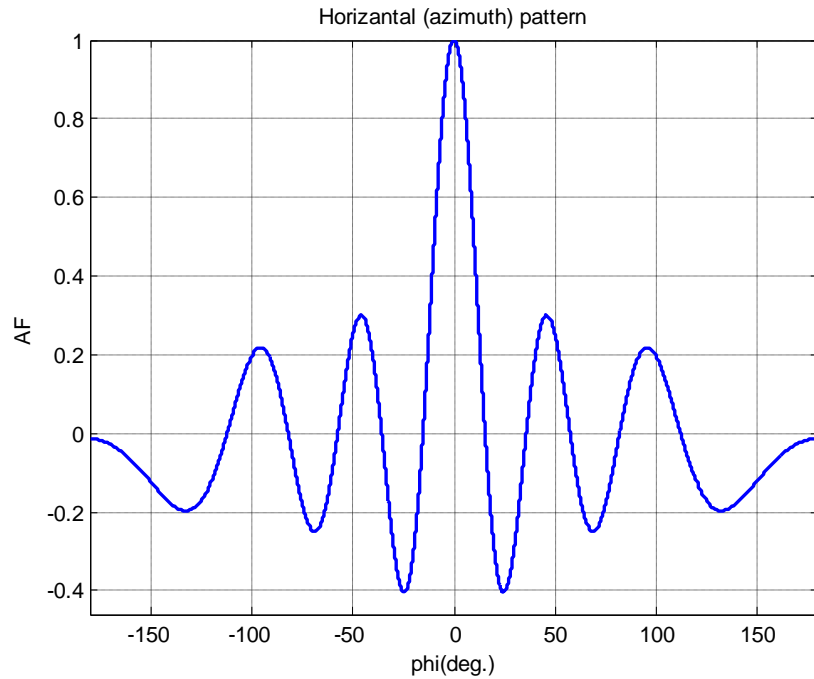


Fig. (2.8) plot of horizontal pattern of circular antenna array for $N = 12, d = 0.75\lambda$

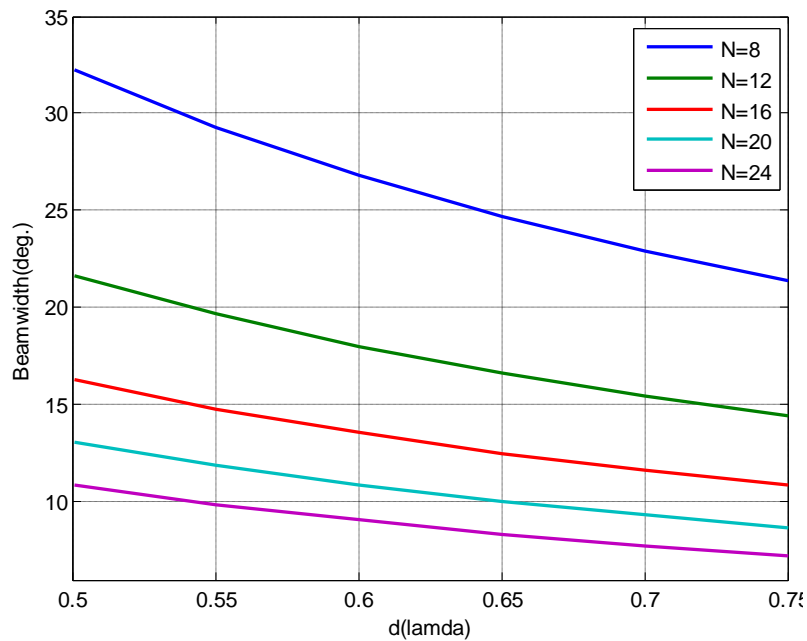


Fig. (2.9) Plot of beamwidth for circular antenna array versus $d(\lambda)$ for different values of N.

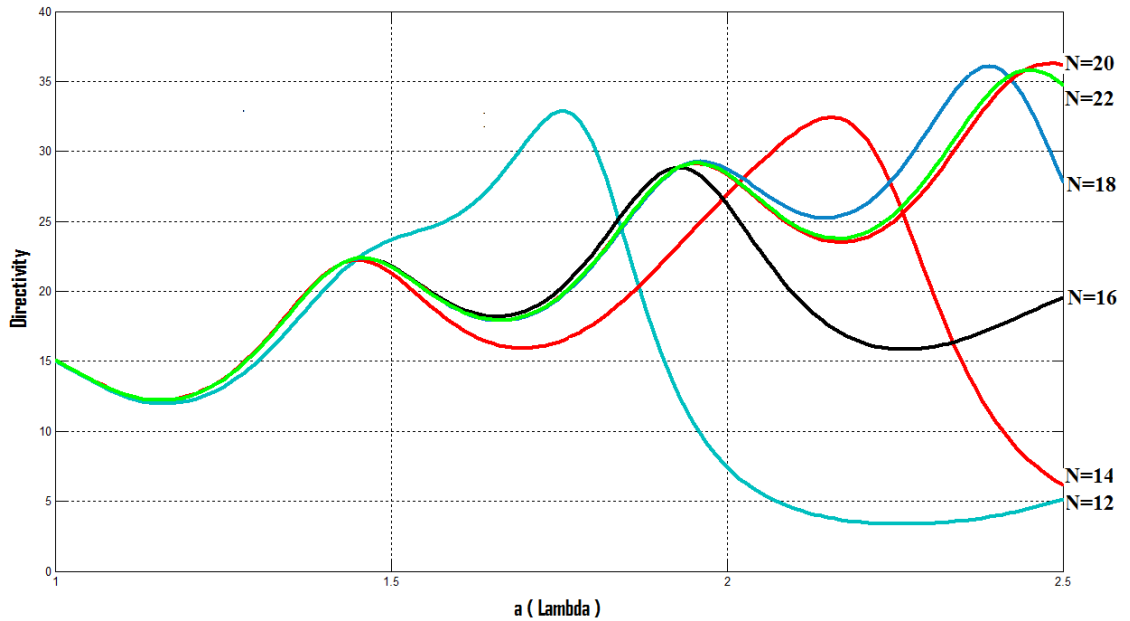


Fig. (2.10) Directivity for uniform circular array versus radius $a(\lambda)$ for different number of elements.

Figure (2.9) shows the beamwidth plot of a uniform circular broadside array of isotropic elements versus spacing between the elements $d(\lambda)$ for different values of 'N'. It is clear from the plot that the beamwidth decreases with the increasing element number 'N' and decrease also with the increasing of the separation between the elements.

Figure (2.10) shows the directivity plot of a uniform circular broadside array of isotropic elements versus radius of the circular antenna $a(\lambda)$ for different values of 'N'.

The plot shows peaks of directivity for each value of N at difference Values of $a(\lambda)$.

Figure (2.11) shows the plots of the null positions and peaks of 1st and 2nd sidelobes versus the spacing between the elements for a uniform circular broadside array of isotropic elements.

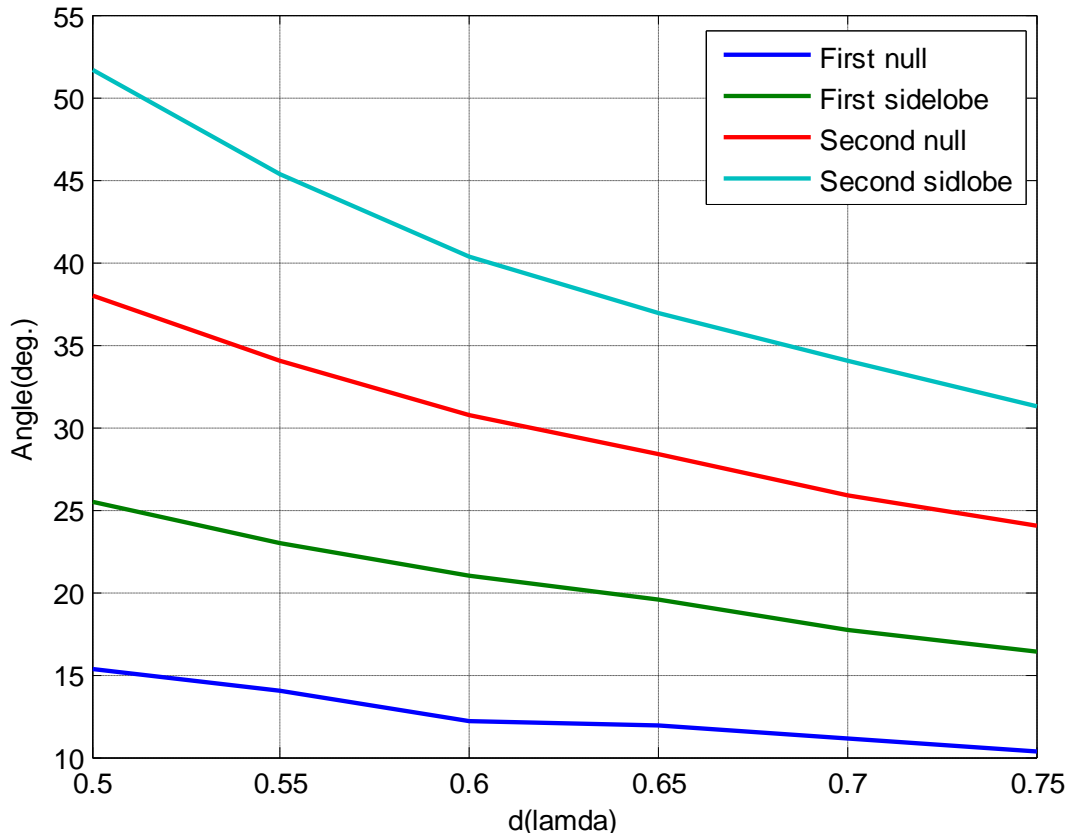


Fig. (2.11) Angular positions of 1st, 2nd null and sidelobes for 18 elements uniform circular array versus elements spacing $d(\lambda)$

2.7- Results of a Uniform circular Array:

In this section, simulations are carried out with various numbers of elements. Tables (2.2) and (2.3) gives results regarding the information about the sidelobes level and sidelobe angular positions in degrees for spacing $d=0.5\lambda$ between the elements for different elements number N. Table (2.4) gives results regarding comparisons between the uniform linear array and uniform circular array at spacing between the elements $d=0.5\lambda$ for different element number N in broadside array.

Table 2.2 Maximum peak sidelobes level in dB for uniform circular broadside arrays at $d=0.5\lambda$.

N	1st	2nd	3rd	4th	5th
8	-8.122				
12	-7.899	-16.39			
18	-7.9	-10.45	-20.88		
24	-7.902	-10.47	-12.05	-26.44	
30	-7.956	-10.53	-12.07	-13.22	-37

Table 2.3 Maximum sidelobe angular positions in degrees for uniform circular broadside arrays at $d=0.5\lambda$

N	1st	2nd	3rd	4th	5th
8	72				
12	39.9	89.6			
18	25.1	51.6	89.6		
24	18.6	35.5	57.5	89.6	
30	14.7	27.8	42.5	62.5	89.7

Table 2.4- Comparisons between the uniform linear array and uniform circular array of spacing between the elements $d=0.5\lambda$ in broadside array.

Array type	N	FSL(dB)	BW(deg.)	Di	FNBW(deg.)
Uniform linear array	12	-13.07	8.5	12	19
	18	-13.18	5.6	18	12.7
	24	-13.23	4.2	24	9.6
Uniform circular array	12	-7.9	21.9	15.4	47.4
	18	-7.9	14.5	22.1	31
	24	-7.9	10.9	28.2	23.1

CHAPTER THREE

Sidelobes Level Reduction of Circular Antenna Array Using Genetic Algorithm

3.1 Introduction:

In the antenna array, the minor lobes of the radiation pattern represent radiation in the undesired directions. Sidelobes level is normally the largest of the minor lobes which causes losses of energy and interface noise signals. Many applications such as radar and communication systems are highly affected by the interfering signals, caused by the high level of sidelobes. Therefore, low sidelobes level is very important to minimize false target indication. Sidelobes level smaller than -30 dB usually requires very careful design and construction [1].

3.2- Genetic algorithm:

A genetic algorithm is basically a probabilistic search algorithm based on the principles and concept of selection and evolution. The evolution usually starts from a population of randomly generated individuals, and is an iterative process, with the population in each iteration called a generation. Each generation is evaluated by a function known as fitness function. Next, new population is generated from the present one through selection, crossover and mutation operations. The purpose of selection mechanism is to select more fit individuals (parents) for crossover and mutation. Crossover causes the exchange of genetic materials between the parents to form offspring, whereas mutation incorporates new genetic material in the offspring.

Commonly, the algorithm terminates when either a maximum number of generations has been produced, or a satisfactory fitness level has been reached for the purpose for which the genetic algorithm was used [31,32].

3.2.1 – Sidelobes level reduction using genetic algorithm:

Reduction of sidelobes level of a circular antenna array can be achieved by using non-uniform amplitude of the excitation currents, phase altering of the excitation currents and distance perturbation between the elements. Here, we used non-uniform excitations for the circular array to achieve sidelobes reduction. One source, out of many, for obtaining the non-uniform weights of the excitation currents is by using genetic algorithm. In antenna array problems, there are many parameters that can be used to evaluate the fitness function which is used as a starting point for genetic algorithm such as gain, sidelobes level area under the curve (AUC). Here, the goal is to design a circular antenna array of reduced sidelobes level. The fitness function which we used here is the area under the curve AUC(area under the sidelobes).The area under the sidelobes can be calculated by:

$$AUC = \int_{-\pi/2}^{-\theta_h} |AF(\theta)| d\theta + \int_{\theta_h}^{\pi/2} |AF(\theta)| d\theta \dots\dots\dots (3.3)$$

$$Fitness = \min\left(\frac{AUC_{reduced}}{AUC_{unreduced}}\right) \dots\dots\dots (3.4)$$

Where $\pm\theta_h$ are the 3 dB angles at either side of the main beam.

Consider N isotropic radiators distributed in a circular ring of radius a placed in x - y plane as shown in Fig.(3.1), the origin of the coordinate system is located at the center of the array. The elements are separated by d in meters and main beam of the pattern is in the boresight of the array, ($\phi_0 = \theta_0 = 0$).

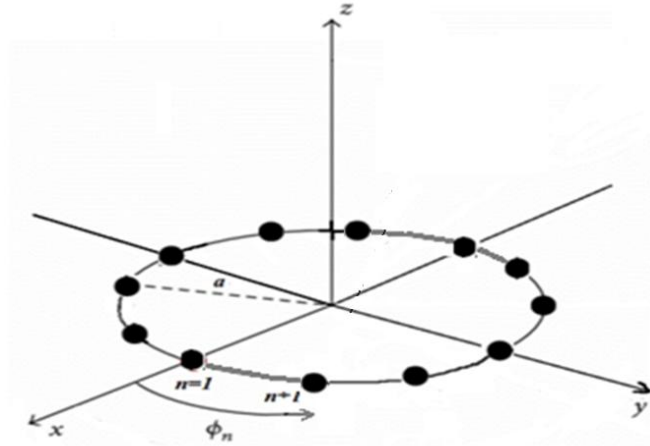


Fig. (3.1) Geometry of a circular antenna array positioned in x-y plane

The array factor can be written as by:

$$AF(\theta, \phi) = \sum_{n=1}^N I_n e^{j(ka \sin \theta \cos(\phi - \phi_n))}$$

The weights for the amplitude excitation represent the initial population in genetic algorithm are.

$$W_n = [w_1, w_2, w_3, \dots, w_N]$$

3.2.2- Results and discussions:

A large number of randomly data was used as an input for genetic algorithm program. The process of the program is to select a suitable excitation current for N -element circular antenna array. The table

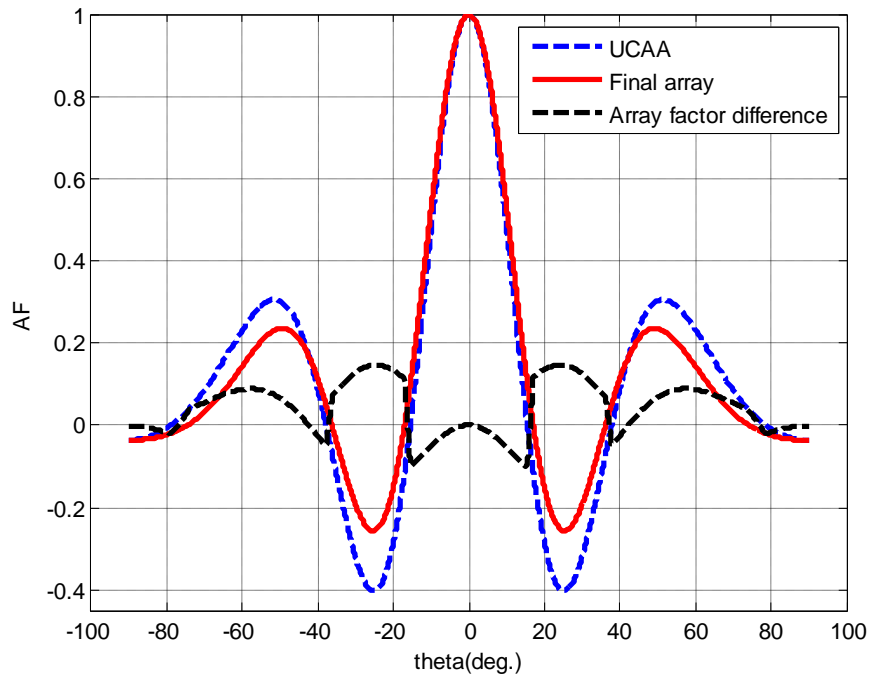
shown below is the results obtained from using the genetic algorithm program for 12, 18 and 20 elements circular antenna array. The table also contains information about the radius, inter-element spacing, beamwidth and directivities of the antenna array.

Table 3.1 Normalized amplitude excitation obtained from genetic algorithm for different number of elements in circular antenna array.

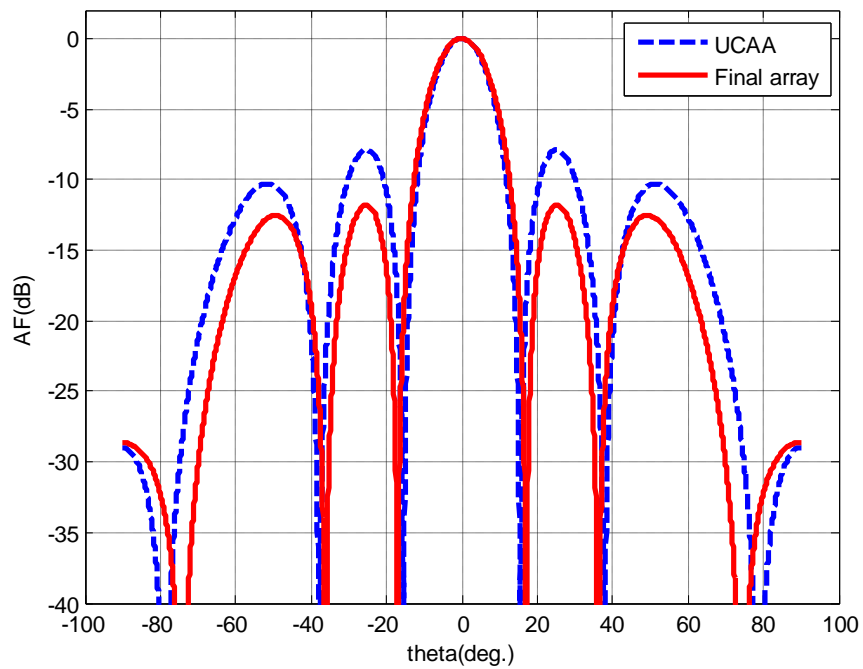
N	$d(\lambda)$	$a(\text{cm})$	Bwi (deg.)	Normalized Excitation w1,w2,w3,.....wN	Bwo (deg.)	FSLL (dB)	Di(dB)	Do(dB)
12	0.75	17.9	14.5	0.6196 0.3933 0.9375 1.0000 0.0151 0.7539 0.5699 0.1940 0.5156 0.7921 0.0606 0.6308	15.4	-11.8	26	31
18	0.75	26.8	9.6	0.1809 0.4998 0.7040 0.9519 0.9696 0.6069 0.3855 0.6617 0.7099 0.6248 0.2305 0.9494 0.7630 0.9672 0.4689 1.0000 0.1943 0.8094	10.5	-12.4	28	32
20	0.75	29.8	8.7	0.4889 0.5513 0.6857 0.5965 0.8815 0.5504 0.2793 0.4954 0.4361 0.8926 0.0523 0.5348 0.7884 0.9814 0.7370 1.0000 0.3578 0.7275 0.2720 0.2042	9.6	-12.2	30	35

Figures (3.2 to 3.4) shows the plots of the radiation patterns, for the uniformly excited 12, 18, 20 elements circular antenna array, and that

for the excitations obtained from genetic algorithm program shown in table 3.1.

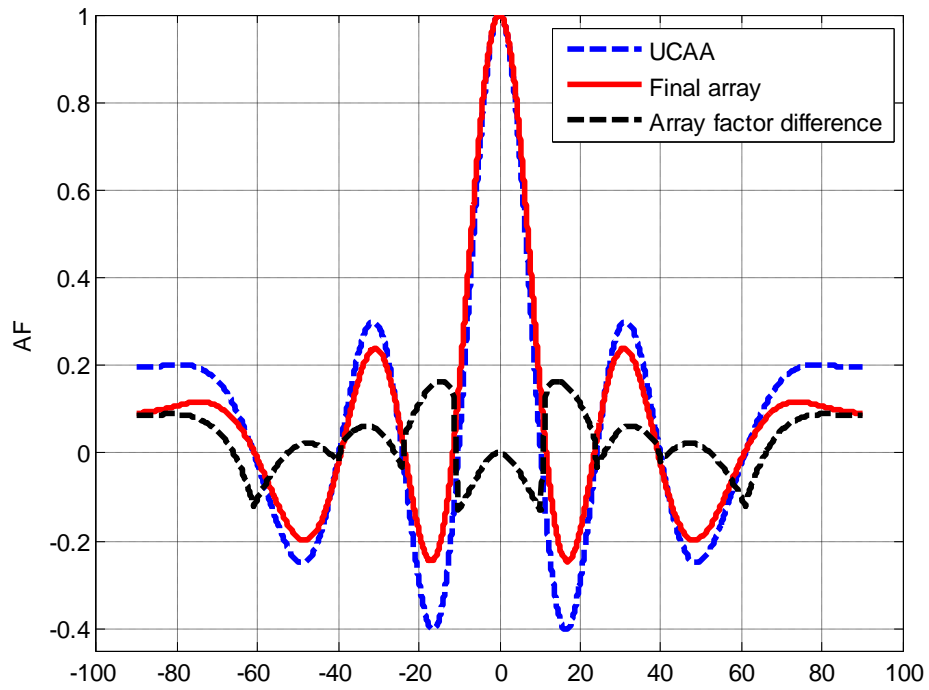


-a-

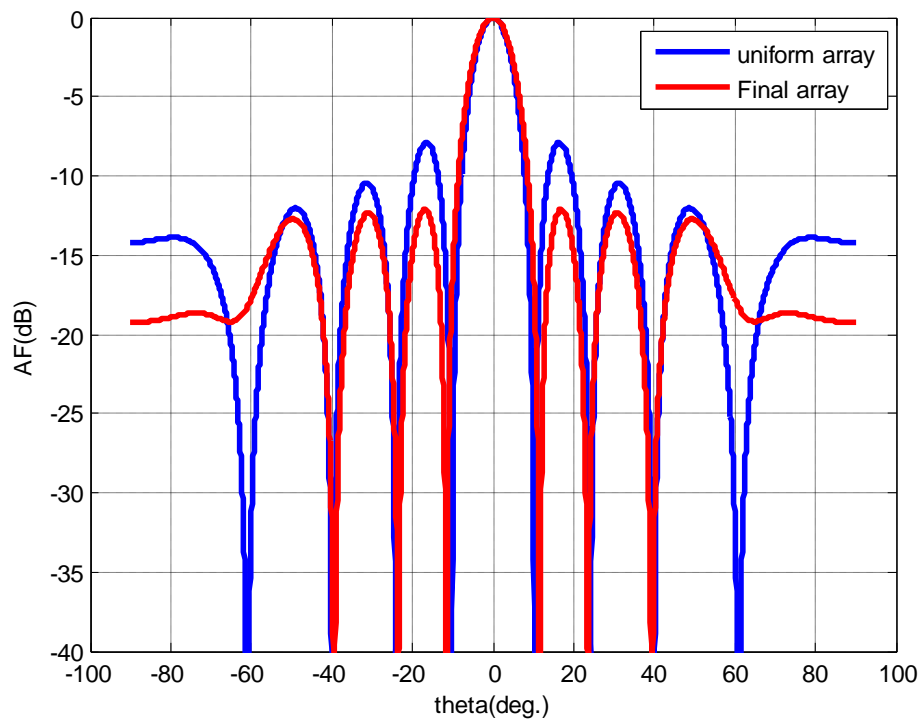


-b-

Fig. (3.2) a&b- Radiation pattern for 12-element circular antenna array using genetic algorithm shows a reduction in the sidelobes level $\phi_0 = 0, \theta_0 = 0$

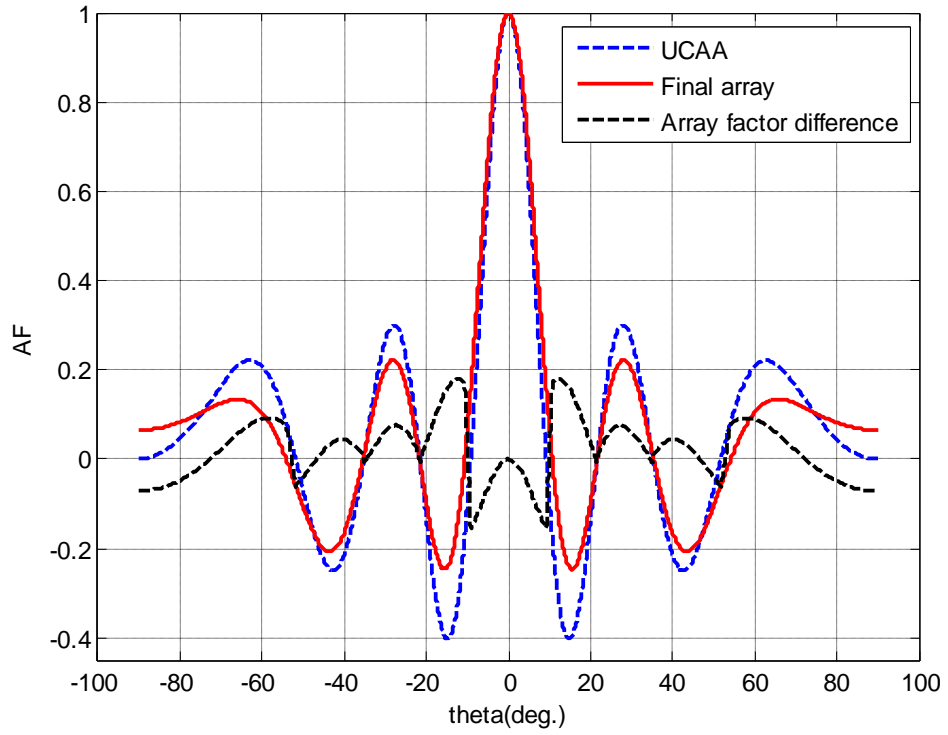


-a-

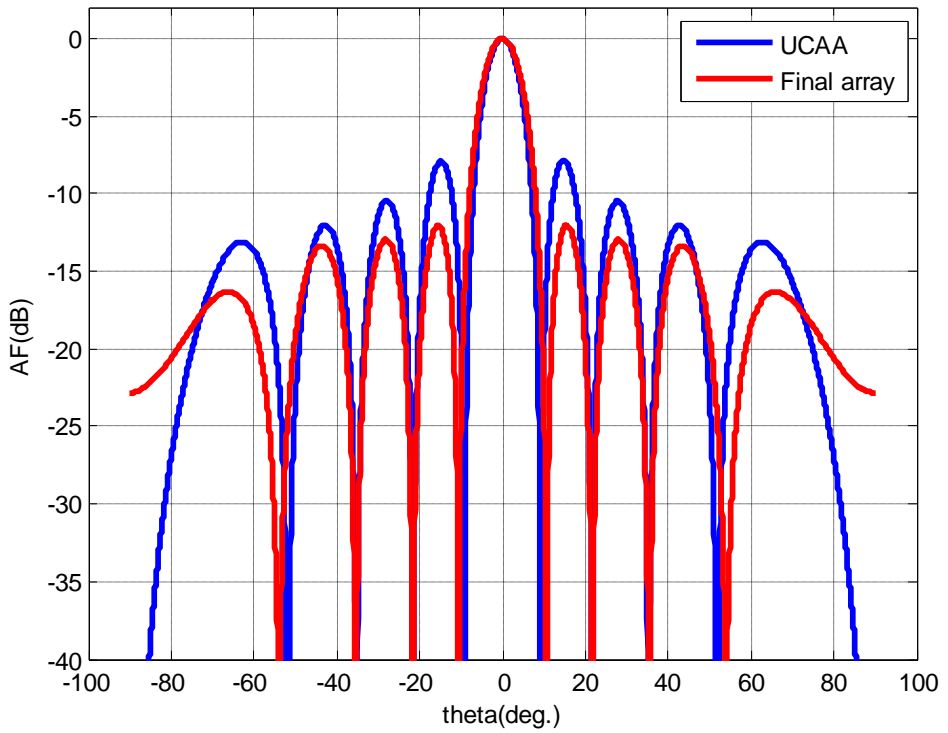


-b-

Fig. (3.3) a&b- Radiation pattern for 18-element circular antenna array using genetic algorithm shows a reduction in the sidelobes level $\phi_0 = 0, \theta_0 = 0$



-a-



-b-

Fig. (3.4)a&b-Radiation pattern for 20elements circular antenna array using genetic algorithm shows a reduction in the sidelobes level $\phi_0 = 0, \theta_0 = 0$

It is clear from the plots and the results given in table 3.1 that, there is a reduction in the value of the sidelobes level with an increase in the values of the directivity. There is also an appreciable unwanted change in the beamwidth values. The plots also show the array factor difference between the absolute values of the array factor of the original array and that of a reduced sidelobes level [12]. The more positive value of the difference the more reduction in the sidelobes level (local improvement). The negative values of this plot around the main beam gives an indication for an increased in the value of the beamwidth, while the positive value reveals a reduction in the value of the beamwidth.

3.3 – Sidelobes level reduction with modification in the selected elements of the uniform circular antenna array:

Modifying the uniform circular antenna array can be done for the existing uniform circular array to enhance its performance. The modification is to change one of the array parameters which are represented by amplitude excitations, phase excitations and spacing between two collinear elements at specified angular positions.

3.3.1- Analysis and results of modified excitations of circular array:

Here we used a modification in the amplitude excitation for certain selected elements of the circular antenna array. Choosing suitable amplitude excitations for 2 or more elements selected at specified ϕ_n angle in the uniform array, will contribute in reducing the sidelobes level of the array pattern.

Fig. (3.5) below shows the improvement factor in the sidelobes reduction versus angular positions for changing the excitation of each opposed pair of elements in the uniform circular array. The more positive values in the improvement factor indicate a more reduction in the sidelobes whereas negative values are for unwanted increasing in the sidelobe structure.

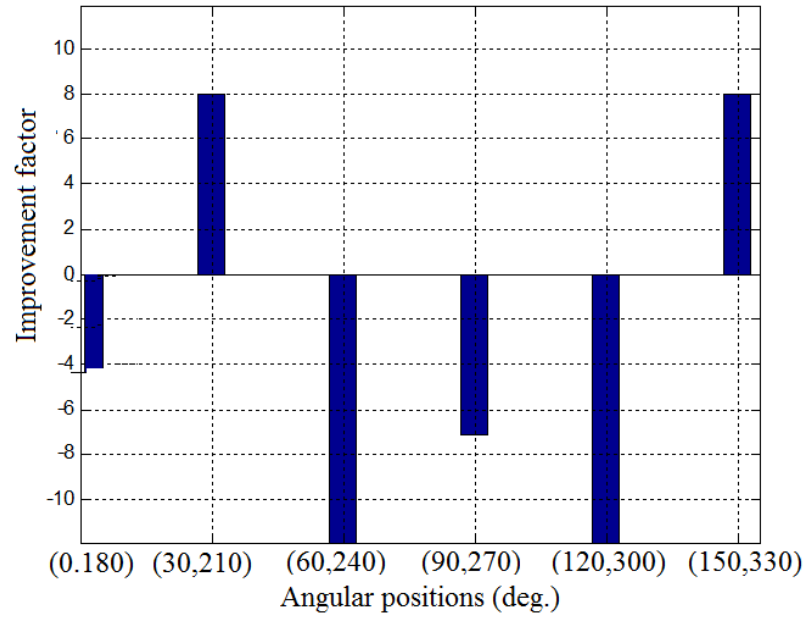


Fig.(3.5) Improvement factor versus angular positions for each pair of elements locations in the resting plane for 12 elements uniform circular array

Consider an array of N isotropic radiators separated by d meters and positioned on the x - y plane, as shown in Fig. (3.6). Modification in the excitation elements involves selection of certain elements from the circular array at certain specified angular positions, then changing their amplitude excitations by tray and error to achieve sidelobes level reduction. From Equation (2.10) (array factor of circular array), assuming the selected elements is two as shown in Fig. (3.6).

$$AF(\theta, \phi) = \sum_{n=1}^N I_n e^{jka[\sin \theta \cos(\phi - \phi_n) - \sin \theta_0 \cos(\phi_0 - \phi_n)]}$$

In broadside array ($\theta_0 = 0, \phi_0 = 0$), the separation between any two opposed selected elements is $d_r = 2a$. The array factor for the selected elements can be written as:

$$AF_{N_r=2} = 2I_r \cos(ka \sin \theta \cos \phi_m) \quad \text{at } \phi = 0 \quad \dots\dots\dots(3.1)$$

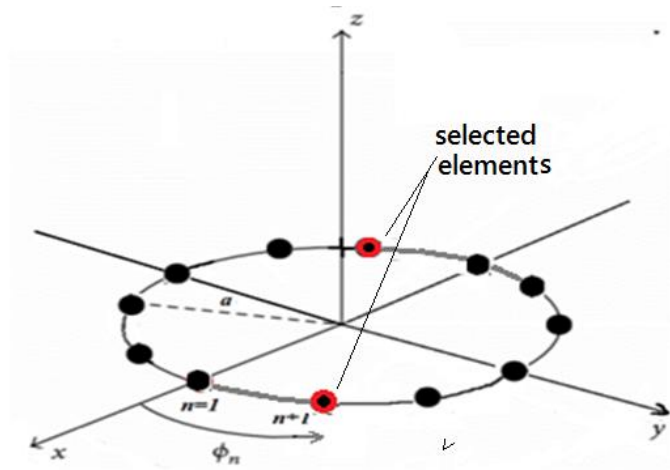


Fig. (3.6) Geometry of modified excitation circular antenna array in x-y plane

Where I_r is the excitation current of these two elements and ϕ_m is angular position for the selected elements in the modified circular array. The total array factor for this circular array is obtained by superimposing the array factor of the 2 elements with the array factor of the N-element circular array. The superimposed array factor is given by:

$$AF_{\text{mod}}(\theta, \phi) = \sum_{n=1}^N I_n \exp(jka \sin \theta \cos \phi_n) \pm 2I_r \cos(ka \sin \theta \cos \phi_m) \quad \dots\dots\dots(3.2)$$

Results and discussions of modified excitation:

We select two elements in collinear with the center (opposed) of the array as an example from the original array with angular position ($\phi_1 = 30^\circ, \phi_2 = 210^\circ$). The sign plus or minus in equation (3.2) represented the increasing or decreasing in the value of amplitude excitation for the selected elements. Here we noted that decreasing the value of I_r to (0.1) of the normalized uniform value of the original array, helped on sidelobes level reduction as shown in Fig. (3.7). The idea of using 2 elements modified amplitude excitation was extended to 4 elements at angular positions of ($30^\circ, 210^\circ, 150^\circ, 330^\circ$) and amplitude excitation for these selected elements is 0.3 of the uniform value as shown in Fig (3.8). To achieve further reduction in sidelobes level simulations were carried out for the original circular antenna array by altering the excitation of many elements of the array.

From table (3.2) it is clear that sidelobes level reduction increased by increasing the number of the modified elements. It is clear from the table that, the directivity increased with altering the excitation of the selected elements.

Table3.2-Normalized amplitude excitations obtained from modified excitation for selected the elements in circular antenna array.

N	$d(\lambda)$	Nr	Bwi (deg.)	Normalized Excitation $w_1, w_2, w_3, \dots, w_n$	Bwo (deg.)	FSL (dB)	Di(dB)	Do(dB)
12	0.75	2	14.5	$(w_1, w_7)=0.1$ $(w_2, w_3, w_4, w_5, w_6)=1$ $(w_8, w_9, w_{10}, w_{11}, w_{12})=1$	15.3	-10.4	26	31
12	0.75	4	14.5	$(w_1, w_5, w_7, w_{11})=0.3$ $(w_2, w_3, w_4, w_6, w_8, w_9, w_{10}, w_{12})=1$	15.9	-13	26	34
18	0.75	4	9.6	$(w_1, w_8, w_{10}, w_{17})=0.1$ $(w_3, w_4, w_5, w_6, w_7, w_8, w_9, w_{12})=1$ $(w_{13}, w_{14}, w_{15}, w_{16}, w_{17}, w_{18})=1$	10.8	-10.6	25	38
18	0.75	6	9.6	$(w_1, w_7, w_8, w_{10}, w_{16}, w_{17})=0.2$ $(w_2, w_3, w_4, w_5, w_6, w_9, w_{11})=1$ $(w_{12}, w_{13}, w_{14}, w_{15}, w_{18})=1$	10.9	-13.2	28	35
24	0.65	6	8.3	$(w_1, w_2, w_{12}, w_{13}, w_{14}, w_{24})=0.1$ $(w_3, w_4, w_5, w_6, w_7, w_8, w_9, w_{10})=1$ $(w_{11}, w_{12}, w_{15}, w_{16}, w_{17}, w_{18})=1$ $(w_{19}, w_{20}, w_{21}, w_{22}, w_{23})=1$	9.6	-10.8	31	39
24	0.65	8	8.3	$(w_1, w_2, w_3, w_{12}, w_{13})=0.1$ $(w_{14}, w_{15}, w_{24})=0.1$ $(w_4, w_5, w_6, w_7, w_8, w_9, w_{10})=1$ $(w_{11}, w_{16}, w_{17}, w_{18}, w_{19}, w_{20})=1$ $(w_{21}, w_{22}, w_{23})=1$	9.7	-13.1	31	36

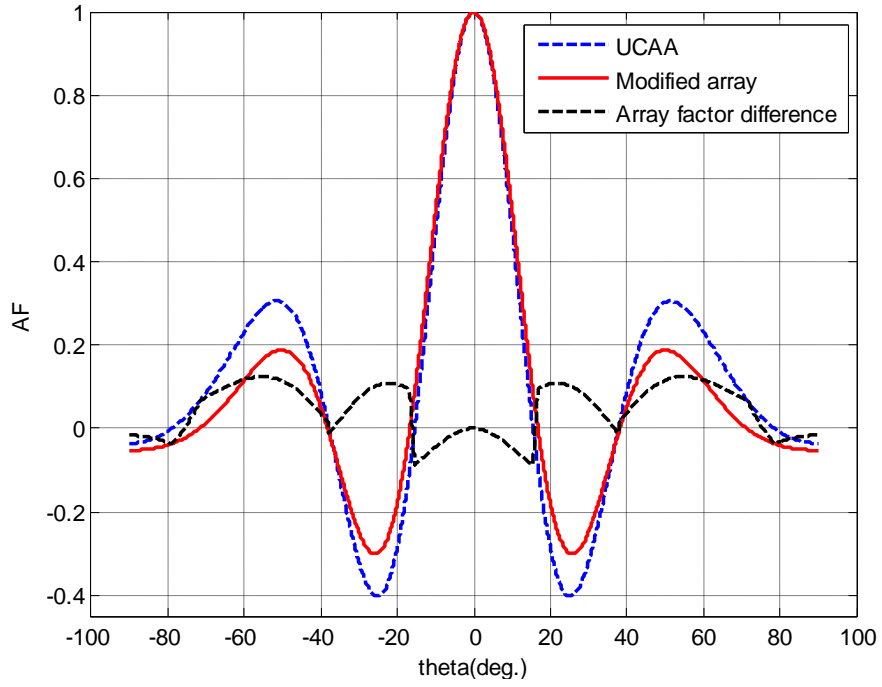
Figures (3.7 to 3.12) are the plots of the array factors of a modified excitation of N-element circular array together with the uniform circular array of the same size. The plots also show the array factor difference between them. It is clear from the plots that good reduction in sidelobes level can be obtained by this method, the penalty here is an appreciable increase in the beamwidth.

Fig. (3.13) show the plot of beamwidth versus the number of elements N. It is clear from the plot that, the beamwidth of the modified array is less than that of the final array (genetic algorithm values) obtained from genetic algorithm, but it is slightly greater than that of the uniform array of equal size. The plot showed also a decrease in beamwidth with increase in 'N'

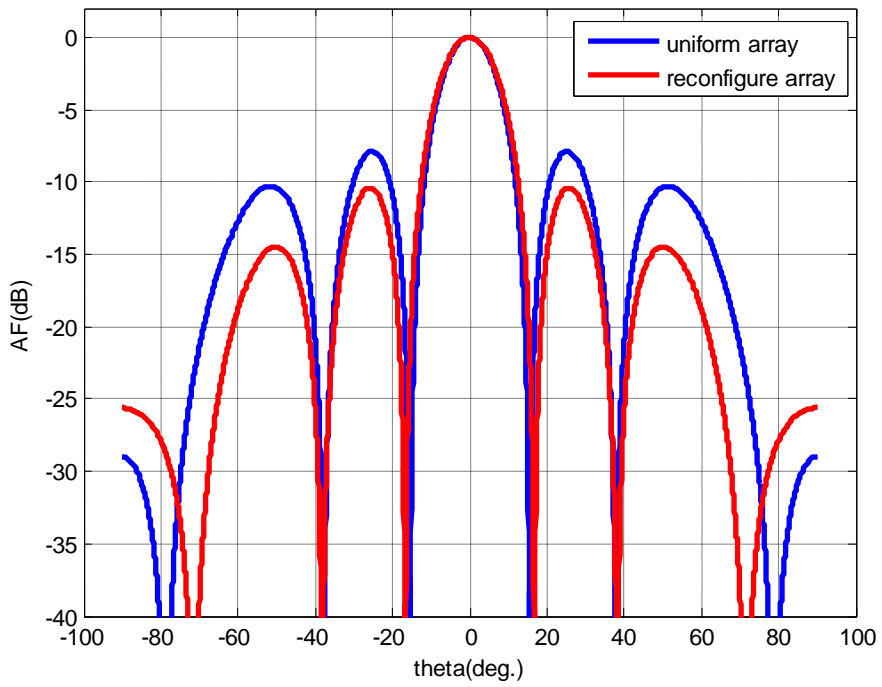
Fig. (3.14) show a plot of the directivity for 12-element circular antenna array versus the excitation of the modified elements. The plot reveals good directivity for 4 elements modified excitation.

Fig. (3.15) shows the plot of the first and second sidelobes level for modified excitation for certain specified elements of a circular antenna array N=12 versus the excitation of the modified elements. The figure shows that, reduction of the sidelobes level for the modified array increases as the excitation value decreases in its specified range.

Fig. (3.16) shows a plot of the beamwidth for the modified excitation circular array versus amplitude excitation for different number of the modified elements. From the plot it is obvious that the beamwidth inversely proportional with the excitation of the modified elements.

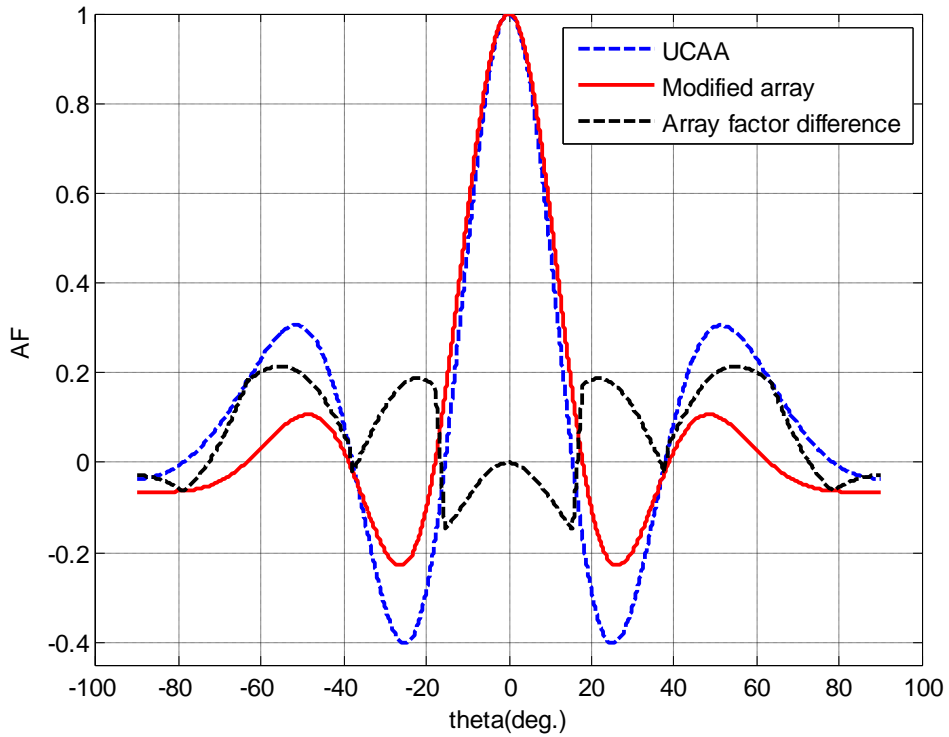


-a-

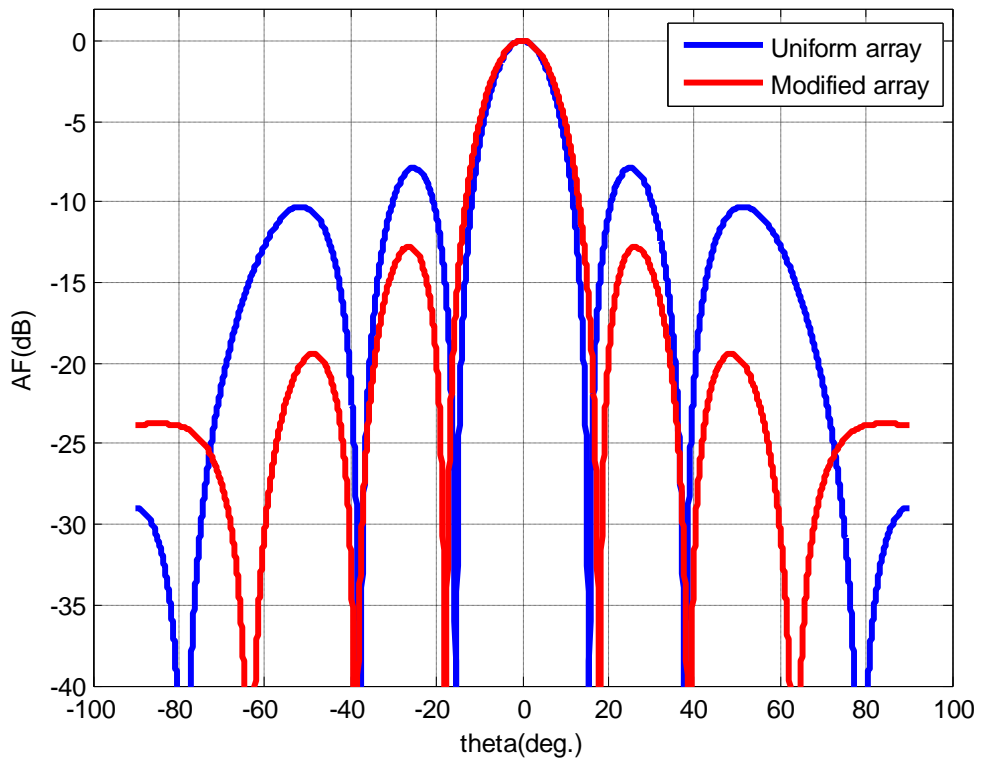


-b-

Fig. (3.7)a&b-Radiation pattern of 12-element circular array with unity excitation of all elements except two elements with 0.1 positioned at angles 30° , 210°

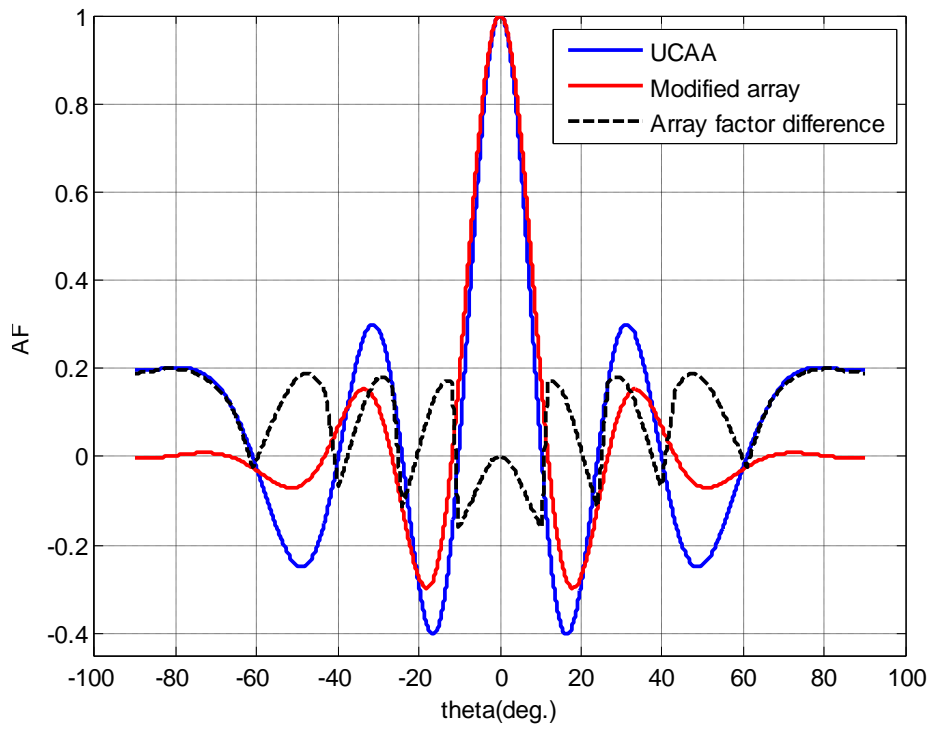


-a-

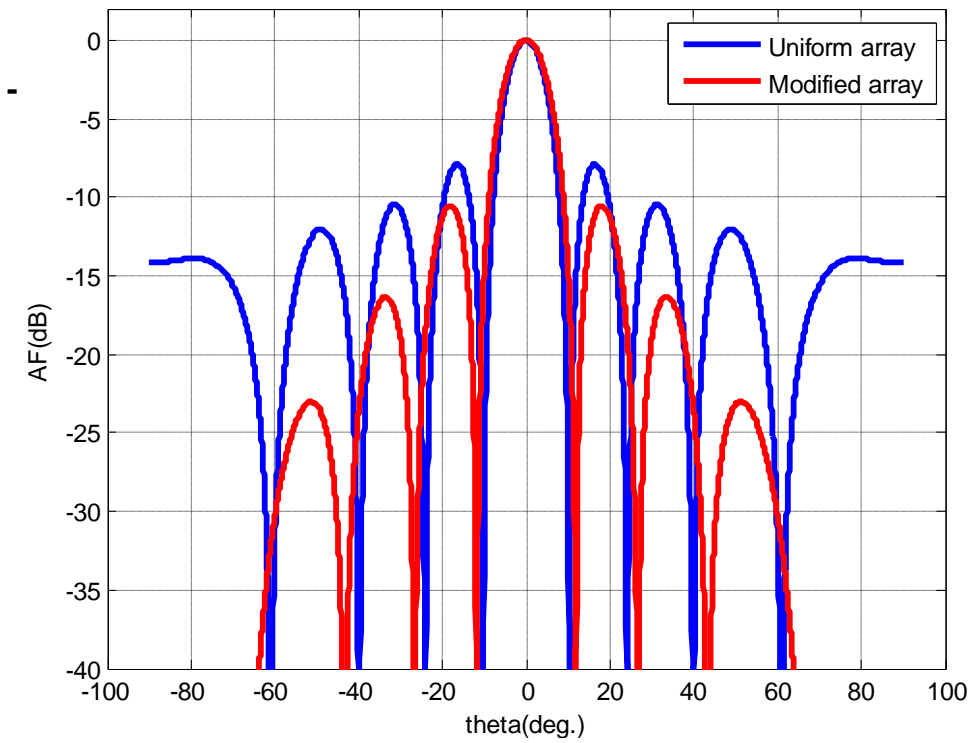


-b-

Fig. (3.8) a&b-Radiation pattern of 12-element circular array with unity excitation of all elements except 4 elements with excitation 0.3 positioned at angles 30° , 210° , 150° , 330°

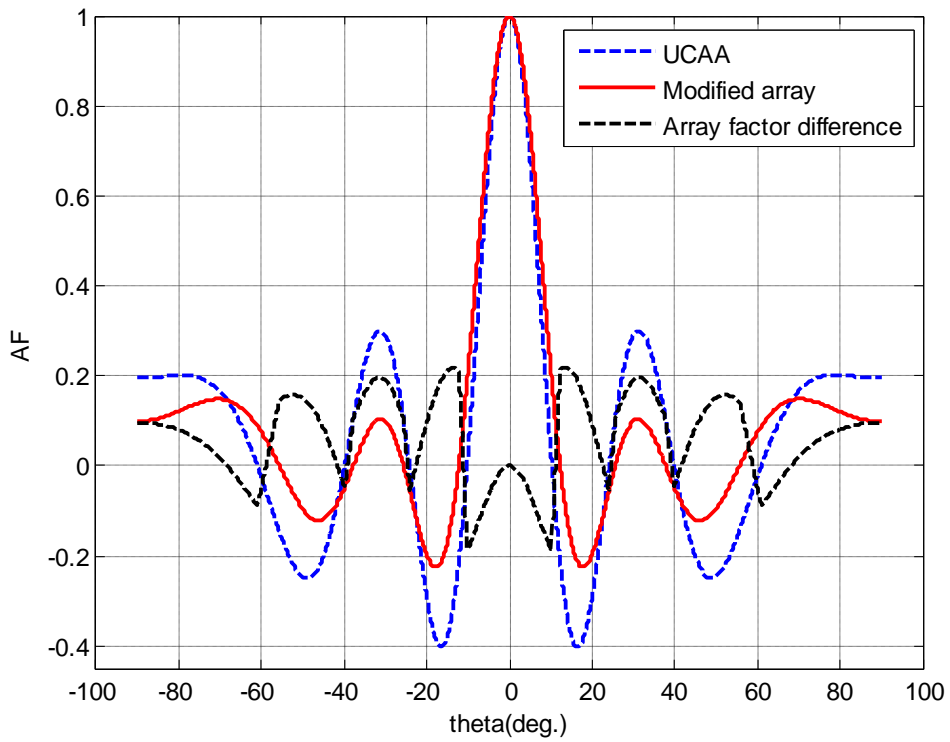


-a-

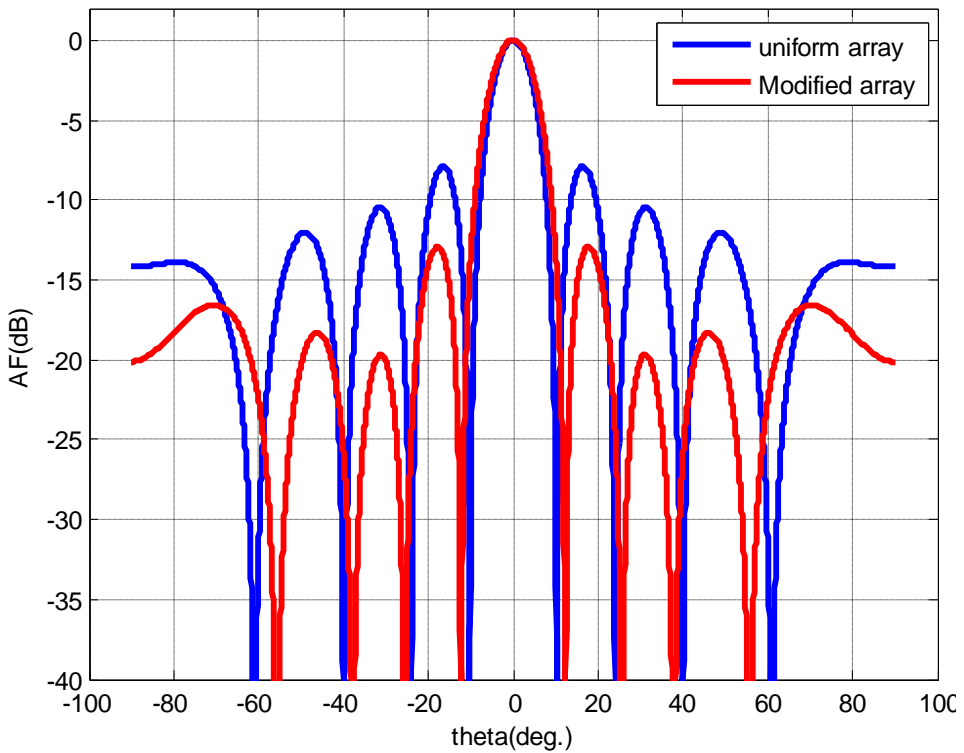


-b-

Fig. (3.9)a&b-Radiation pattern of 18-element circular array with unity excitation of all elements except 4 elements with excitation 0.1 positioned at angles 20° , 160° , 200° , 340°

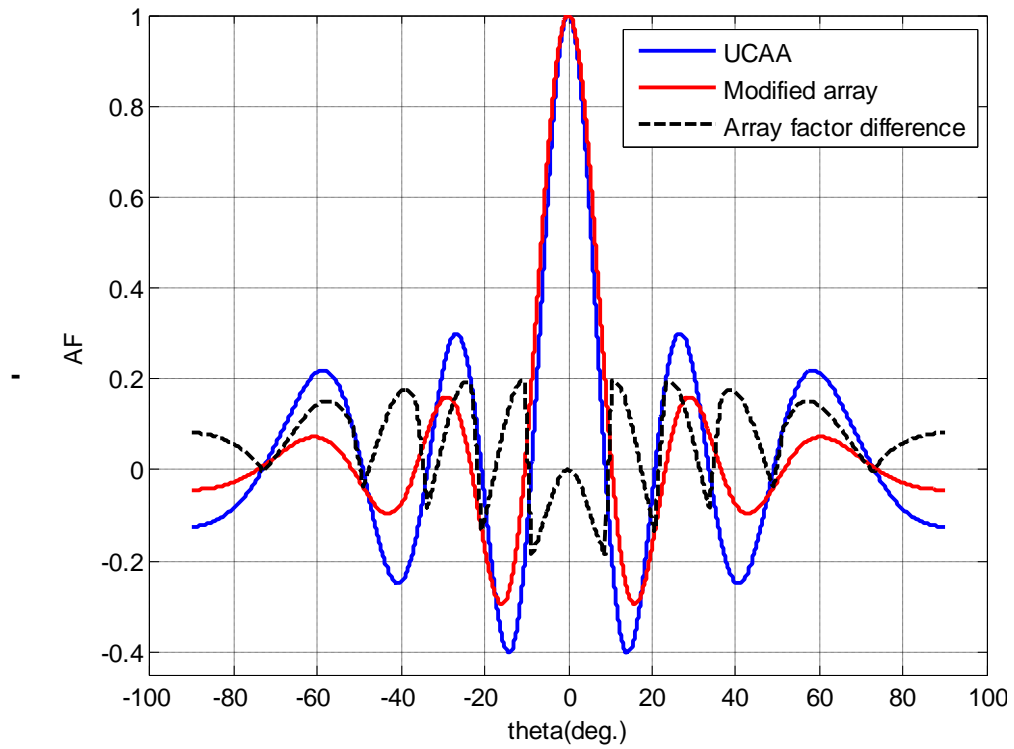


-a-

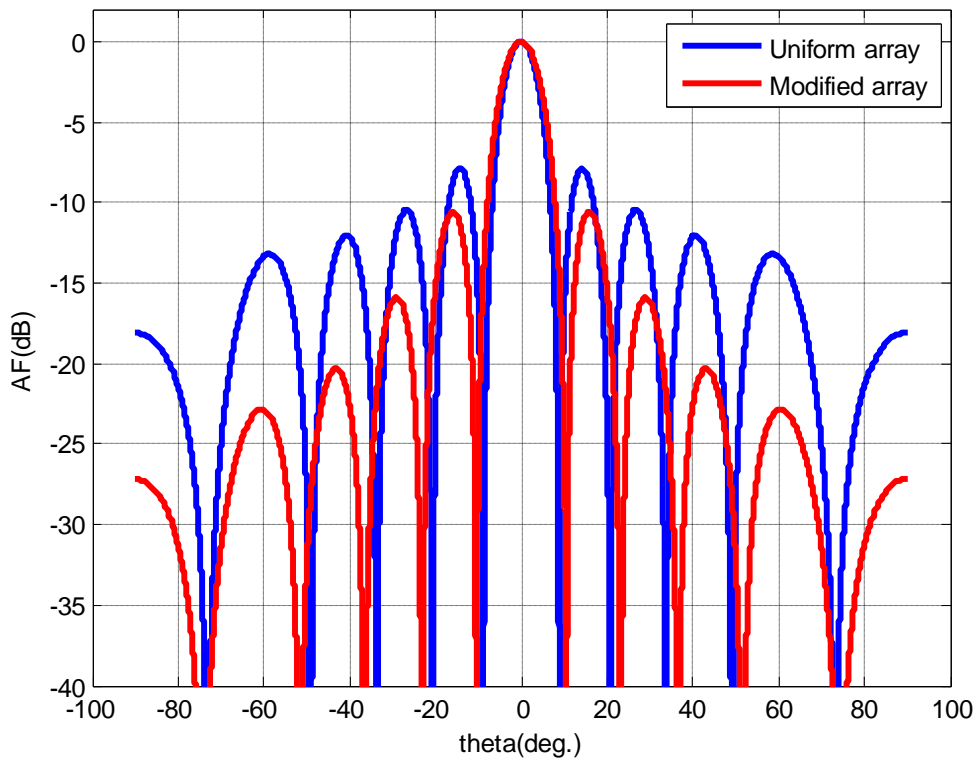


-b-

Fig. (3.10)a&b-Radiation pattern of 18-element circular array with unity excitation of all elements except 6 elements with modified excitation 0.2 at angular positioned in(deg.)20,140,160,200,320,340

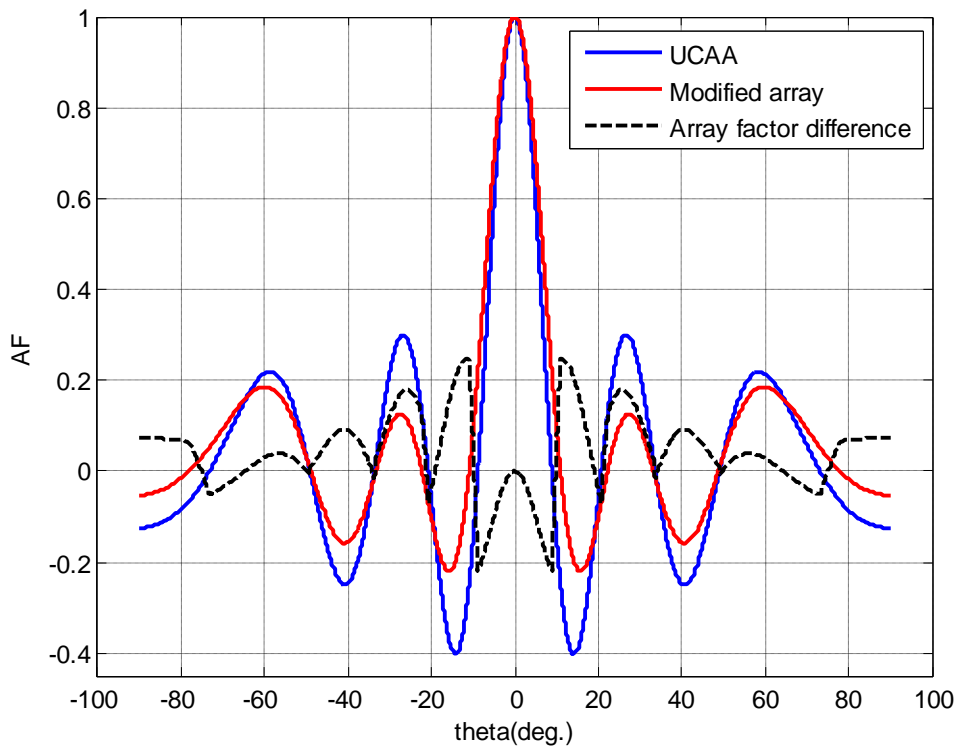


-a-

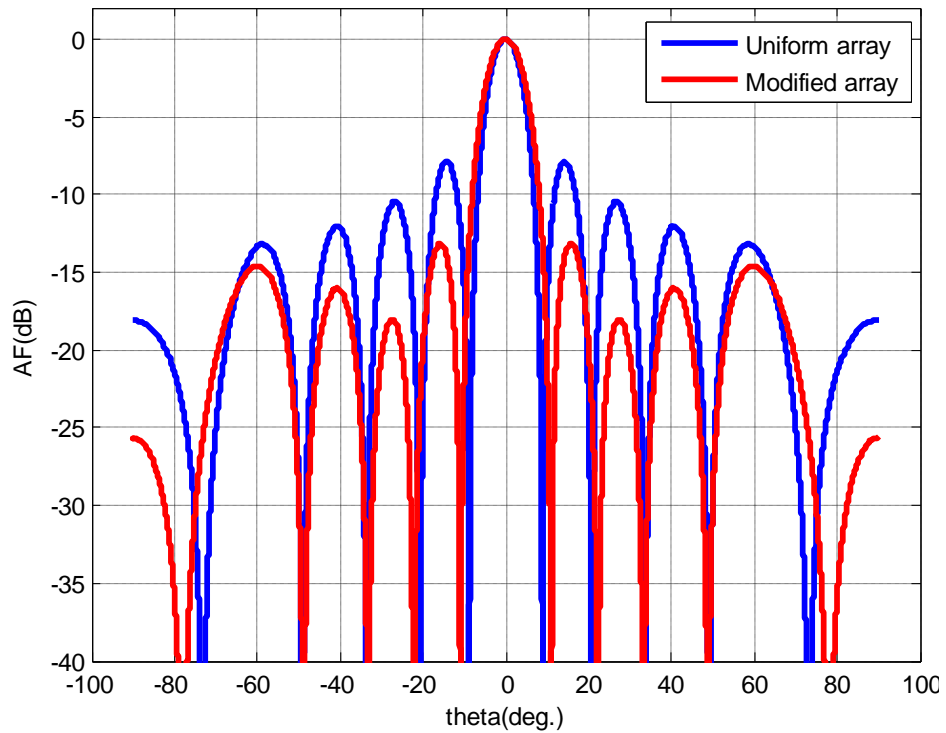


-b-

Fig. (3.11) a&b-Radiation pattern of 24-element circular array with unity excitation of all elements except 6 elements with excitation 0.1 positioned at angles in (deg.) 15,30,180,195,210,360



-a-



-b-

Fig. (3.12) a&b Radiation pattern of 24-element circular array with unity excitation of all elements except 8 elements with modified excitation 0.1 at angular position in (deg.) 15, 30, 45, 180, 195, 210, 225, 360

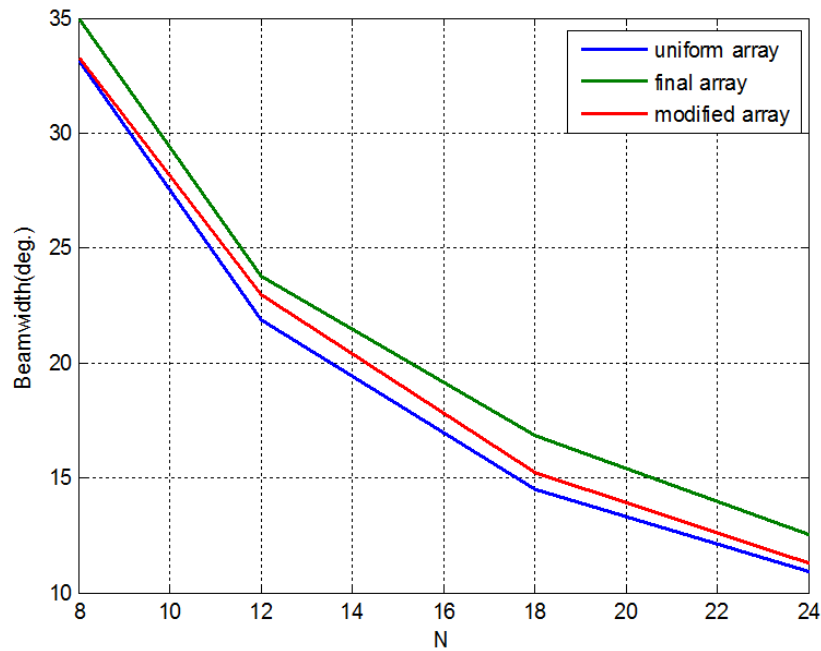


Fig. (3.13) Plot of beamwidth for uniform circular array, final array and modified array versus N at $d=0.5\lambda$

Fig. (3.17) shows plot of the ratio of area under the sidelobes for the modified array, to that of N-element uniform circular array, versus amplitude excitation. It is clear from the plot that, the area ratio increases as amplitude excitation increases. The plot shows good curve for area ratio when number of the modified elements equal to 4 in the case when the total number of the array elements equal to 12.

Fig. (3.18) shows the plot of the first and second sidelobe level for modified excitation of circular antenna array $N=24$ versus amplitude excitation of modified elements. The figure shows that, the sidelobes level reduction of the modified array increases as the excitation value decreases.

Fig. (3.19) shows the plot of the beamwidth for modified excitation of circular antenna array $N=24$ versus amplitude excitation of the modified elements. The figure shows that, beamwidth at the selected

elements 2 are better than that of the selected elements 6 or 8 but the penalty is an increasing in the area ratio of the modified array.

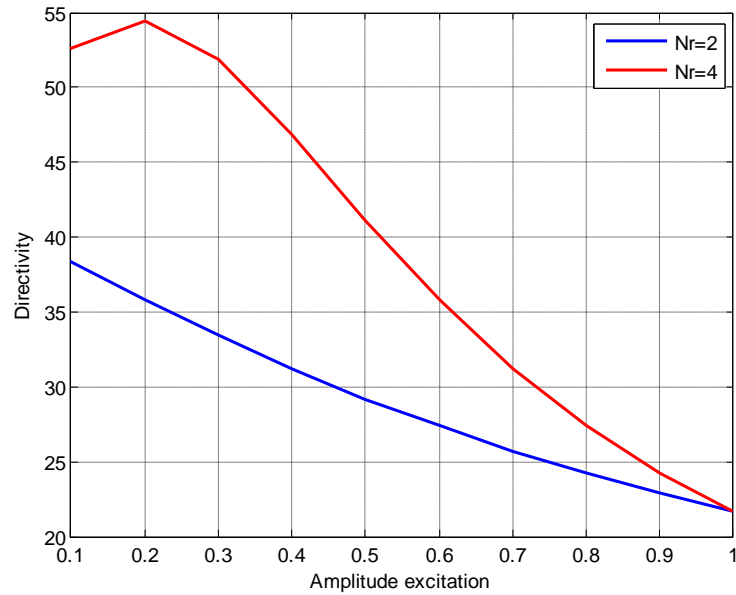


Fig. (3.14) Plot of directivity for modified excitation circular antenna array with $N=12$ & $d=0.75\lambda$ versus amplitude excitation for selected elements, $Nr=2$ at $(\phi_1 = 30^\circ, \phi_7 = 210^\circ)$ and $Nr=4$ at $(\phi_1 = 30^\circ, \phi_5 = 150^\circ, \phi_7 = 210^\circ, \phi_{11} = 330^\circ)$

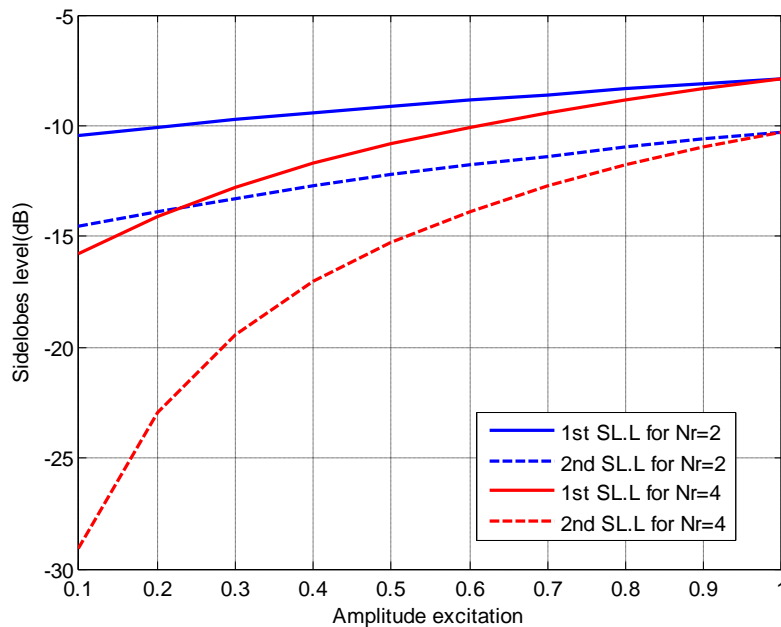


Fig. (3.15) Plot of first and second Sidelobes level for modified excitation circular antenna array with $N=12$ & $d=0.75\lambda$ versus amplitude excitation for selected elements, $Nr=2$ at $(\phi_1 = 30^\circ, \phi_7 = 210^\circ)$ and $Nr=4$ at $(\phi_1 = 30^\circ, \phi_5 = 150^\circ, \phi_7 = 210^\circ, \phi_{11} = 330^\circ)$

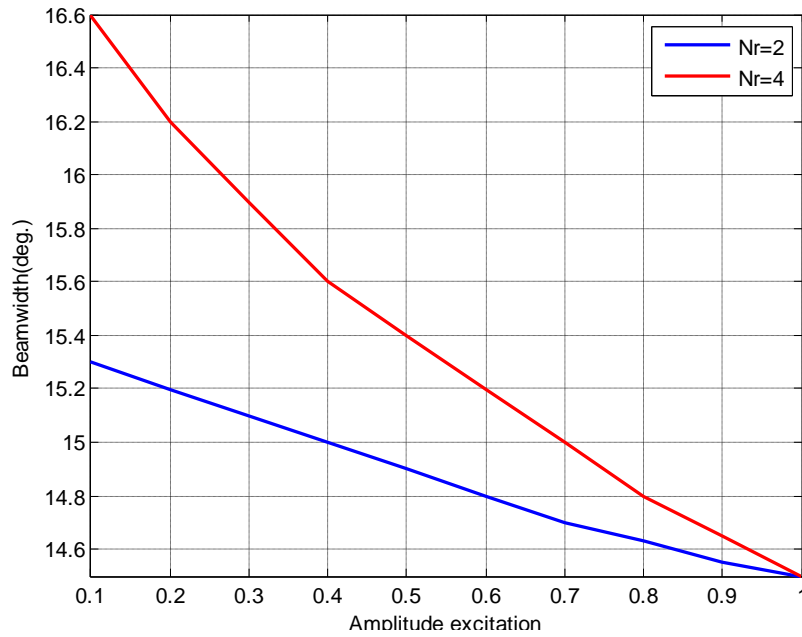


Fig. (3.16) Plot of beamwidth for modified excitation circular antenna array with $N=12$ & $d=0.75\lambda$ versus amplitude excitation for selected elements, **Nr=2** at $(\phi_1 = 30^\circ, \phi_7 = 210^\circ)$ and **Nr=4** at $(\phi_1 = 30^\circ, \phi_5 = 150^\circ, \phi_7 = 210^\circ, \phi_{11} = 330^\circ)$

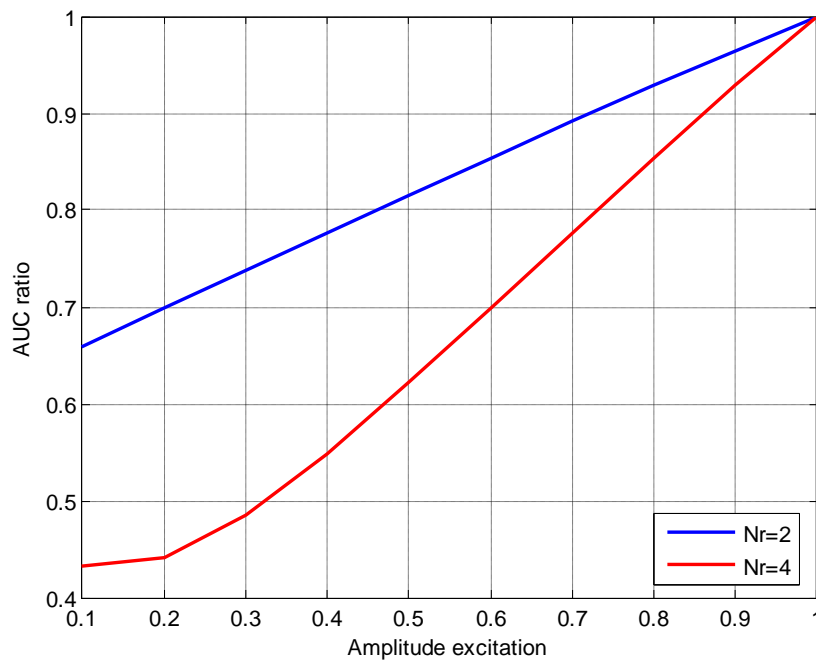


Fig. (3.17) Plot of AUC ratio for modified excitation circular antenna array with $N=12$ & $d=0.75\lambda$ versus amplitude excitation for selected elements, **Nr=2** at $(\phi_1 = 30^\circ, \phi_7 = 210^\circ)$ and **Nr=4** at $(\phi_1 = 30^\circ, \phi_5 = 150^\circ, \phi_7 = 210^\circ, \phi_{11} = 330^\circ)$

Fig. (3.20) shows plot of the ratio of area under the sidelobes for the modified array, to that of N-element uniform circular array, versus amplitude excitation. It is clear from the plot that, the area ratio increases as amplitude excitation increases. The plot shows good curve for area ratio when the number of the modified elements equal to 6 in the case when the total number of the array elements equal to 24.

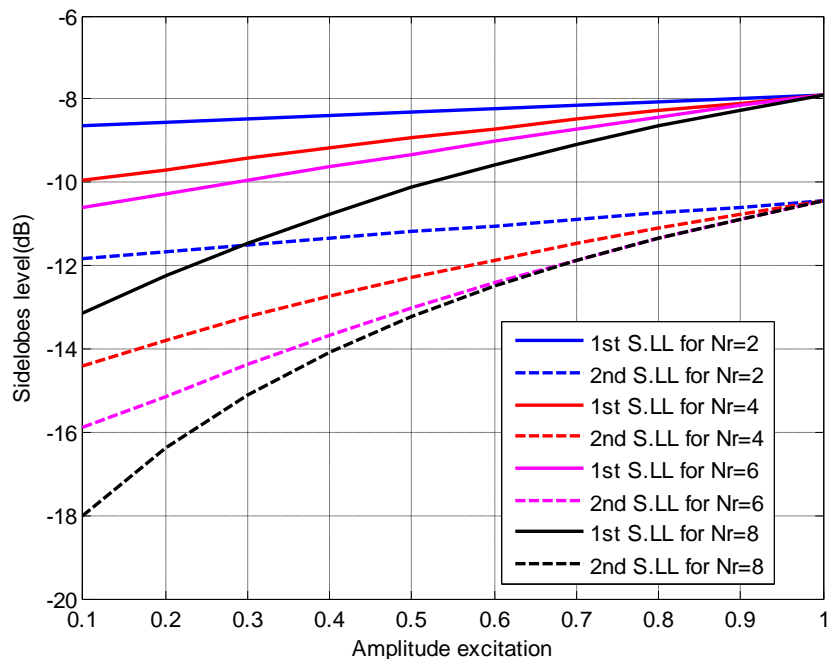


Fig. (3.18) Plot of first and second Sidelobes level for modified excitation circular antenna array with $N=24$ & $d=0.65\lambda$ versus amplitude excitation for selected elements,
Nr=2 at $(\phi_1 = 15^\circ, \phi_{13} = 195^\circ)$
Nr=4 at $(\phi_1 = 15^\circ, \phi_2 = 30^\circ, \phi_{13} = 195^\circ, \phi_{14} = 210^\circ)$
Nr=6 at $(\phi_1 = 15^\circ, \phi_2 = 30^\circ, \phi_{12} = 180^\circ, \phi_{13} = 195^\circ, \phi_{14} = 210^\circ, \phi_{24} = 360^\circ)$
Nr=8 at $(\phi_1 = 15^\circ, \phi_2 = 30^\circ, \phi_3 = 45^\circ, \phi_{13} = 195^\circ, \phi_{14} = 210^\circ, \phi_{15} = 225^\circ, \phi_{16} = 240^\circ, \phi_{24} = 360^\circ)$

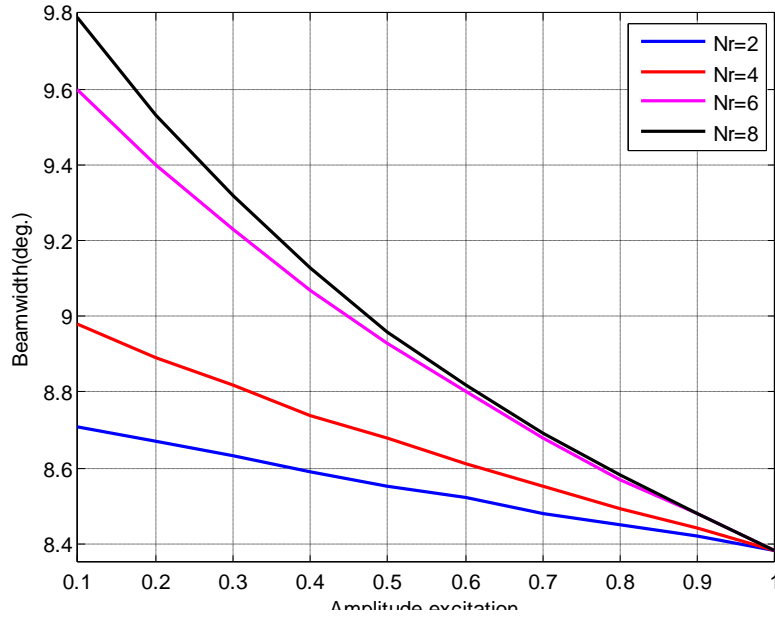


Fig. (3.19) Plot of beamwidth for modified excitation circular antenna array with $N=24$ & $d=0.65\lambda$ versus amplitude excitation of the selected elements $Nr=2$ at $(\phi_1 = 15^\circ, \phi_{13} = 195^\circ)$, $Nr=4$ at $(\phi_1 = 15^\circ, \phi_2 = 30^\circ, \phi_{13} = 195^\circ, \phi_{14} = 210^\circ)$

$Nr=6$ at $(\phi_1 = 15^\circ, \phi_2 = 30^\circ, \phi_{12} = 180^\circ, \phi_{13} = 195^\circ, \phi_{14} = 210^\circ, \phi_{24} = 360^\circ)$

$Nr=8$ at $(\phi_1 = 15^\circ, \phi_2 = 30^\circ, \phi_3 = 45^\circ, \phi_{13} = 195^\circ, \phi_{14} = 210^\circ, \phi_{15} = 225^\circ, \phi_{16} = 240^\circ, \phi_{24} = 360^\circ)$

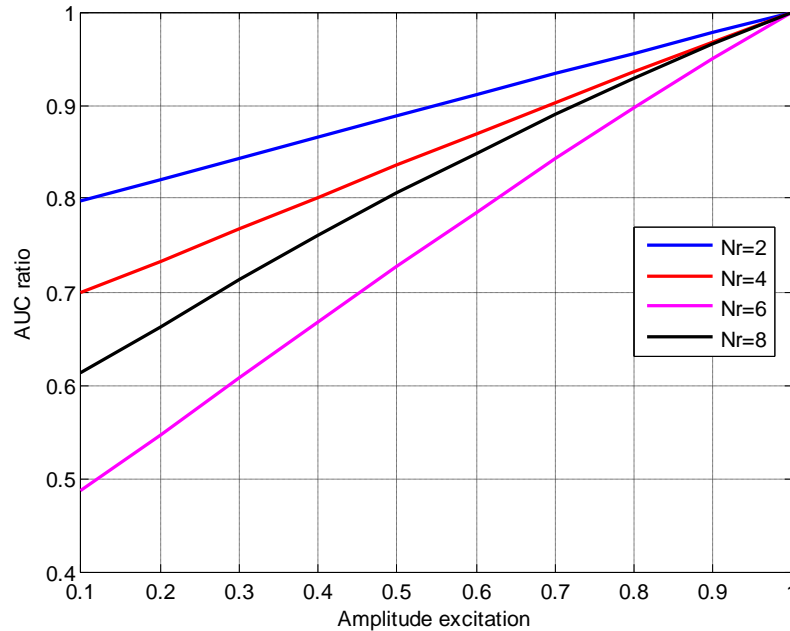


Fig. (3.20) Plot of area ratio under the curve for the modified excitation circular antenna array with $N=24$ & $d=0.65\lambda$ versus amplitude excitation of the selected elements $Nr=2$ at $(\phi_1 = 15^\circ, \phi_{13} = 195^\circ)$

$Nr=4$ at $(\phi_1 = 15^\circ, \phi_2 = 30^\circ, \phi_{13} = 195^\circ, \phi_{14} = 210^\circ)$

$Nr=6$ at $(\phi_1 = 15^\circ, \phi_2 = 30^\circ, \phi_{12} = 180^\circ, \phi_{13} = 195^\circ, \phi_{14} = 210^\circ, \phi_{24} = 360^\circ)$

$Nr=8$ at $(\phi_1 = 15^\circ, \phi_2 = 30^\circ, \phi_3 = 45^\circ, \phi_{13} = 195^\circ, \phi_{14} = 210^\circ, \phi_{15} = 225^\circ, \phi_{16} = 240^\circ, \phi_{24} = 360^\circ)$

3.3.2– Sidelobes level reduction using modified spacing between two collinear elements at specified angular positions:

Consider an array of N isotropic radiators separated by d meters and positioned on the x - y plane. Modification of the space between selected elements is to reconfigure the circular array as shown in Fig. (3.21).

In the uniform circular antenna array the straight collinear distance between any two elements passing through the origin of the array depends on the equation shown below. All elements were arranged on the peripheral of a circle with elements separation d value depends on the equation shown below.

$$d = 2a \sin\left(\frac{\pi}{N}\right)$$

Where a is the radius of the circular array.

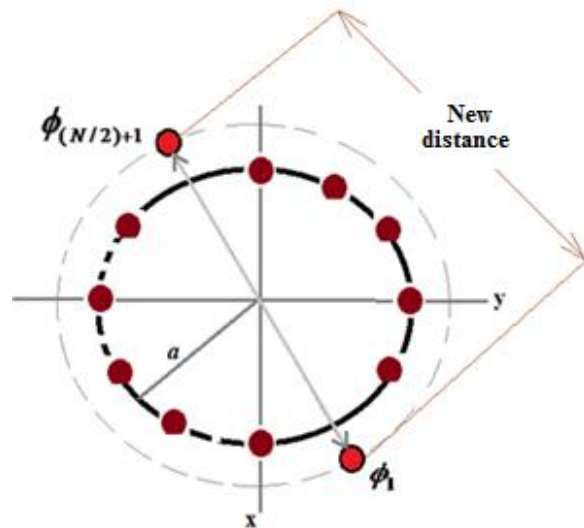


Fig. (3.21) Geometry of reconfigured circular antenna array in x - y plane.

Reconfiguration of the array is to modify the distance between the selected elements that lies at the two ends of any diameter of the

circular array. The new distance is less or more than the radius of the circular array. In broadside array ($\theta_0 = 0, \phi_0 = 0$), the distance between the two selected elements is $2d_r$. The array factor for the two selected elements can be written as:

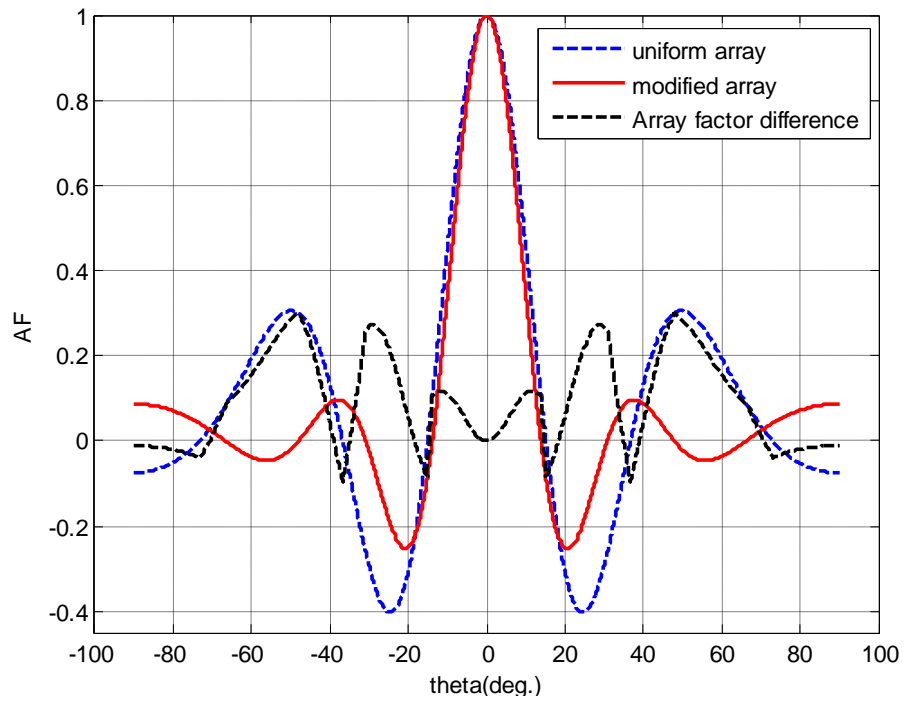
$$AF_{N_r=2} = 2I_r \cos(kd_r \sin \theta \cos \phi_{rn}) \quad \text{at } \phi = 0 \quad \dots\dots\dots(3.3)$$

The array factor of the modified array can be written as:

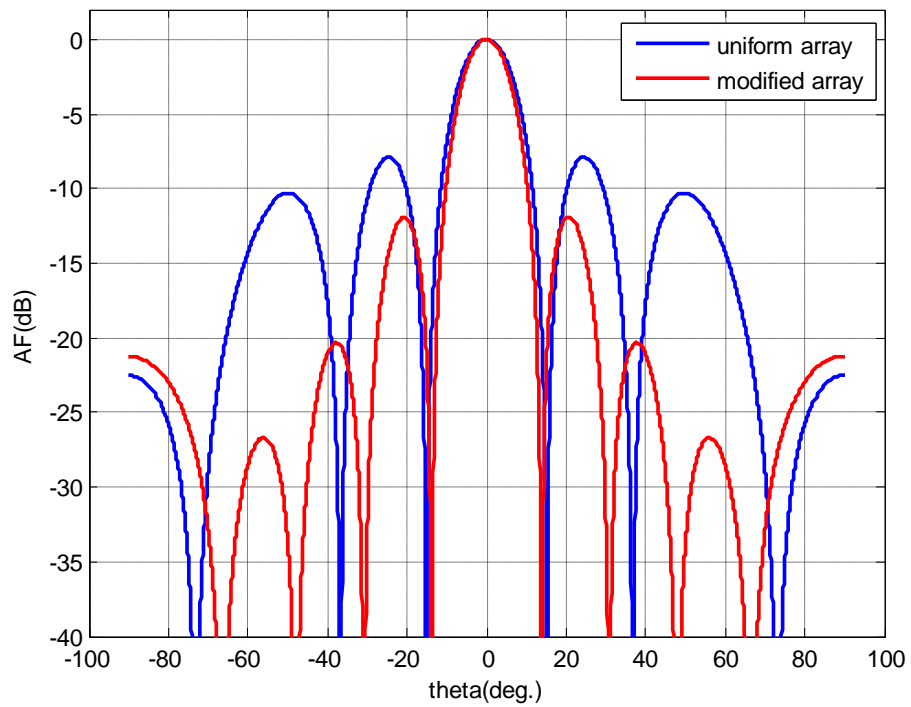
$$AF_r(\theta, \phi) = \sum_{n=1}^N I_n \exp(jka \sin \theta \cos \phi_n) \pm 2I_r \cos(kd_r \sin \theta \cos \phi_{rn}) \quad \dots\dots\dots (3.4)$$

Fig.(3.22) shows the plot of the array factor pattern of 12 elements antenna circular array of uniform excitations. The plot also shows the pattern of the modified array. The two selected elements for the modified array are at angular position ($\phi_1 = 30^\circ, \phi_2 = 210^\circ$). It is clear from the plot that there is good reduction in sidelobes level with appreciable decrease in beamwidth.

Fig. (3.23) shows modified amplitude excitation with modified spacing between two collinear elements in the array. This form of the array leads to good reduction in sidelobes level as compared with the modified in their collinear spacing only.

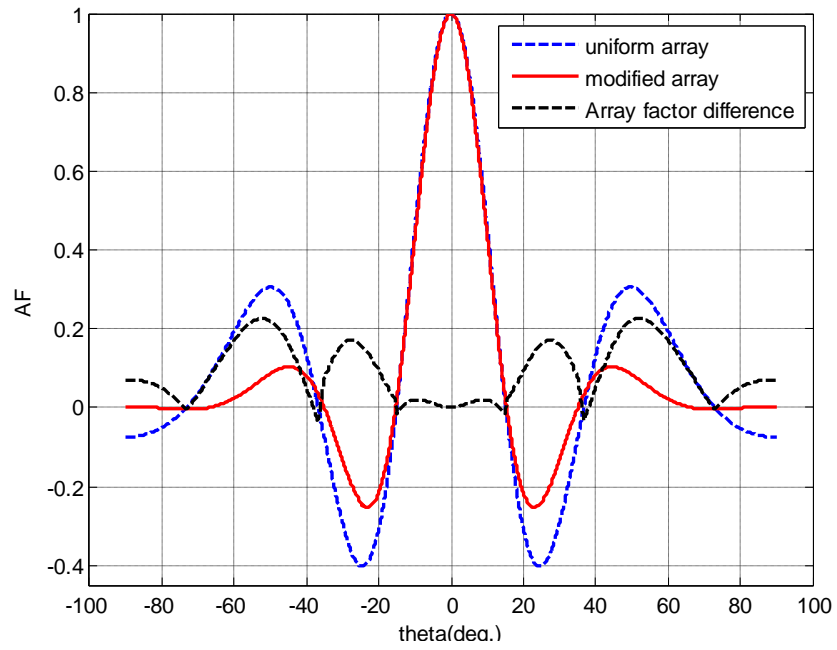


-a-

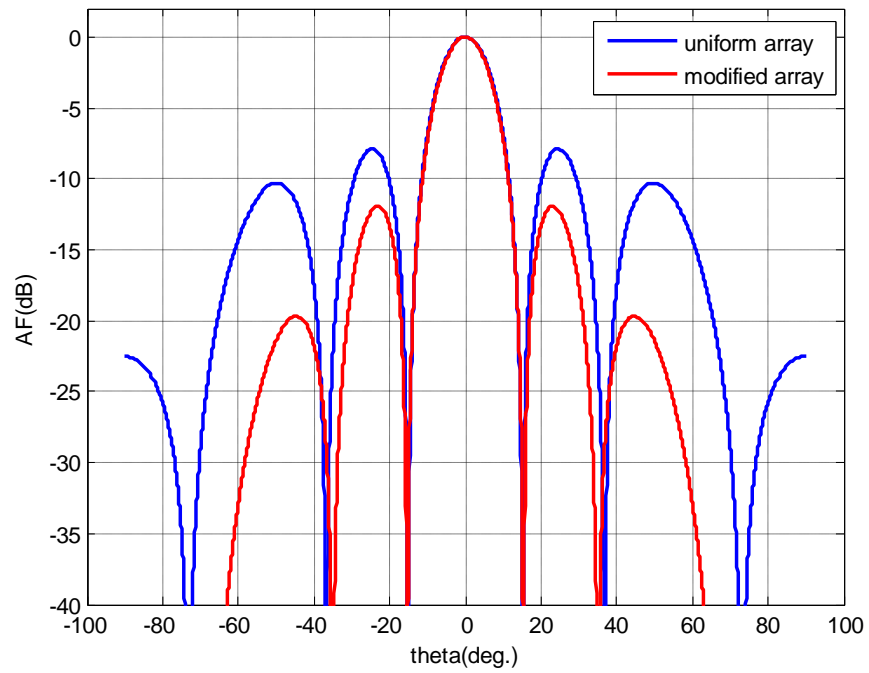


-b-

Fig(3.22) a&b-Radiation pattern of 12-element uniform circular antenna array with radiation pattern of 12-element modified spacing between the two collinear selected elements



-a-



-b-

Fig(3.23) a&b-Radiation pattern of 12-element uniform circular antenna array with radiation pattern of 12-element for modified spacing between the two collinear elements and modified excitation for the same selected elements

Fig. (3.24) shows the first and second sidelobes level for the reconfigured array. Sidelobes level were plotted versus the distance between the two reconfigured elements. It is clear from the plot that sidelobes level reduction change with distance separation between the two selected elements.

Fig. (3.25) shows the plot of the area ratio between the reduced sidelobes level of the reconfigured circular array to that of a uniformly excited circular array of equal size, versus the distance d_r between the two selected elements. The plot indicates a reduction in the area ratio at certain values of d_r . The reduction in the area ratio means a reduction in the sidelobes level. The plot also shows this area ratio plotted versus d_r for modified excitations of the selected elements of the reconfigured array. The plot of the area ratio for the reconfigured circular array of modified excitation for the selected elements gives better result as that compared to that of the reconfigured array with uniform excitation.

Fig. (3.26) shows the improvement factor plotted against the reconfigured distance. The figure shows two plots, one for the reconfigured array with uniform excitation and the other for the reconfigured array with modified excitation. The improvement factor represents the total area under the pattern of the array factor difference. The more positive value of the improvement factor is the more reduction in the sidelobes level.

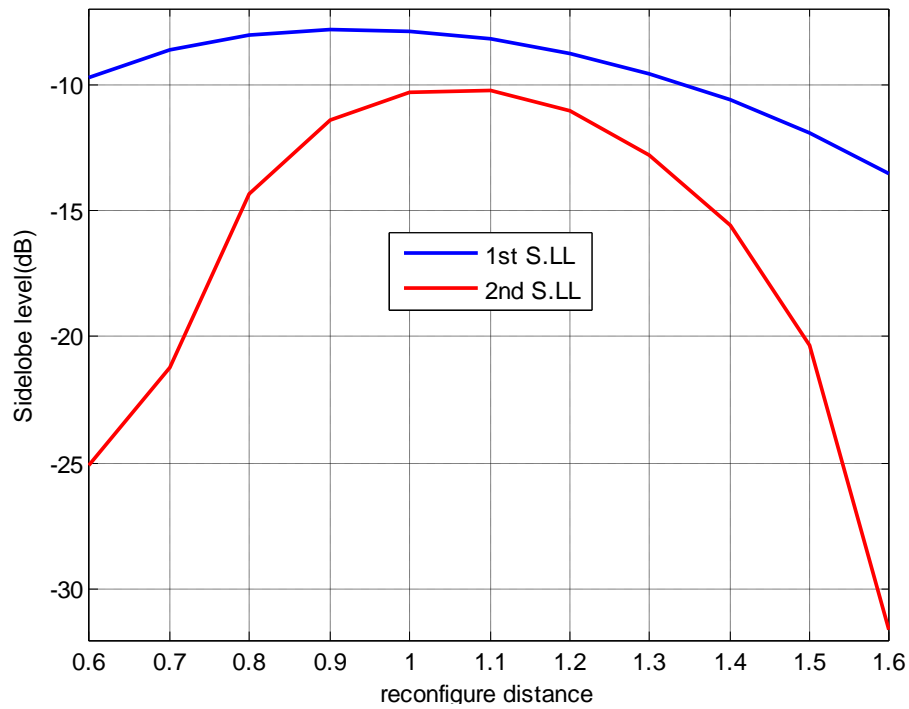


Fig. (3.24) Plot of first and second sidelobes level for N=12 modified circular array versus spacing between the two collinear elements at $(\phi_1 = 30^\circ, \phi_7 = 210^\circ)$

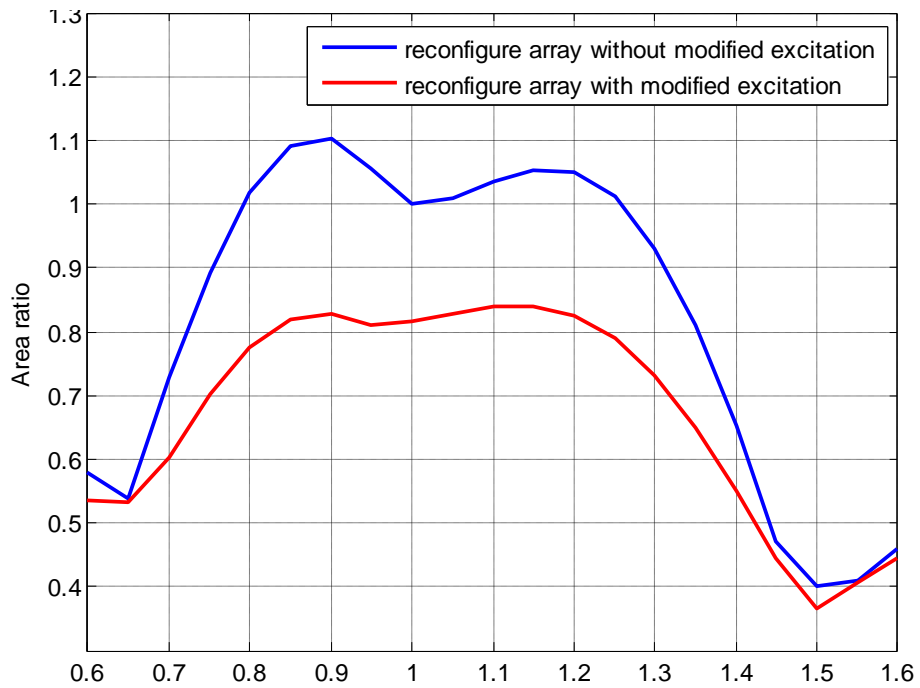


Fig. (3.25) Plot of ratio of area under the curve for N=12 modified circular array versus spacing between the two collinear elements at $(\phi_1 = 30^\circ, \phi_7 = 210^\circ)$

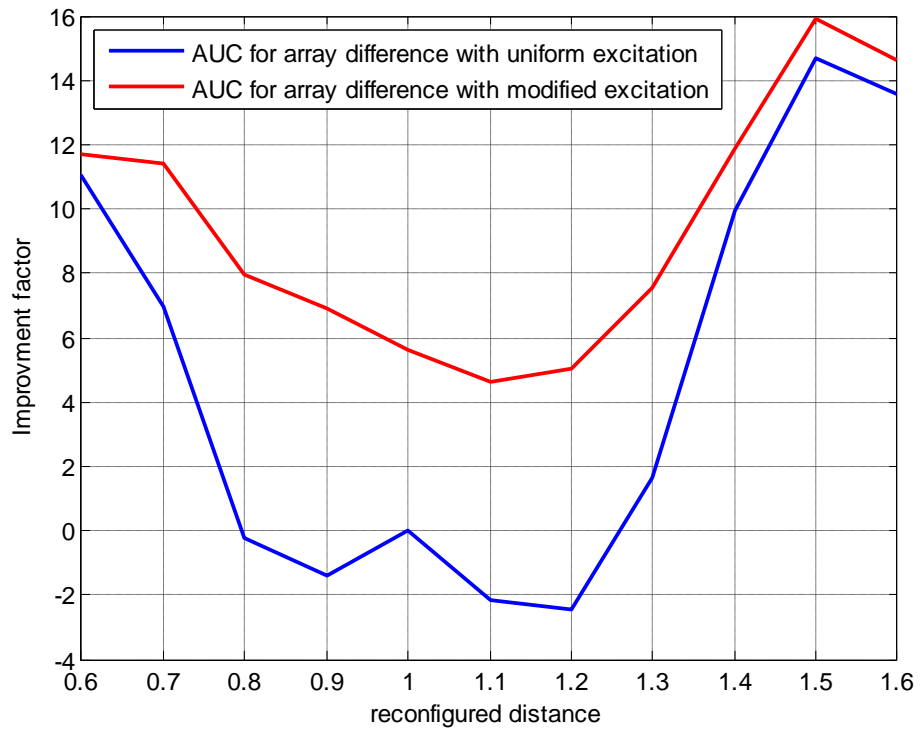


Fig. (3.26) Plot of the improvement factor versus modified spacing between the two collinear elements at $(\phi_1 = 30^\circ, \phi_7 = 210^\circ)$

CHAPTER FOUR

Sidelobes level Reduction Using Concentric Circular Antenna Array

4.1 Introduction:

Among the different types of antenna arrays, concentric circular antenna arrays (CCAA) has been of considerable interest in a numerous applications which comprises sonar, radar, mobile and commercial satellite communications systems[33-36]. It is worthwhile to search for a method of minimizing the sidelobes level of the circular antenna array. One, out of many solutions of reducing the sidelobes level of a circular antenna array is by using a concentric circular antenna array as shown in Fig. (4.1).

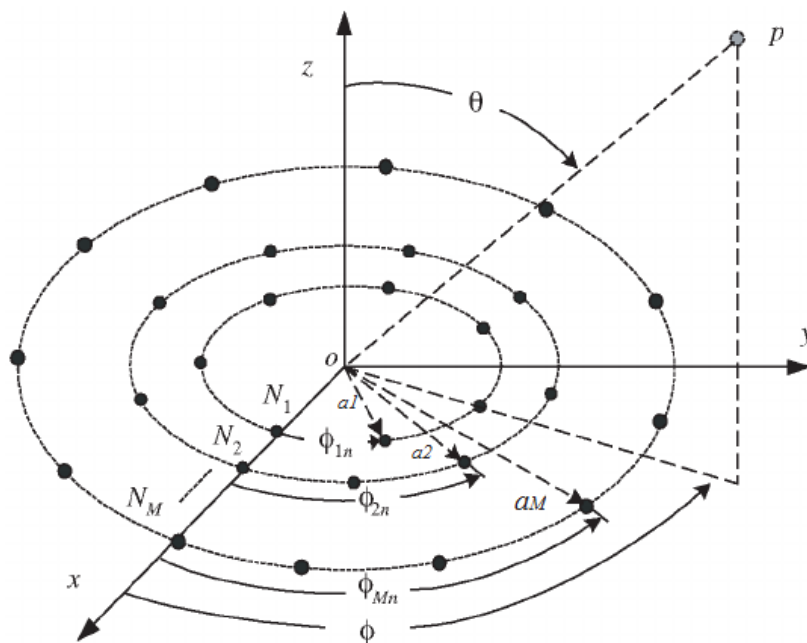


Fig. (4.1) Geometry of Concentric circular antenna array positioned in x-y plane.

Concentric circular antenna array has a number of advantages including the flexibility in array pattern synthesis and design both in narrowband and broadband beam forming techniques.

Since a concentric circular array does not have edge elements, directional patterns synthesized with a concentric circular array can be electronically rotated in the plane of the array without a meaningful change of the beam shape.

4.2 Equation of concentric circular array:

The geometry of a concentric circular antenna array is shown in Fig. (4.1) this array was placed in x-y plane where there are M concentric circular rings. The m th ring has a radius a_m and corresponding number of elements is N_m where ($m = 1, 2, \dots, M$). If all elements are assumed to be isotropic sources, then the radiation pattern of a concentric circular antenna array can be written in terms of its array factor:

$$AF(\theta, \phi) = \sum_{m=1}^M \sum_{n=1}^{N_m} I_{mn} e^{j(ka_m \sin \theta \cos(\phi - \phi_{nm}) + \alpha_{nm})} \dots (4.1)$$

$$a_m = \frac{d_m}{2 \sin \frac{\pi}{N_m}} \dots (4.2)$$

a_m = Radius of m th ring.

M = Number of rings.

N_m = Number of elements in m th ring.

d_m = Inter-element spacing of m th ring.

I_{mn} = Amplitude excitation of the n element of the m th ring

ϕ_{mn} = Angular position of concentric circular array with respect to $\phi = 0^\circ$

$$\phi_{mn} = \frac{2\pi n}{N_m}, \quad n = 1, 2, \dots, N_m, \quad m = 1, 2, \dots, M \quad \dots \dots \dots (4.3)$$

α_{mn} = Phase excitation of the n th element (the phase difference between the individual elements in the array) given by:

$$\alpha_{mn} = -ka_m \sin(\theta_0) \cos(\phi_0 - \phi_{mn}) \quad n = 1, 2, \dots, N_m, \quad m = 1, 2, \dots, M \quad \dots \dots (4.4)$$

It was shown in equation 2.14 that when all elements of the uniform circular array are equally spaced. The pattern for such a circular array can be approximated as:

$$AF(\theta, \phi) \cong NIJ_{mN}(k\rho)$$

For M concentric rings in the array, and each ring contains a "large number" of elements. The array factor will be approximately written as [30]:

$$AF(\theta, \phi) \cong \sum_{m=1}^M N_m I_m J_0(k\rho_m) \quad \dots \dots \dots (4.5)$$

$$\rho_m = ka_m \sin \theta \quad (m = 1, 2, \dots, M) \quad \text{For vertical pattern}$$

$$\rho_m = 2ka_m \sin \frac{\phi}{2} \quad (m = 1, 2, \dots, M) \quad \text{For horizontal pattern}$$

4.3 – Sidelobes level reduction by using concentric circular array:

Since circular antenna array suffers from high sidelobes level as shown in chapter 2, a method, out of many used for reduction. These sidelobes in circular antenna array is to apply concentric circular antenna array of different number of elements and radii [11, 21].

Simulations were carried out for concentric circular antenna array of two rings with various numbers of elements to investigate sidelobes reduction by selection of suitable radii; this means selection of a suitable inter-element spacing d between their elements.

4.3.1-Sidelobes reduction for 12elements two concentric circular array:

Fig. (4.2) shows the radiation patterns of a 12-element circular array together with the array pattern of 12-element concentric circular array. The inter-element spacing of the 12-element circular array is 0.5λ . In this figure, the level value of the first sidelobe of this circular array pattern is of order -7.89 dB and the beamwidth of the main beam is 21.9° . The same 12 elements were then distributed between two concentric rings. The inner ring contains 4 elements with radius equal to 0.51λ and the outer ring contains 8 elements with radius equal to 1.21λ . The inner and the outer rings has inter-element spacing of 0.8λ and 0.95λ respectively.

It is clear from the figure shown that there is good reduction in the first sidelobe level as compared with that of the circular array of the same number of elements.

The figure also shows the plot of the array factor difference were its positive value is responsible in sidelobes reduction.

4.3.2-Sidelobes reduction for 14elements concentric circular array:

Fig. (4.3) shows the radiation patterns of a 14-element circular array together with the array pattern of 14-element concentric circular array. The inter-element spacing of the 14-element circular array is 0.5λ . In this figure, the value of the first sidelobe level of the circular array

pattern is of order -7.89 dB and the beamwidth of the main beam is 18.7° . The same 14 elements were then distributed between two concentric rings. The inner ring contains 4 elements with radius equal to 0.51λ and the outer ring contains 10 elements with radius equal to 1.3λ . The inner and the outer ring has inter-element spacing of 0.8λ and 0.815λ respectively.

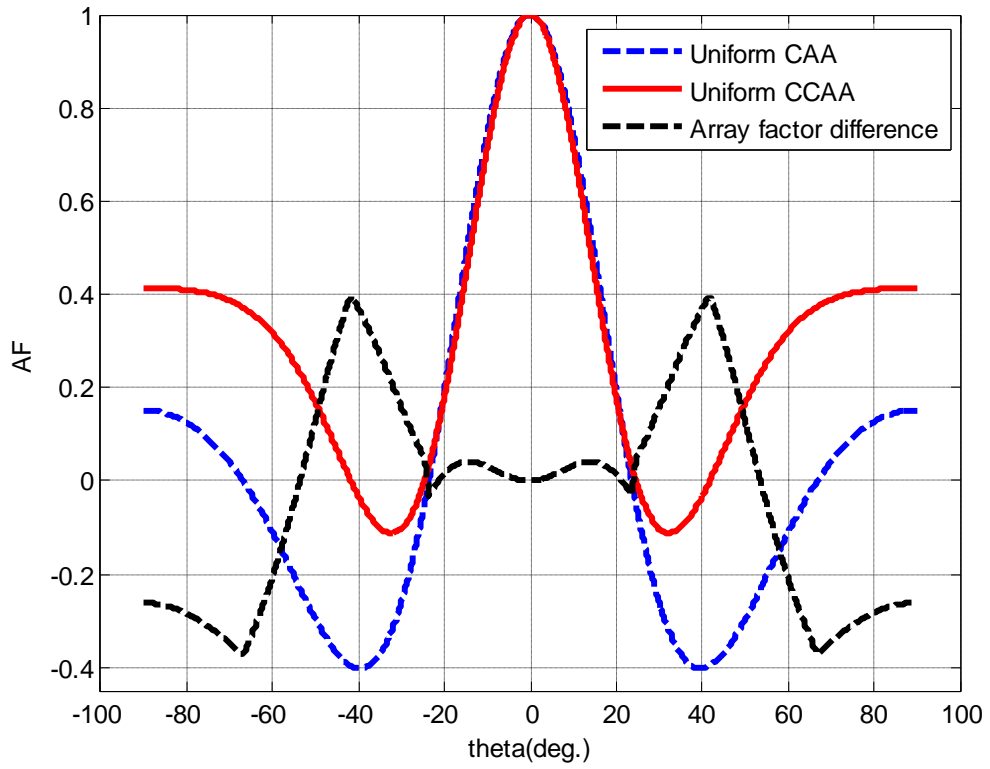
It is clear from the Fig. (4.3) with its plot of the array factor difference that there is good reduction in first and second sidelobes level as compared with that of the circular array of the same number of elements.

4.3.3- Sidelobes reduction for 18 elements concentric circular array:

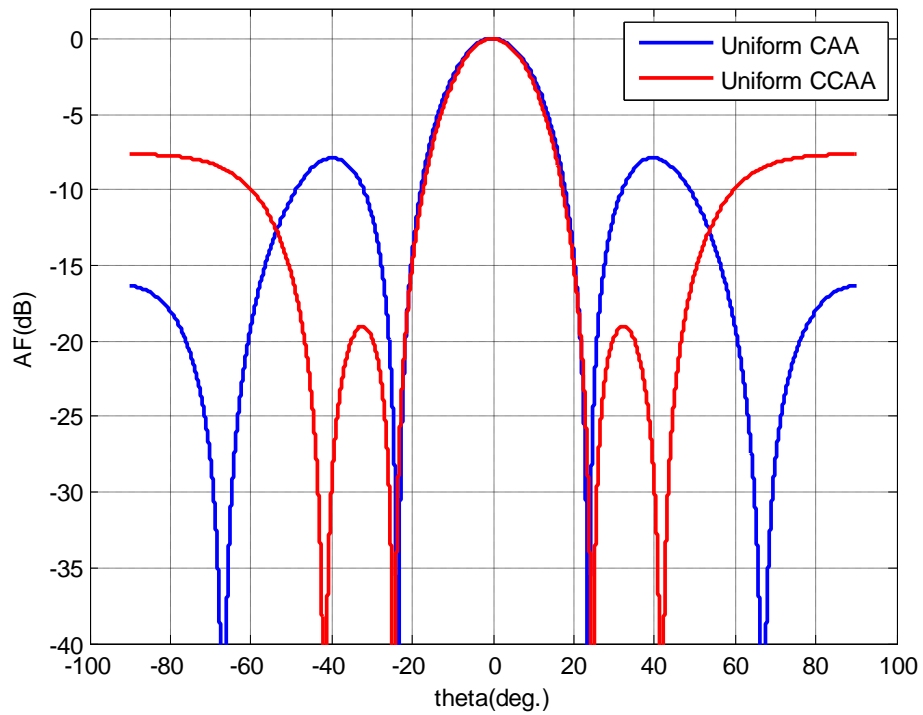
Fig. (4.4) shows the radiation patterns of an 18-element circular array together with the array pattern of 18-element concentric circular array. The inter-element spacing of the 18-element circular array is 0.5λ . In this figure, the value of the first sidelobe level of the circular array pattern is of order -7.89 dB and the beamwidth of the main beam is 14.5° . The same 18 elements were then distributed between two concentric rings. The inner ring contains 6 elements with radius equal to 0.765λ while the outer ring contains 12 elements with radius equal to 1.72λ . The inner and the outer ring has inter-element spacing of 0.8λ and 0.9λ respectively.

It is clear from the figures shown that there is good reduction in the sidelobes level as compared with that of the circular array of the same size.

The same figure also shows the difference of the array factor between the absolute values of the array factor of the two arrays. The positive value of the array factor difference indicates a reduction in the sidelobes level.

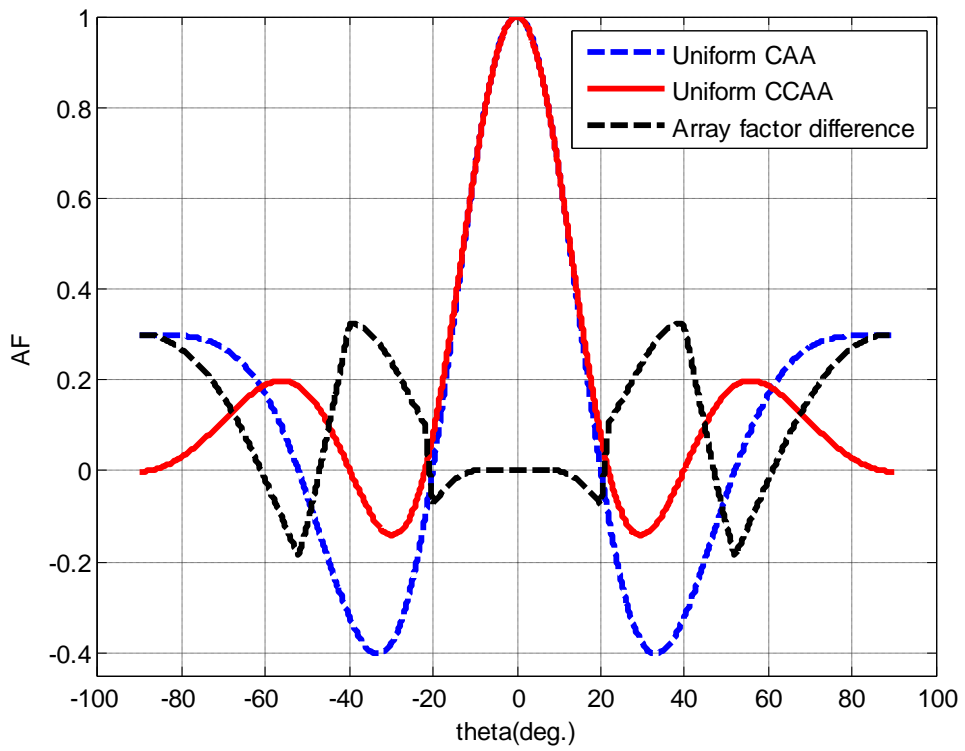


-a-

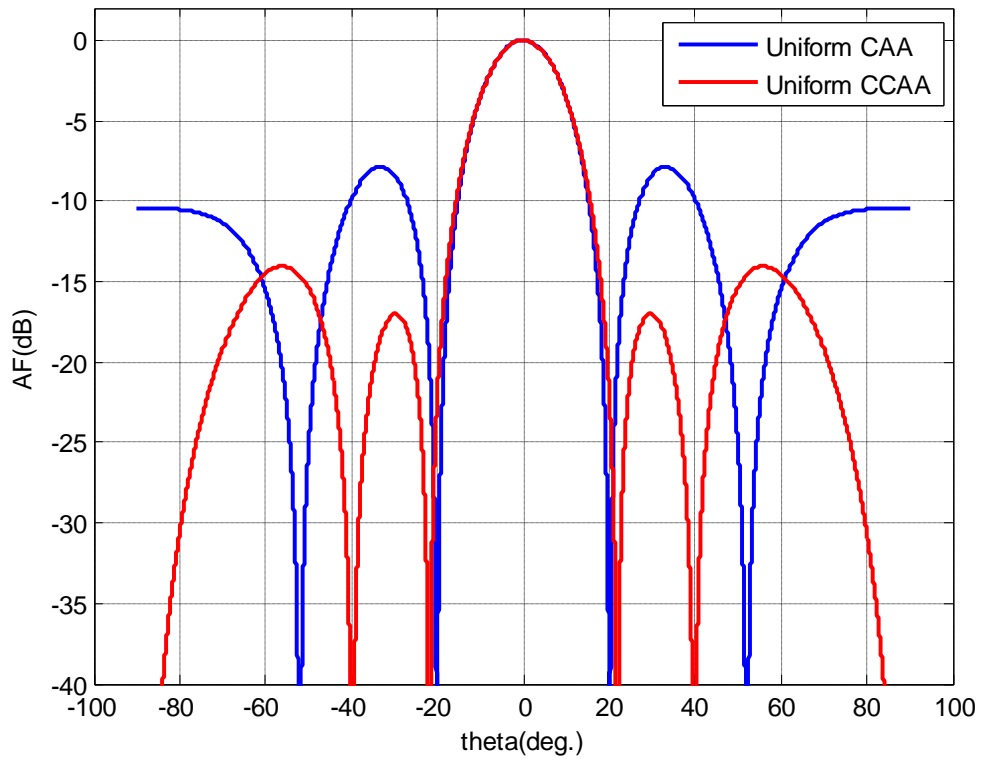


-b-

Fig. (4.2) a&b- Radiation pattern for concentric circular array with inner ring of 4 elements and outer ring of 8 elements



-a-



-b-

Fig. (4.3) a&b- Radiation pattern for concentric circular array with inner ring of 4 elements and outer ring of 10 elements

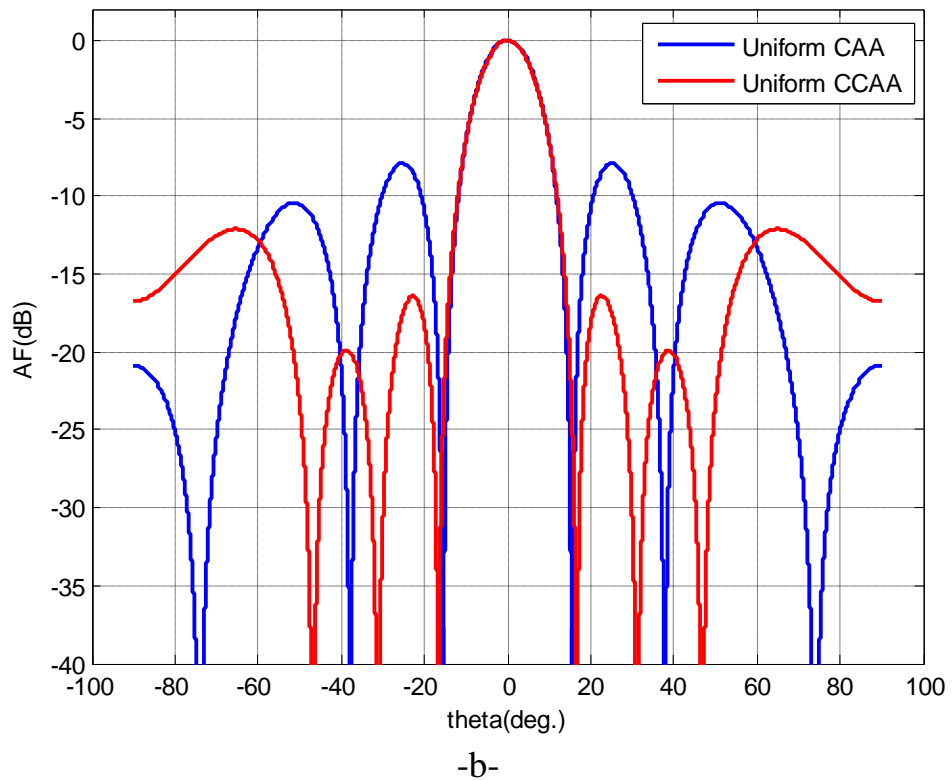
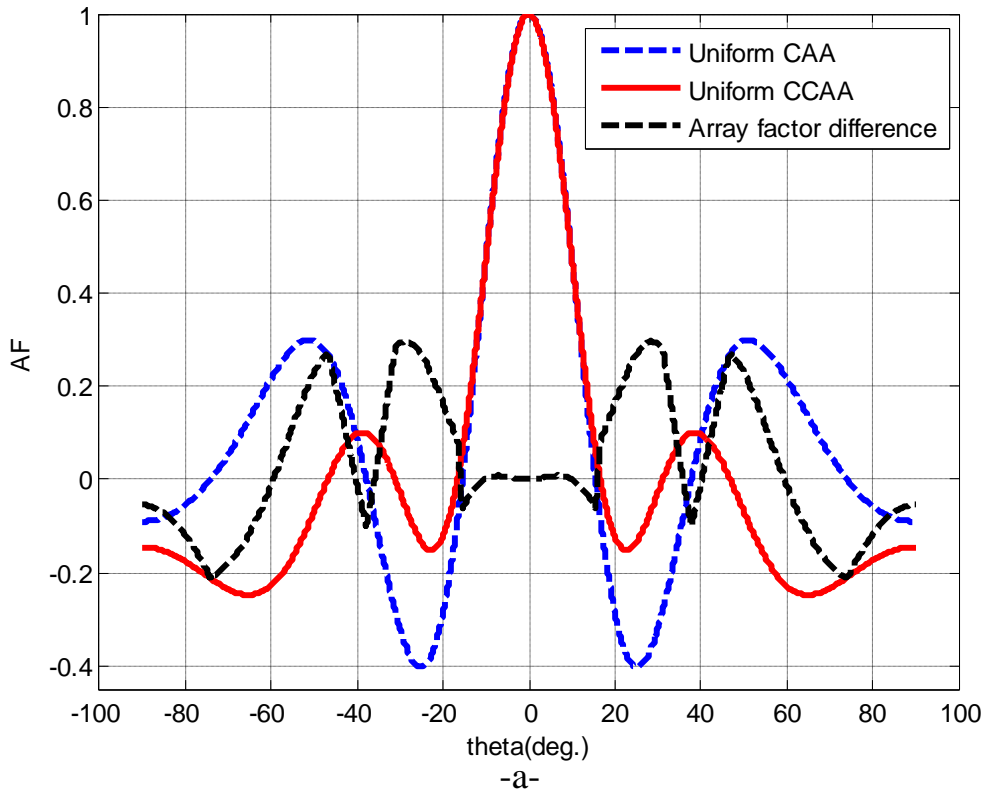


Fig. (4.4) a&b-Radiation pattern for concentric circular array using 18 elements in two rings, inner ring of 6 elements and outer ring of 12 elements

4.3.4- Sidelobes level reduction for 24 elements circular array:

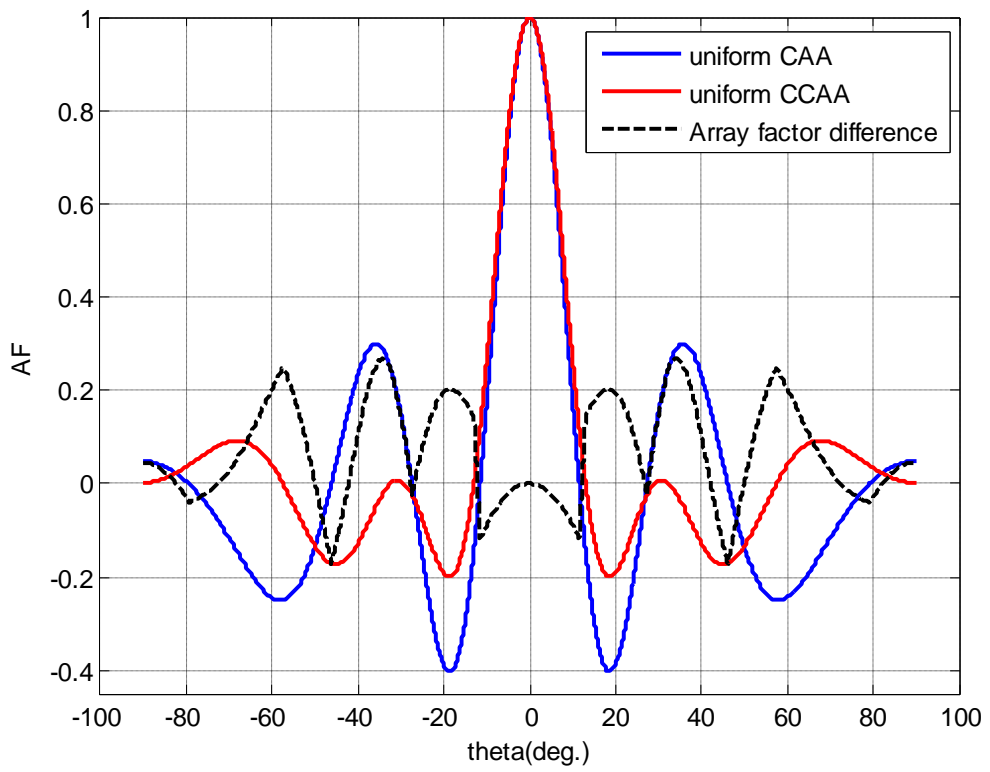
Simulation was carried out for 24-element concentric circular array of many configurations according to the number of elements contained in ring of the concentric circular array.

a- (10-14) concentric circular array:

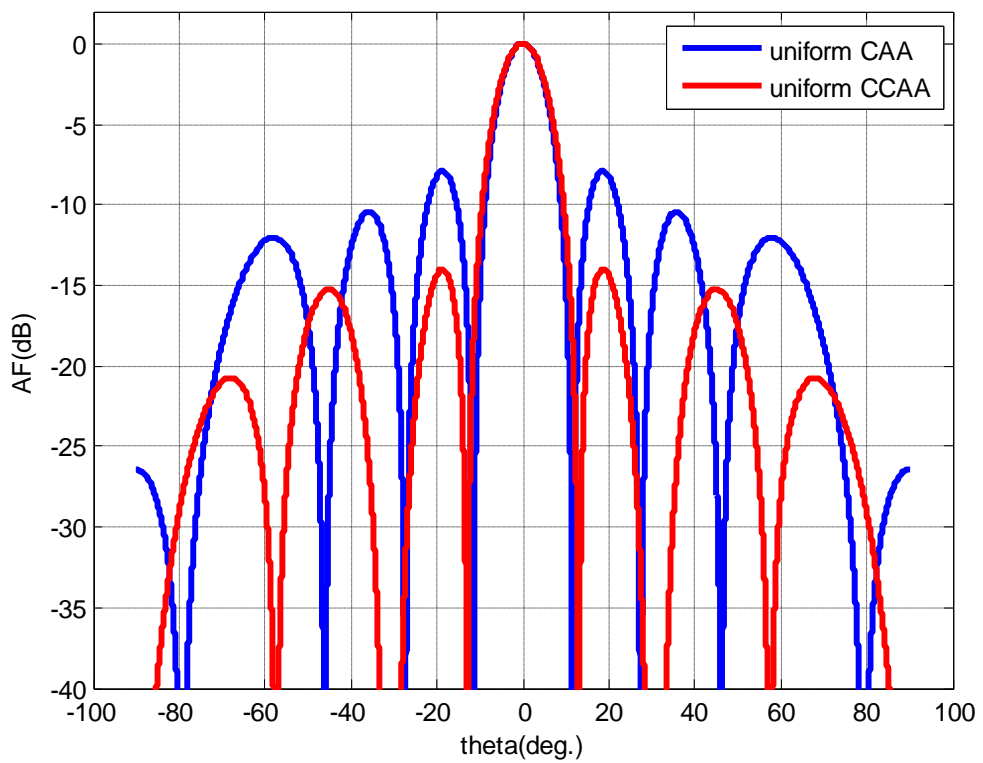
Fig. (4.5a,b) shows the radiation patterns of a 24-element circular array together with the array pattern of 24 elements concentric circular array. The inter-element spacing of the 24-element circular array is 0.5λ . In this figure, the level value of the first sidelobe of this circular array pattern is of order -7.89 dB and the beamwidth of the main beam is 10.9° .

The same 24 elements were then distributed between two concentric rings. The inner ring contains 10 elements and the outer ring contains 14 elements. The inner and the outer rings have inter-element spacing of 0.75λ and 0.98λ respectively. The radius of the inner ring is equal to 1.2λ and that of the outer radius is 2.15λ .

The plot shows good reduction in the sidelobes level as compared with that of the circular array of the same number of elements. This is clear from the plot of the difference array factor in the same figure. The more positive of the area under the difference array factor is the more reduction in the sidelobes level.



-a-



-b-

Fig. (4.5) a&b-Radiation pattern for concentric circular array using two rings with inner ring contains 10 elements and outer ring contains 14 elements

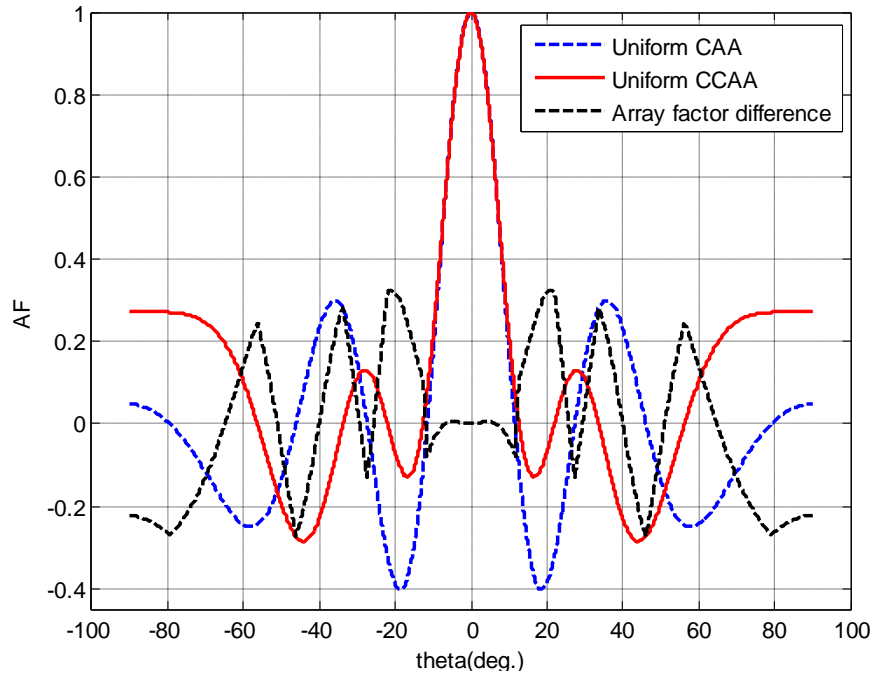
b- (8-16) concentric circular array:

Fig. (4.6a,b) shows the radiation patterns of a 24 elements circular array together with the array pattern of 24 elements concentric circular array CCAA. The inter-element spacing of the 24 elements circular array is 0.5λ . In this figure, the value of the first sidelobe of the circular array pattern is of order -7.89 dB and the beamwidth of the main beam is 10.9° .

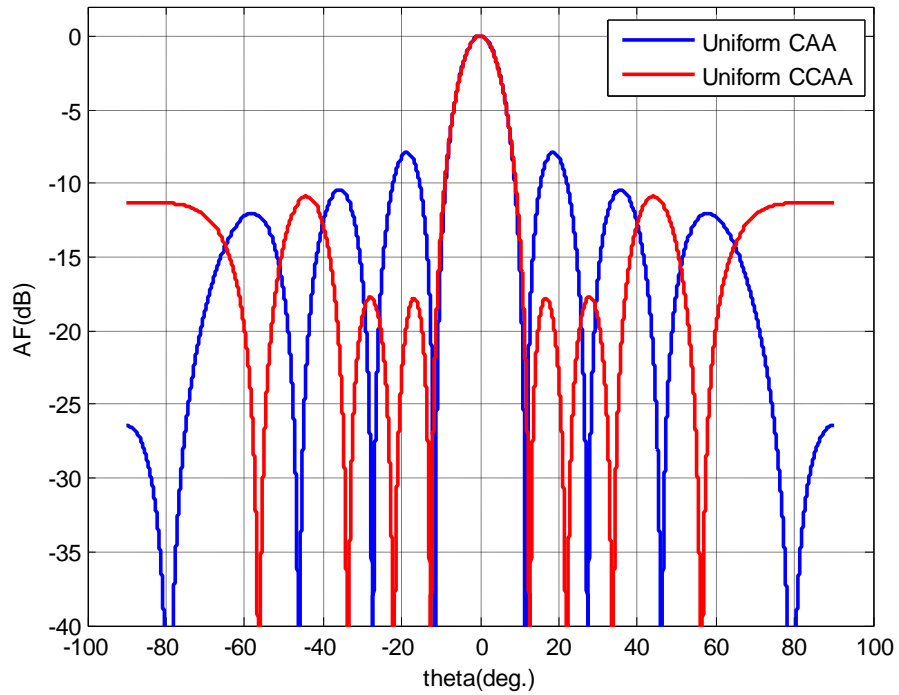
The same 24 elements were then distributed between two concentric rings. The inner ring contains 8 elements and the outer ring contains 16 elements. The inner and the outer rings has inter-element spacing of 0.75λ and 0.9λ respectively. The radius of the inner ring is equal to 1.25λ and that of the outer radius is 2λ . The plot shows good reduction in the sidelobes level as compared with that of the circular array of the same number of elements. Again this is also clear from the plot of the difference array factor which indicates that the more positive of the area under the difference array factor is the more reduction in the sidelobes level.

For the same 24 elements of the two concentric rings discussed above, we used a modified amplitude excitation for selected elements in the inner and outer rings. The modified excitation for the two elements of the inner ring was performed for the two opposite elements of the array at the angular positions $(\phi_1 = 45^\circ, \phi_5 = 225^\circ)$ and that for the outer ring were performed for the two opposite elements of the array at the angular positions $(\phi_1 = 22.5^\circ, \phi_9 = 202.5^\circ)$. Amplitude excitations for the two inner elements are $(w_1=w_5=0.1)$ and that for the two outer elements are $(w_1=w_9=0.1)$. This modified in amplitude excitation resulted in better sidelobes reduction level as compared to the case

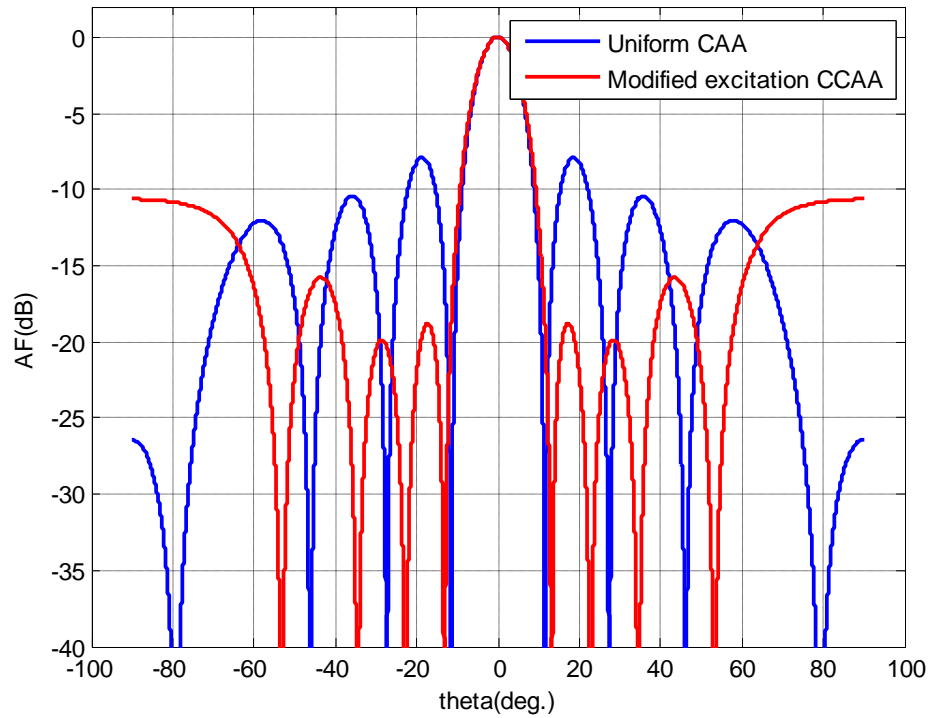
with uniform excitation for both rings. This result is clearly shown in Fig. (4.6c).



-a-



-b-



-c-

Fig. (4.6) a&b- Radiation pattern for concentric circular array using (8 -16) element of uniform excitation, c- Radiation pattern for concentric circular array for(8-16) using modified amplitude excitation for specified element.

c- (6-18)concentric circular array:

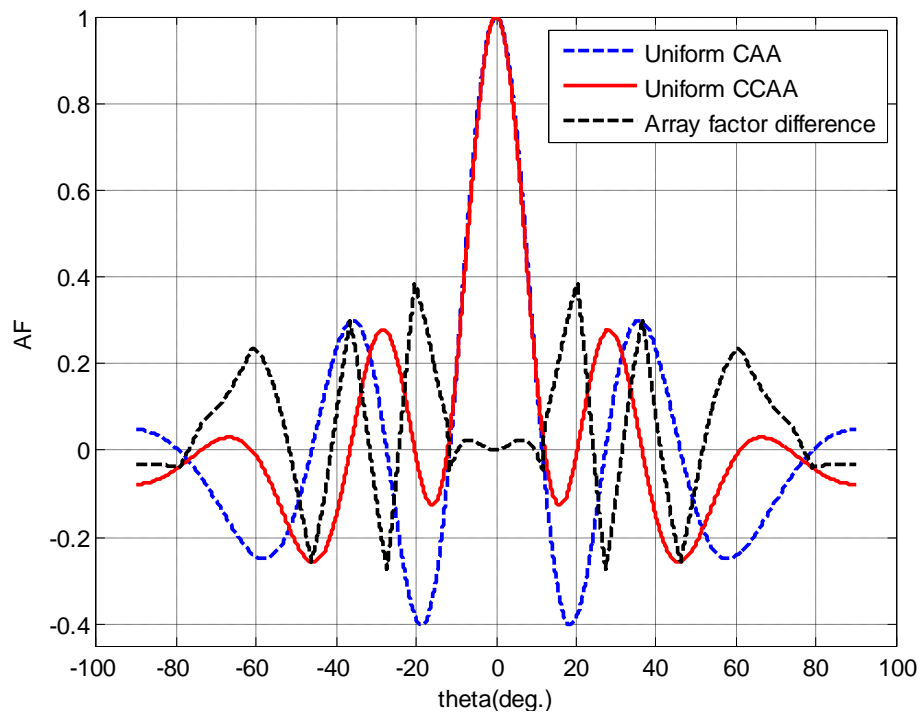
Fig. (4.7a,b) shows the radiation patterns of a 24-element circular array together with the array pattern of 24elements concentric circular array. The inter-element spacing of the 24-element circular array is 0.5λ . In this figure, the value of the first sidelobe of the circular array pattern is of order -7.89 dB and the beamwidth of the main beam is 10.9° .

The same 24 elements were then distributed between two concentric rings. The inner ring contains 6 elements and the outer ring contains 18 elements. The first and the second rings are of inter-element spacing of 0.7λ and 0.8λ respectively .The radius of the inner ring is equal to 0.6λ and that of the outer radius is 2.3λ .

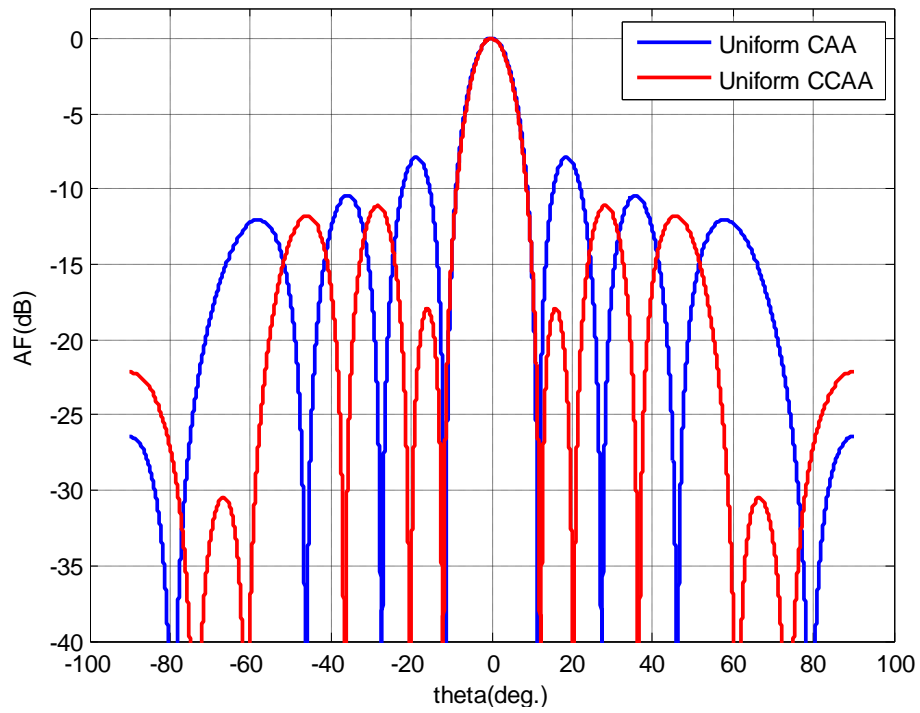
It is clear from the plot that there is good reduction in the sidelobes level as compared with that of the circular array of the same number of elements. Fig. (4.7a) shows the difference of the array factor between the two arrays. The positive area value of the array factor difference gives a degree about the amount of the reduction in the sidelobes level.

For the same (6-18) two concentric rings discussed above, we modified the excitation for the elements in the outer ring for the two opposite elements of the array that are located at angular positions ($\phi_1 = 20^\circ, \phi_2 = 40^\circ, \phi_{10} = 200^\circ, \phi_{11} = 220^\circ$).

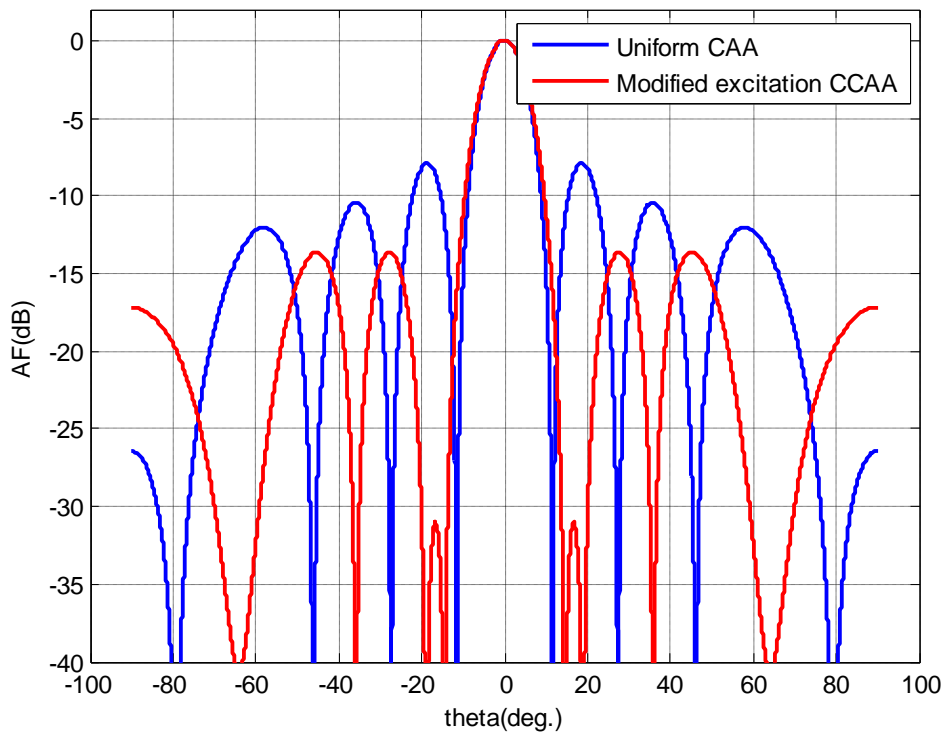
The modified excitation values for these selected elements in the outer ring are ($w_1=w_{10}=0.1$) and ($w_2=w_{11}=0.5$) respectively. This modifications in amplitude excitations resulted in better sidelobes reduction as compared to the case with uniform excitation for both rings. This result is clearly shown in Fig. (4.7c).



-a-



-b-



-c-

Fig. (4.7) a&b-Radiation pattern for concentric circular array using (6-18) element antenna for uniform array, c-Radiation pattern for concentric circular array for (6-18) using modified amplitude excitation for specified element.

4.4 Discussions for the results of concentric circular antenna array:

The results shown in the following figures were taken from three cases:

Case one represents the performance of the concentric circular array as a function of inter-element spacing for the two rings that constitute the array.

Fig. (4.8) shows plots of beamwidth versus spacing between the elements for different configurations of 24 elements concentric circular array. It is clear from the plot that the beamwidth is inversely proportional with inter-element spacing. The plot gives also indication that, when the numbers of elements in the outer ring increase the beamwidth decrease.

Fig. (4.9) shows the plot of the area ratio (area under the sidelobes of the concentric circular array to that of the original circular array) for different state of concentric circular antenna array versus spacing between the elements. The figure indicates that whenever the area ratio is below the value of unity, there will be a local reduction in the sidelobes level of the array.

Fig. (4.10) shows the plot of the directivity for different state of concentric circular antenna array versus spacing between the elements.

Fig. (4.9) and Fig. (4.10), reveal that whenever the area ratio is below the value of unity, there will be a local increase in the value of directivity. The directivity reaches maximum when the area ratio reach minimum.

Case two represents the performance of the concentric circular array as a function of the spacing between the two rings of the array keeping the radius of the inner ring fixed at specified value.

Fig. (4.11) represents the first, second and third sidelobes level plotted versus spacing between the two rings for different forms of concentric circular array. In this figure the radius of the inner ring is kept constant at 1.12λ while the spacing between the two rings was varied between $(1.6-2.8)\lambda$. The figure reveals that good sidelobes reduction for the first and second sidelobes is for the concentric circular array of 10 elements in the inner ring and 14 elements in the outer ring.

Fig. (4.12) represents the plot of the beamwidth and beamwidth difference versus the spacing between the two rings for different forms of concentric circular array. The beamwidth difference represents the difference in beamwidth between the original circular antenna array and that of the concentric circular antenna array of the same number of elements. In this figure the radius of the inner ring is kept constant at 1.12λ while the spacing between the two rings was varied between $(1.6-2.8)\lambda$. The figure shows decreasing in beamwidth with increasing the spacing between the two rings. The figure also shows decreasing in beamwidth when the outer ring contains more elements as compared with the inner ring; this is also clear from the relation of the beamwidth given in section 2.5.3

The positive value of the beamwidth difference represents improvement in the beamwidth of the concentric circular antenna array as compared with the beamwidth of the original single ring circular antenna array.

Fig. (4.13) shows the plot of the area ratio for different state of concentric circular antenna array. In this figure the radius of the inner ring is kept constant at 1.12λ while the spacing between the two rings

was varied between $(1.6 - 2.8)\lambda$. The figure indicates that whenever the area ratio is below the value of unity, there will be a reduction in the sidelobes level.

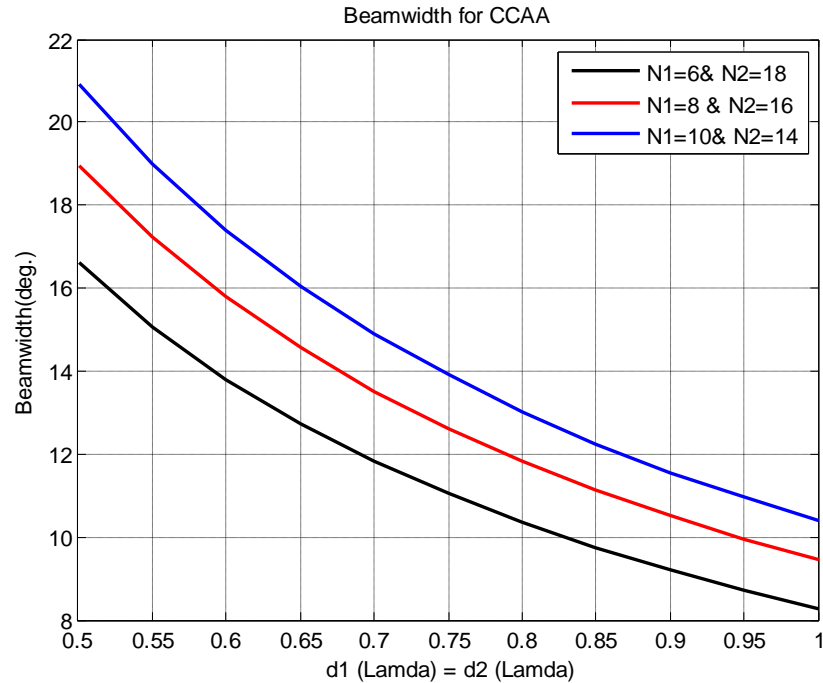


Fig. (4.8) Plot of Beamwidth for concentric circular antenna array versus spacing between the elements at 'd1=d2'

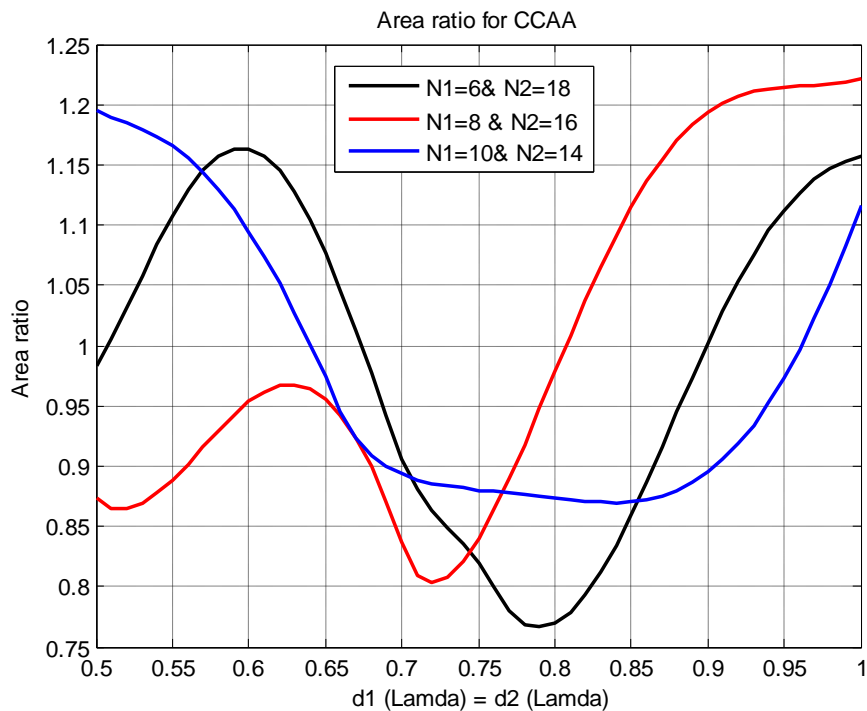


Fig. (4.9) Plot of ratio of area under the curve for different state of concentric circular antenna array versus spacing between the elements for 'd1=d2'.

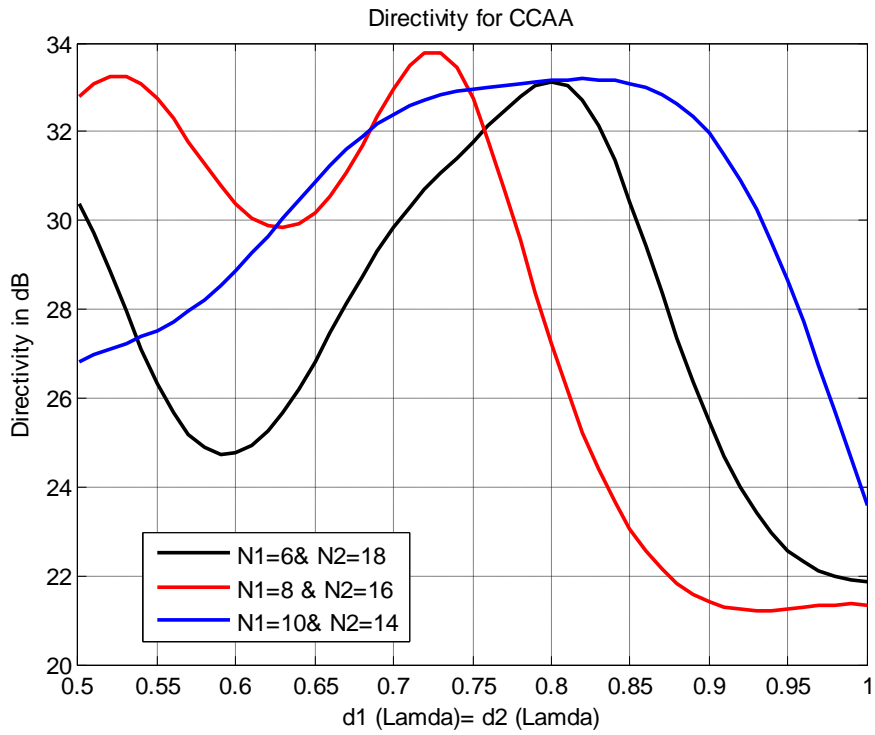
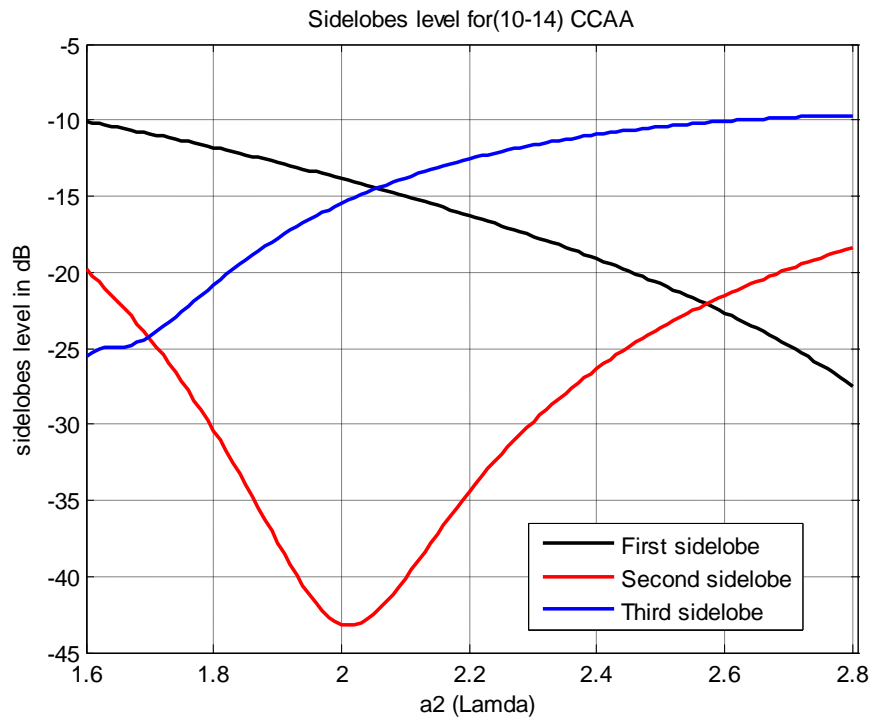
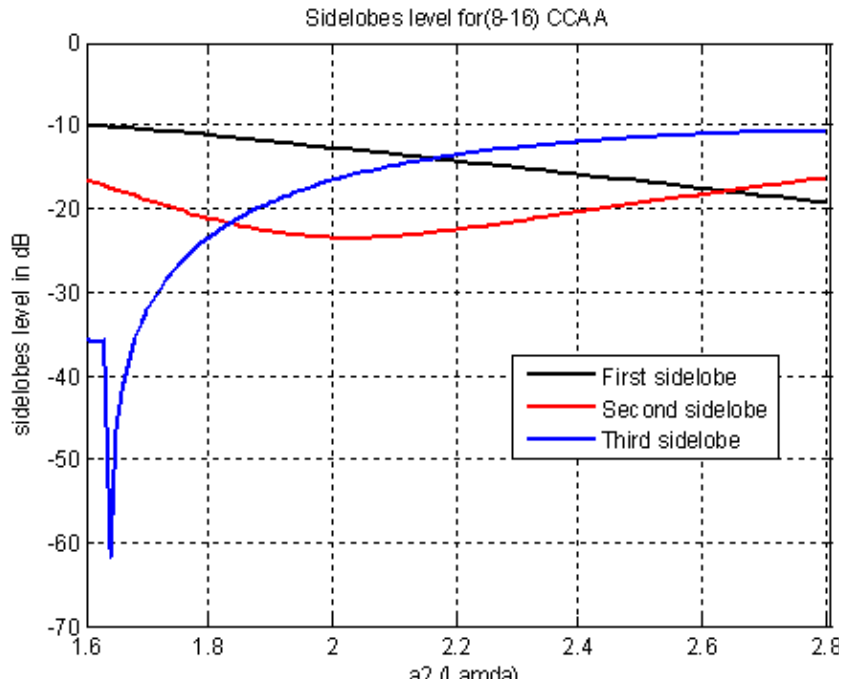


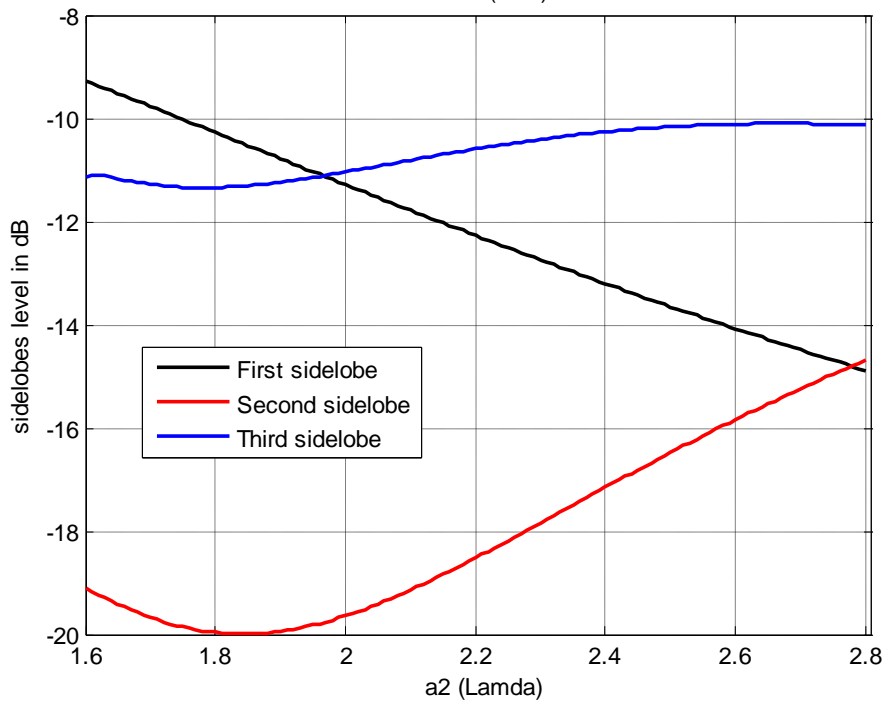
Fig. (4.10) Plot of directivity for different state of concentric circular antenna array versus spacing between the elements for ' $d1=d2$ '



-a-

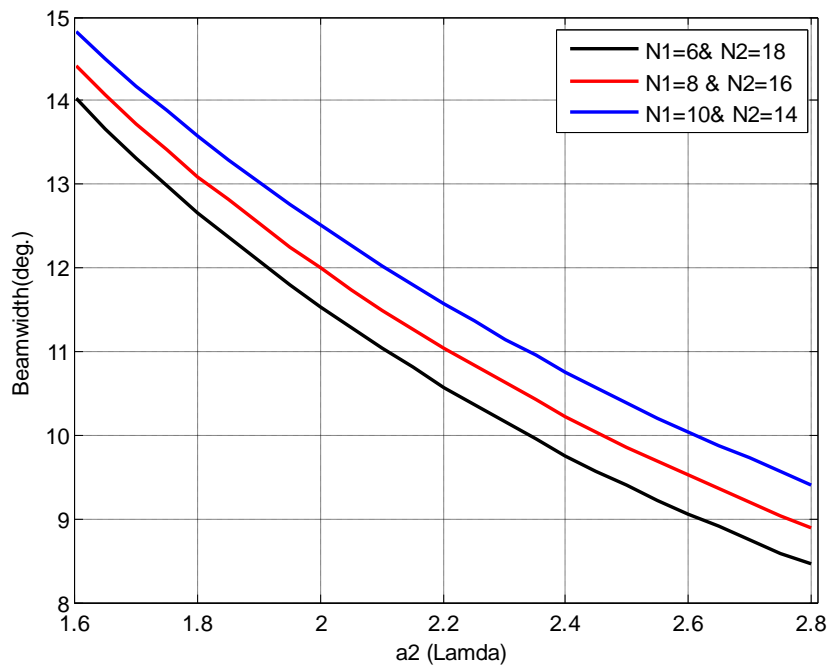


-b-

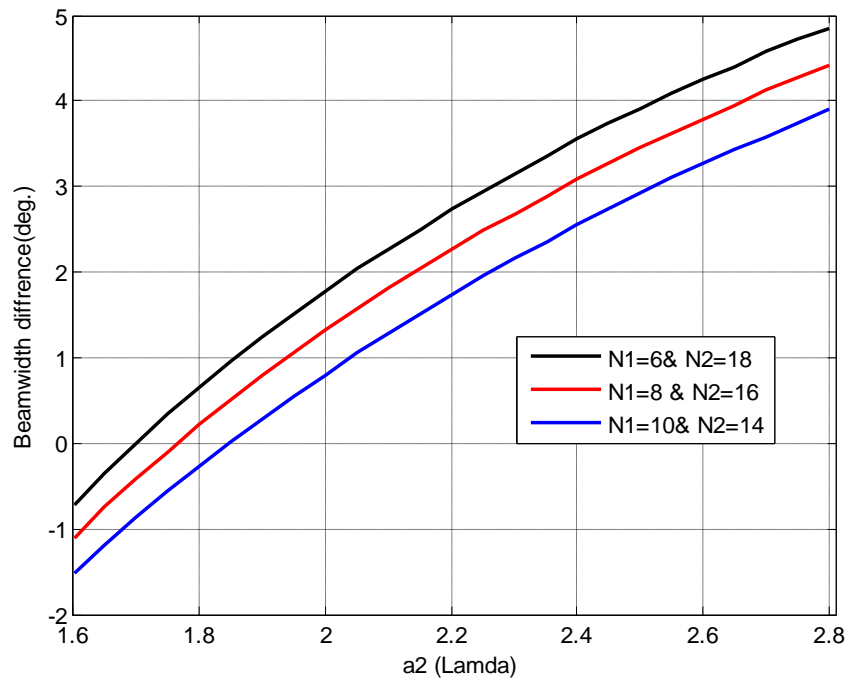


-c-

Fig. (4.11) Plot of sidelobes level versus spacing between the rings for
a- uniform concentric circular array $N_1=10, N_2=14$
b- uniform concentric circular array $N_1=8, N_2=16$
c- uniform concentric circular array $N_1=6, N_2=18$



-a-



-b-

**Fig. (4.12)a-Plot of beamwidth for concentric circular antenna array versus spacing between the rings.
b-Plot of the beamwidth difference for concentric circular array versus spacing between the rings.**

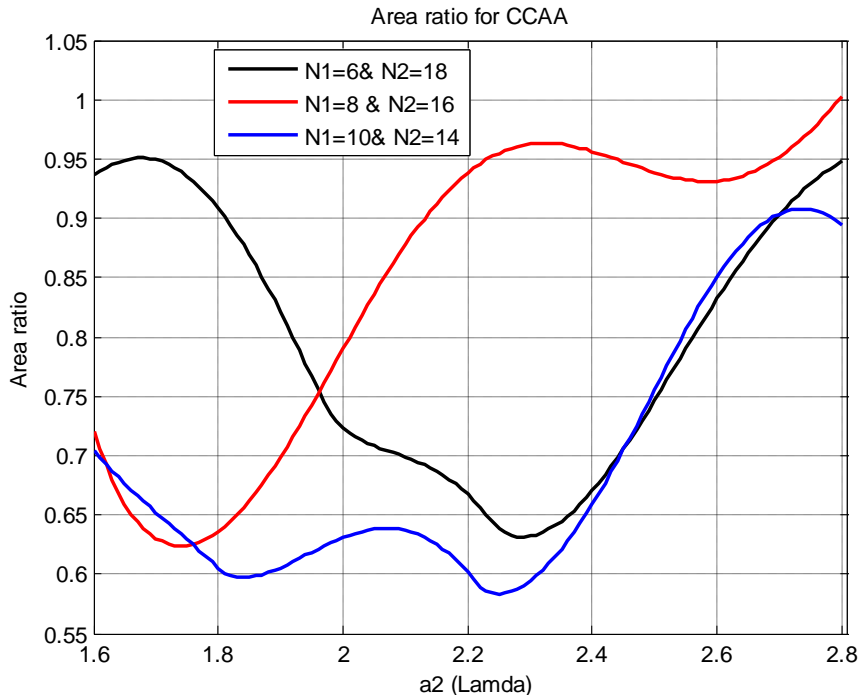


Fig. (4.13) Plot of ratio of area under the curve for different state of concentric circular antenna array versus spacing between the rings

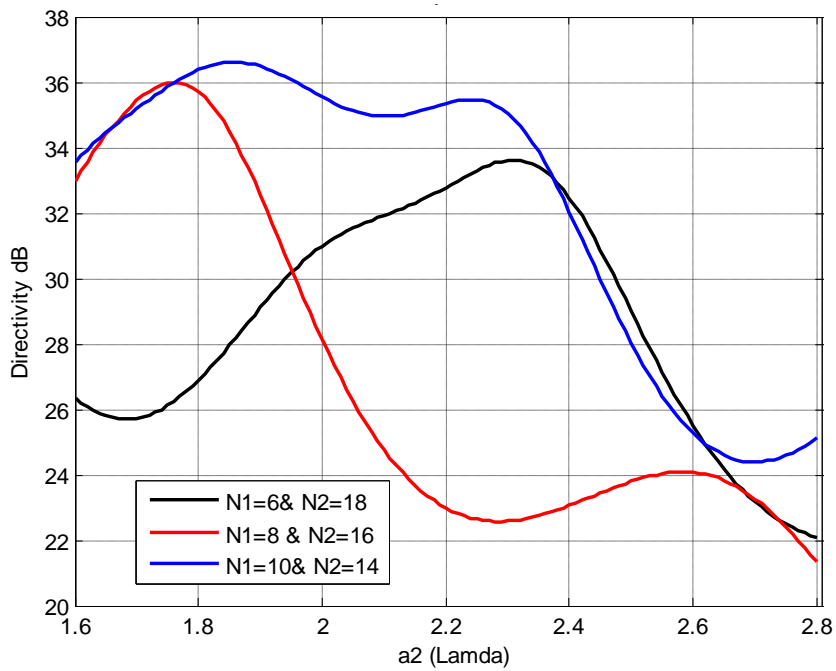


Fig. (4.14) Plot of directivity for different state of concentric circular antenna array versus spacing between the rings

Fig. (4.14) shows the plot of the directivity for different state of concentric circular antenna array. In this figure the radius of the inner ring is kept constant at 1.12λ while the spacing between the two rings

was varied between $(1.6-2.8)\lambda$. Fig. (4.13) and Fig. (4.14), reveals that whenever the area ratio is below the value of unity toward minimum value, there will be an increase in the value of directivity toward maximum value. Comparing the results when the radius of the two rings in the concentric circular array is varied with the results when the radius of the first ring is kept constant while we vary the radius of the outer ring. Better results were obtained for the latter case when only the radius of the outer ring is varied.

Case three represents the performance of the concentric circular array as a function of the spacing between the two rings of the array keeping the radius of the outer ring fixed at radius of the original array value.

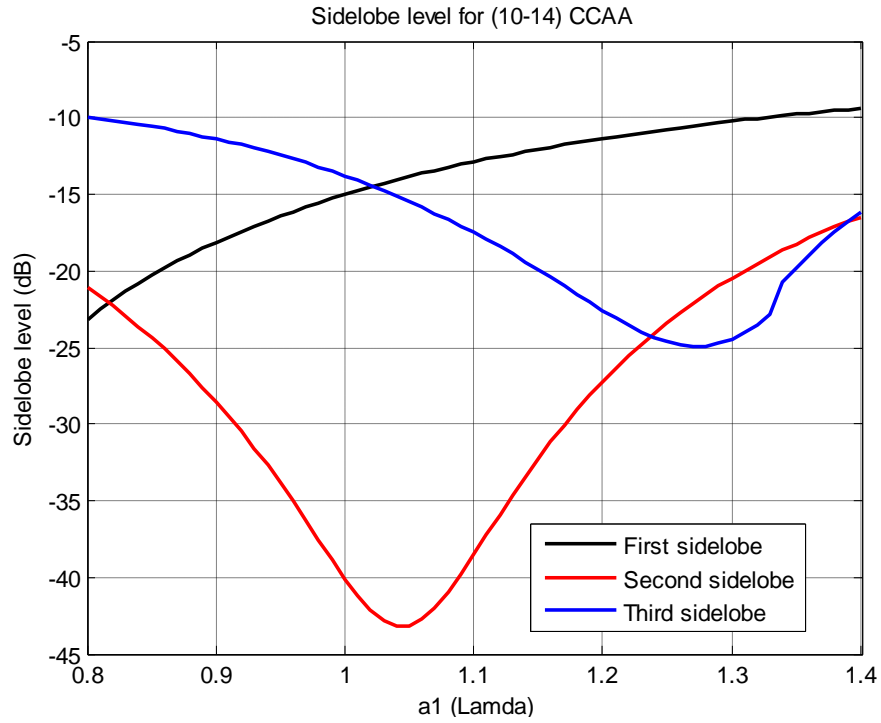
In figures(4.15 to 4.18) the radius of the outer ring is kept constant at 1.9λ which is the same value of the original circular antenna array for 24 elements while the spacing between the two rings was varied between $(0.8-1.4)\lambda$.

Fig. (4.15) represents the first, second and third sidelobes level plotted versus spacing between the two rings for different forms of concentric circular antenna array. The figure reveals that good sidelobes reduction for the first and second sidelobes is for the concentric circular array of 10 elements in the inner ring and 14 elements in the outer ring.

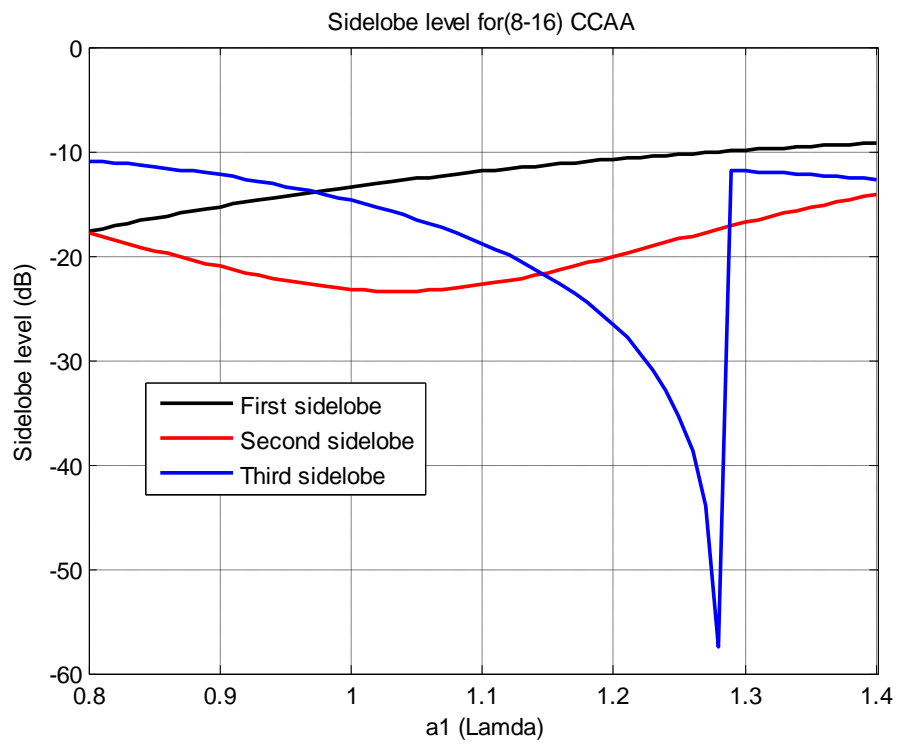
Fig.(4.16) represents the plot of the beamwidth versus the spacing between the two rings for different forms of concentric circular array. The figure shows decreasing in beamwidth with increasing the spacing between the two rings. The figure also shows decreasing in beamwidth when the outer ring contains more elements with respect to the inner ring.

Fig. (4.17) shows the plot of the area ratio for different state of concentric circular antenna array versus spacing between the two rings

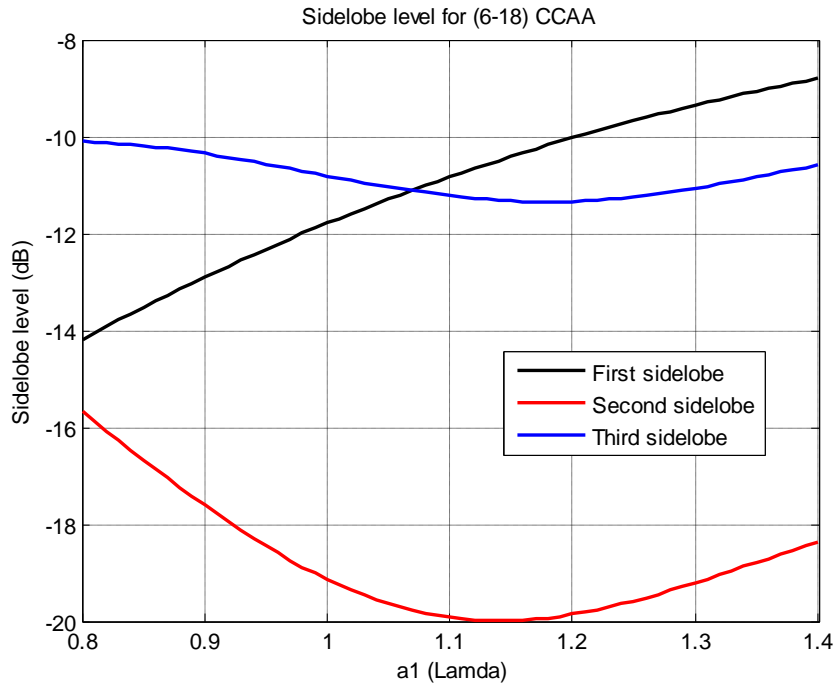
for different forms of concentric circular antenna array. The figure indicates that whenever the area ratio is below the value of unity, there will be a reduction in the sidelobes level.



-a-



-b-



-C-

Fig. (4.15) Plot of sidelobes level versus spacing between the rings for
a- uniform concentric circular array $N_1=10, N_2=14$
b- uniform concentric circular array $N_1 =8, N_2=16$
c- uniform concentric circular array $N_1 =6, N_2=18$

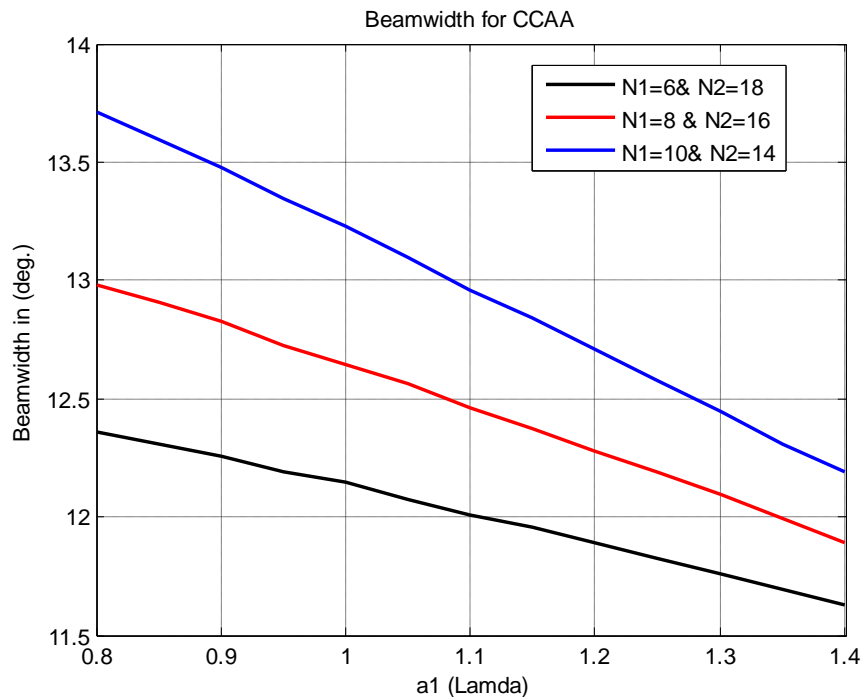


Fig. (4.16) Plot of beamwidth for concentric circular antenna array versus spacing between the rings.

Fig. (4.18) shows the plot of the directivity for different state of concentric circular antenna array. It is clear from this figure that maximum directivity happen, in concentric circular array for 10 elements in inner ring and 14 elements in outer ring at radius of inner ring equal to 1.22λ

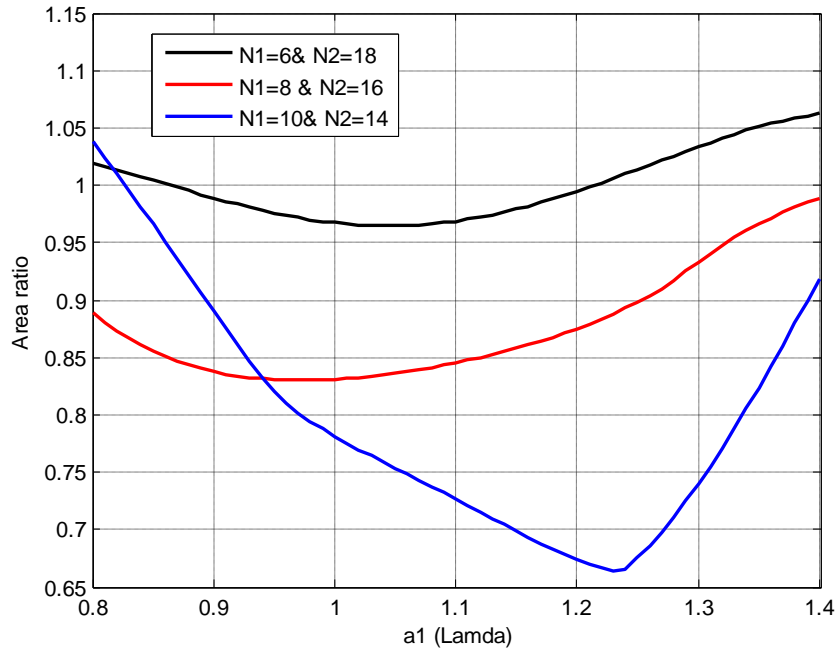


Fig. (4.17) Plot of ratio of area under the curve for different state of concentric circular antenna array versus spacing between the rings

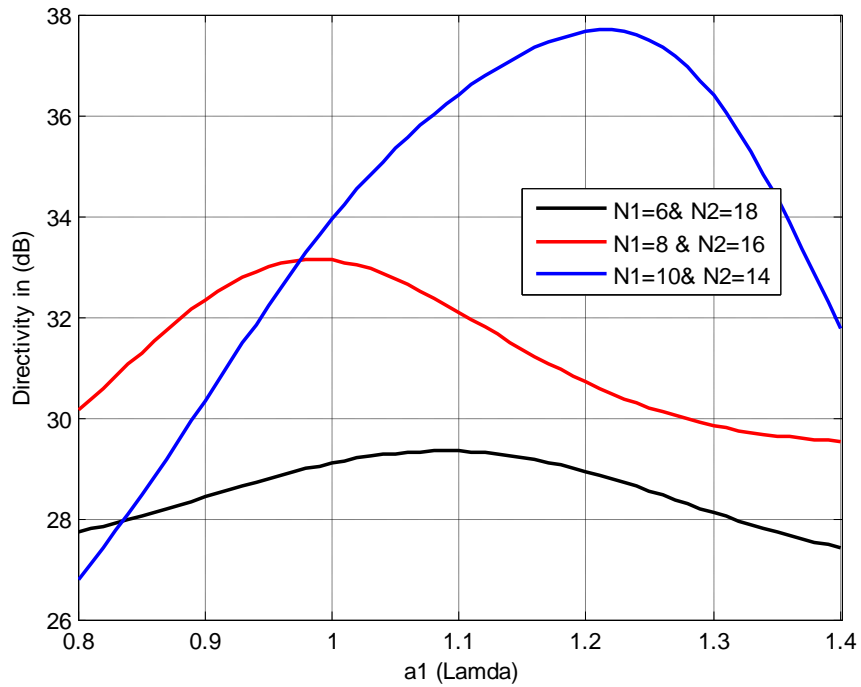


Fig. (4.18) Plot of directivity for different state of concentric circular antenna array versus spacing between the rings

CHAPTER FIVE

Conclusions and Suggestions for Future Work

Antenna arrays have been widely used in different applications including radar, sonar, and communication systems. The radiation pattern of an antenna array is composed of main beam in the direction of the wanted signals and sidelobes in the direction of the unwanted signals. The high level of the sidelobes is responsible for interferences with the main signal in many applications. Therefore, it is desirable to design an antenna array with a high directivity and low sidelobes level to avoid radiation of electromagnetic energy in directions other than the direction of its main beam.

Sidelobes level for antenna array are different from type to another depend on the array configuration such as linear, circular, concentric circular and planer array. There are many ways to reduce the sidelobes level of the antenna array pattern such as using genetic, particle and swarm, neural network algorithms and aperture tapers. These methods help in obtaining optimized weights for the excitation, phase excitation and inter-element spacing between the elements that can be used for constructing the array. Modifying these parameters will leads in reducing the sidelobes level of the array. Moreover the proposed techniques can be used in improving the radiation pattern of an existing antenna. The process is simply done by selection a pair of elements on the array then adjusting its parameters such as amplitude, phase of the excitation currents, and the elements spacing.

5.1 Circular Antenna Arrays:

The uniform circular array has sidelobes level of -7.89 dB with inter-elements spacing at half wavelength. Sidelobes level reduction can be achieved by genetic algorithm, modified excitation of the array elements, reconfiguring the array and by concentric circular array.

It is worthwhile to state the following conclusions.

Applying genetic algorithm for designing circular antenna resulted in the following conclusions:

1- Design a non-uniform circular antenna array with optimized weights for amplitude excitation using the genetic algorithm leads to reduce the sidelobes level for a given number of array elements with respect to the corresponding uniform excited circular antenna array.

Using genetic algorithm technique makes three main contributions

a-The first Sidelobe level is reduced more than 3dB.

b-Since the reduction of the sidelobes level is at the expense of the increase in the beamwidth of the mainbeam, we have taken into account that the increase does not exceed 1.5 degree.

c-Increasing in the value of the directivity for the antenna array.

2- Sidelobes level reduction using modified amplitude excitation:

Adjustments were made in the excitations for certain selected elements in the circular antenna array. These adjustment leads in good reduction in the values of the sidelobes level. For instance, in 12-element circular antenna array, modifying the amplitude excitation for only 2 elements of a uniformly excited array at specified angular

positions, gives sidelobes level of -10.5dB and -14.5 dB for the first and second sidelobes respectively.

Selecting 4 elements in modified excitation array imposes sidelobes level with -14.2dB and -23 dB for the first and second sidelobes respectively.

Using modified excitation array technique gives the following conclusions:

a –Reducing the amplitude excitation of the selected elements in the uniform circular antenna array to 0.1 of its value uniform value, it is possible to reduce the sidelobes level of the uniform circular antenna array.

b – There is a maximum reduction in the value of the sidelobes level for the modified arrays at certain excitation value of the selected elements in the array.

c – Ratio of the area under the sidelobes of the modified excitation array to that of the uniform array, reaches minimum value at certain excitation value of the selected elements for each size of the main array.

d – Directivity of the modified antenna array reaches a maximum value when the area ratio reaches minimum at certain excitation of the selected elements for each size of the main array.

Using 4, 6 and 8 elements with modified excitations in the uniform circular array leads to the following conclusions:

a – With suitable excitations for 4 specified angular positions of the selected elements in circular antenna array gives better reduction in the sidelobes level as compared with that obtained using two elements modified excitations.

b – Ratio of area under sidelobes of the modified excitations circular array to that of the uniform circular array, reaches minimum value at certain excitations of the modified selected elements.

c – Directivity of the modified excitation circular array reaches maximum at certain excitations value for the selected elements.

3- Sidelobes level reduction using reconfigured array:

Changing the locations of two elements in radial distance of N-element circular antenna array can serve in reducing the sidelobes level of the array. The two elements lie at the ends of the diameter of the main array at specified angular positions. The selected two elements in 12-element circular array imposes sidelobes level of -12dB, -20 dB and -26 dB for the first, second and third sidelobes respectively.

Using reconfigured circular array gives us the following conclusions.

a – Sidelobes level reduction depends on the separation between the two selected elements in the N-element circular array.

b – Ratio of area under sidelobes of the reconfigured circular array to that of the main circular array, reaches minimum value at certain separation between the two selected elements.

c – With suitable separation distance between the two selected elements and suitable excitations for the two elements in the reconfigured circular antenna array, good reductions in sidelobes level can be obtained as compared with that obtained by using the uniform excitation.

d – Directivity of the reconfigured circular antenna array reaches maximum value at certain separation between the selected elements and certain excitations for these two elements.

4-sidelobes level reduction using concentric circular antenna array:

Concentric circular antenna array is one of many solutions for obtaining low sidelobes level. For instance in 24-element circular antenna array it is possible to reform it in two concentric rings circular antenna array. The inner ring contains as an example 10 elements and the outer ring contains 14 elements. This array possesses better performance as compared with one ring circular antenna of the same number of elements. The following conclusions can be found by using concentric circular array.

- a-** Sidelobes level of concentric circular array is reduced more compared with circular antenna array of equal number of elements.
- b-** Reduction of the sidelobes level is at the expense of an increase in the beamwidth of the circular array.
- c-** Increase in the directivity as compared with circular antenna array of equal number of elements.
- d-** For narrower beamwidth the outer ring must contain more elements as compared with the inner ring.

5.2 Suggestions for Future Work:

The future work regarding sidelobes canceling techniques for circular antenna can be focused on the following:

- 1- Using genetic algorithm for sidelobe level reduction by optimizing the spacing between the elements (non-uniform spacing).
- 2- Extending the use of modification in the amplitude excitations for certain specified antenna elements to the planar linear arrays for sidelobe reduction.
- 3- Using modification in the phase excitations for certain specified antenna elements for sidelobe reduction.

References:

- [1] Ballanis, C.A., "Antenna theory analysis and design", 3rd edition, JohnWiley and Son's Inc. New York, 2005.
- [2] Cockrell, C. R. and Crosswell, W. F. "A general method for designing circular array antennas to obtain quasi-omnidirectional patterns", NASA, WASHINGTON D.C.,(1967).
- [3] Hodjat, F. and Shahen, A., "Non-uniformly spaced linear and planar array antennas for sidelobe reduction", IEEE Trans. on Antennas and propagation, Vol. AP-26, No. 2, pp.198-204, March, 1978.
- [4] Tseng, F., "Synthesis of arrays for suppressing a wide-band jammer", IEEE Trans. Electromagn. Compat. , Vol. EMC-22, No. 2, May. 1980.
- [5] Hassan, M. A., "Simple iterative method for pattern synthesis using non-uniformly spaced arrays", Electronics letters, Vol. 26, No.13, pp. 891,1990.
- [6] Tennant, A., Dawoud, M. M. and Anderson, A. P., "Array pattern nulling by element position perturbations using a genetic algorithm", Electronics letters 30.3, pp. 174-176, 1994.
- [7] Mitchell, R. J., Chambers,B. and Anderson , A. P., "Array pattern synthesis in the complex plane optimised by a genetic algorithm", Electronics letters 32.20 , pp.1843-1845,1996.
- [8] Keen-Keong,Y., and Yilong, L., "Sidelobe reduction in array-pattern synthesis using genetic algorithm.", IEEE Transactions on Antennas and Propagation 45.7 , pp.1117-1122,1997.
- [9] Preetham, B. K., and Branner, G. R., "Design of unequally spaced arrays for performance improvement", IEEE Transactions on Antennas and Propagation 47.3 pp. 511-523, 1999.
- [10] Dennis, G. and Yahya, R.S., "Particle swarm optimization for reconfigurable phase differentiated array design", Microwave and Optical Technology Letters, Vol. 38, No.3, 5, pp. 168-175, 2003.
- [11] Dessouky, M., Sharshar,H and Albagory,Y.," Efficient sidelobe reduction technique for small-sized concentric circular arrays" ,Progress In Electromagnetics Research, PIER 65, pp.187–200, 2006.
- [12] Sayidmarie, K. H., and Aboud H.A. "Improvement of array radiation pattern by element position perturbation." Systems, Signals and Devices, IEEE SSD. 5th International Multi-Conference on. IEEE, 2008.

- [13] Najjar, Y., Shihab, M., Dib, N. and Khodier, M., "Design of non-uniform circular antenna arrays using particle swarm optimization.", *Journal of electrical engineering* 59.4 ,pp.216-220,2008.
- [14] Zuniga, V., Haridas, N., Erdogan, A. T. and Arslan, T., "Effect of a central antenna element on the directivity, half-power beamwidth and side-lobe level of circular antenna arrays", *Adaptive Hardware and Systems, 2009. AHS 2009. NASA/ESA Conference on. IEEE, 2009.*
- [15] Mandal, D., Ghoshal, S. P., and Bhattacharjee, A. K., "Design of concentric circular antenna array with central element feeding using particle swarm optimization with constriction factor and inertia weight approach and evolutionary programming technique", *Journal of Infrared, Millimeter, and Terahertz Waves*, pp. 667-680,2010.
- [16] Siddharth, P., Basak, A., Das, S., Abraham, A., and Zelinka, I., "Concentric Circular Antenna Array Synthesis Using a Differential Invasive Weed Optimization Algorithm", *Electronics and Telecommunication Engg., IEEE*, pp.395-400, 2010.
- [17] Singh, U. and . Kamal, T. S., "Design of non-uniform circular antenna arrays using biogeography-based optimisation." *IET microwaves, antennas & propagation*, pp. 1365-1370, 2011.
- [18] Das, S., and Mandal, D., "Synthesis of broadside uniform circular antenna array with low on-surface scanning", *Antenna Week (IAW), IEEE, Indian*, 2011.
- [19] Ghosh, P., Banerjee, J., Das, S., and Chaudhuri, S. S. "Design of non-uniform circular antenna arrays using an evolutionary algorithm based approach", *Progress In Electromagnetics Research B*, 43, pp.333-354, 2012.
- [20] Reddy, B. R., Vakula, D., and Sarma, N. V., "Circular antenna array pattern analysis using radial basis function neural network." *IOP Conference Series: Materials Science and Engineering*. Vol. 44. No. 1. IOP Publishing, 2013.
- [21] Albagory ,Y. A., " Analysis of Sidelobe Level and Beamwidth of Uniform Concentric Circular Arrays Utilizing Kaiser Amplitude Weighting", *International Journal of Advanced Research in Computer Engineering & Technology*, Vol 3, Issue 9, September 2014.

- [22] Mohab,A., Hassan,,M. and Mohamed,T.," Design of time modulated concentric circular and concentric hexagonal antenna array using hybrid Enhanced particle swarm optimisation and differential evolution algorithm", Electrical and Electronics Engineering, IET Microw. Antennas & Propagation, pp. 1–9, 2014.
- [23] Recioui, A. "Optimization of circular antenna arrays using a differential search algorithm", vol. 128, issue, 2015.
- [24] Devi, G. G., Raju, G. S. N. and Sridevi, P. V., "Design Of Concentric Circular Antenna Arrays For Sidelobe Reduction Using Differential Evolution Algorithm." , AMSE JOURNALS , Vol. 89, pp. 45-57, March, 2016.
- [25] Mohammed, J. R., and Sayidmarie, K. H., " Synthesizing Asymmetric Side Lobe Pattern with Steered Nulling in Non-uniformly Excited Linear Arrays by Controlling Edge Elements", International Journal of Antennas and Propagation, pp.1-7, 2017.
- [26] Davies, D. E. N. "Circular arrays." The handbook of antenna design 2, pp. 299-329, 1983, chapter 12. [https://books.google.iq/books?id=QjYtNJZmWLEC&printsec=frontcover&dq=the+hand+book+of+antenna+design+2&hl=+](https://books.google.iq/books?id=QjYtNJZmWLEC&printsec=frontcover&dq=the+hand+book+of+antenna+design+2&hl=)
- [27] Elliott, R. S., "Antenna Theory and Design", Revised Edition, John Wiley, New Jersey, 2003.
- [28] Collin, R. E., "Antenna and Radio-wave Propagation", McGraw-Hill, New York, 1985.
- [29] Bogdan, L. and C. Comsa, "Analysis of circular arrays as smart antennas for cellular networks", Proc. IEEE Int. Symp. Signals, Circuits and Systems.03, Vol. 2, pp. 525-528, 2003.
- [30] Ma, Mark T., " Theory and application of antenna arrays", John Wiley & Sons, pp.191-202, 1974. chapter 3
- [31] Haupt, R.L. and Douglas, H.W., " Genetic Algorithms in Electromagnetics", IEEE Press & John Wiley & Sons, New Jersey, 2007.
- [32] Hermawanto, D., "Genetic algorithm for solving simple mathematical equality problem " , Indonesian Institute of Sciences, Indonesia, pp.1-9, 2013.
- [33] Bogdan, L. and Comsa, C., " Analysis of circular arrays as smart antennas for cellular networks", In Proceedings of IEEE international symposium on signals, circuits and systems 03 Vol. 2, pp. 525–528, 2003.

- [34] Chan, S. C. and Chen, H. H. , " Uniform concentric circular arrays with frequency-invariant characteristics theory, design, adaptive beamforming and DOA estimation", *IEEE Transactions on SignalProcessing*, 55(1), pp. 165–177,2007.
- [35] Li, Y., Ho, K. C. and Kwan, C., "A novel partial adaptive broadband beamformer using concentric ring array", In *Proceedings of IEEE ICASSP '04*, pp.177-180, Montreal, Quebec, Canada, May 2004.
- [36] Nofal,M., Aljahdali, S, and Albagory, Y., "Simplified Sidelobe Reduction Technique for Concentric Ring Arrays", *Wireless Personal Communications*, Vol. 71, No. 4, Springer, pp. 2981-2991, 2013.

الخلاصة

أن نظم الاتصالات والرادار تتطلب نمط إشعاع ذي توجيهية عالية و مستوى منخفض للفصوص الجانبية، ومن الضروري البحث عن هوائي لتحقيق ذلك الغرض، ان مصفوفة الهوائيات يمكنها ان تساعدنا في تحقيق هذا الهدف حيث ان مصفوفة الهوائيات تتمتلك نمط إشعاع ذي توجيهية عالية ومستوى منخفض للفصوص الجانبية مقارنة بهوائي ذو عنصر واحد. لكن لازال هوائي المصفوفة يمتلك فصوص جانبية عالية لابد من تخفيضها للتعلب على الاشارات او المعلومات الغير مرغوب فيها. في هذا العمل استخدمنا مصفوفة هوائيات دائرية، حيث تم استخدام العديد من الطرق للحصول على صيغ توزيع التيار لعناصر المصفوفة التي لها فصوص منخفضة.

الخوارزمية الجينية هي تقنية استخدمت في هذه الأطروحة لتقليل الفصوص الجانبية في نمط إشعاع لمصفوفة هوائيات دائرية. تم استعمال المساحة تحت الفصوص الجانبية لتمثيل دالة اللياقة المستخدمة في هذه الخوارزمية. للحصول على نتائج جيدة في الحد من مستوى الفصوص الجانبية. يجب أن نحصل على أدنى قيمة لدالة اللياقة ، مع الأخذ بعين الاعتبار الزيادة في عرض الحزمة الرئيسية .

إن نتائج التمثيل على الحاسبة لمصفوفة الهوائيات الدائرية عند استخدام الخوارزميه الجينية أظهرت انخفاض جيد في تركيبة الفصوص الجانبية.

ومن الطرق المقدمة في هذه الأطروحة لتخفيض الفصوص الجانبية هو تعديل أوزان التيار أو المسافة الشعاعية لبعض العناصر المحددة في مصفوفة الهوائيات الدائرية وتشمل هذه الطريقة تعديل أوزان التيار لبعض العناصر أو المسافة الشعاعية بين عنصرين معينين أو كليهما. تم تطوير فكرة تعديل أوزان التيار من عنصرين إلى أربعة وستة وثمانية.

أظهرت نتائج التمثيل على الحاسبة انخفاضا أفضل في الفصوص الجانبية مقارنة بتلك التي تم الحصول عليها من استخدام الخوارزمية الجينية.

ومن الطرق المقدمة أيضا مصفوفة الهوائيات الدائرية متعددة الحلقات متحدة المركز ،حيث انه تم توزيع العناصر المستخدمة في مصفوفة الهوائيات ذات حلقة واحدة إلى حلقتين متحدة المركز .

تم استخدام ثلاثة أمثلة لمصفوفة الهوائيات الدائرية متعددة الحلقات متحدة المركز ،المثال الأول قمنا بقياس أداء المصفوفة من خلال تغير إنصاف أقطار الحلقتين اعتمادا على نسبة العناصر في الحلقة الخارجية إلى تلك الموجودة في الحلقة الداخلية ، المثال الثاني فانه تم قياس أداء المصفوفة الدائرية متعددة الحلقات متحدة المركز من خلال تغير نصف قطر الحلقة الخارجية مع الحفاظ على نصف قطر الحلقة الداخلية دون تغير عند قيمة اقل من نصف قطر المصفوفة الأصلية،أما في المثال الثالث فقد تم قياس أداء المصفوفة الدائرية متعددة الحلقات متحدة المركز من خلال تغيير نصف قطر الدائرة الداخلية مع الحفاظ على نصف قطر الدائرة الخارجية عند قيمة تساوي لنصف قطر المصفوفة الدائرية أحادية الحلقة .

إن نتائج التمثيل على الحاسبة أظهرت أداء أفضل لمصفوفة الهوائيات الدائرية متعددة الحلقات متحدة المركز بالمقارنة مع المصفوفة الدائرية ذات الحلقة الواحد.

شكر وتقدير

الحمد لله رب العالمين والصلاة والسلام على خاتم الأنبياء والمرسلين سيدنا محمد (صلى الله عليه وسلم) وعلى آله وصحبه أجمعين.

وبعد التوفيق من الله عز وجل في إتمام هذا البحث أود إن أعرب عن جزيل شكري واحترامي إلى مشرفي "الدكتور عبدالله حسن عبود" الذي قدم لي النصح والإرشاد والملاحظات القيمة التي كان لها الأثر الكبير في إخراج البحث بهذا الشكل.

وأود أن أخص بالشكر والتقدير إلى "الأستاذ الدكتور خليل حسن سيد مرعي" لما قدمه من ملاحظات قيمة أثناء فترة الدراسة والبحث.

وكما أقدم شكري وامتناني إلى رئيس قسم هندسة الاتصالات والسادة أعضاء الهيئة التدريسية وجميع زملائي لما أبدوه من تعاون معي أثناء فترة البحث.

وأخيراً، أود أن أشكر جميع أفراد عائلتي وخاصة أبي وأمي على دعمهم وتشجيعهم وصبرهم طوال مدة هذا العمل.

الباحث



جامعة الموصل

كلية هندسة الالكترونيات

دراسة طرق تخفيض الفصوص الجانبية في مصفوفة الهوائيات الدائرية

رسالة تقدم بها

محمد زهير محمد فوزي

إلى

مجلس كلية هندسة الالكترونيات

جامعة الموصل

كجزء من متطلبات نيل شهادة الماجستير

في

هندسة الاتصالات

بإشراف

الدكتور عبدالله حسن عبود

2018م

1439هـ



جامعة الموصل
كلية هندسة الالكترونيات

دراسة طرق تخفيض الفصوص الجانبية في مصفوفة الهوائيات الدائرية

محمد زهير محمد فوزي

رسالة ماجستير
هندسة الاتصالات

بإشراف

الدكتور عبد الله حسن عبود

2018م

1439 هـ